DYNAMICS OF GENE NETWORKS WITH TIME DELAYS

A Dissertation

Presented to the Faculty of the Graduate School

of Cornell University

in Partial Fulfillment of the Requirements for the Degree of

Doctor of Philosophy

by

Anael Verdugo

May 2009

DYNAMICS OF GENE NETWORKS

WITH TIME DELAYS

Anael Verdugo, Ph.D.

Cornell University 2009

The study of time delays and their influence on gene network dynamics is the central topic of this thesis. Three different gene models with delay are studied:

(1) a single gene-mRNA-protein model

(2) a multiple gene network model

(3) a continuous gene network model

Chapters 2 and 3 present a brief introduction to the fields of gene regulatory networks and delay differential equations, respectively. Previous results relevant for this thesis are presented and a friendly overview with figures and examples is given. The purpose of these two chapters is to present a self-contained introduction of the main ideas to the rest of the thesis.

Chapter 4 presents a linear and nonlinear analysis of (1) a single gene-mRNA-protein system given by

$$\begin{aligned} \dot{M} &= \alpha_m \left(\frac{1}{1 + \left(\frac{P_d}{P_0}\right)^n} \right) - \mu_m M \\ \dot{P} &= \alpha_p M - \mu_p P \end{aligned}$$

The study of this model is divided into three cases:

Case 1: Perturbation Methods with Constant Delay

Case 2: Center Manifold Reduction with Constant Delay

Case 3: Perturbation Methods with State-Dependent Delay

Theoretical proof that the model exhibits oscillatory behavior of mRNA and protein expressions was found. The final outcome results in closed form expressions for the limit cycle amplitude and frequency of oscillation. An important result of these findings is the theoretical evidence that delays can drive oscillations in gene activity.

Chapter 5 presents a study of a network model of N coupled gene units. This analysis is the natural extension of a single-gene model by considering multiple gene-mRNA-protein units interconnected. Two different cases are studied and theoretical and numerical results are presented.

Chapter 6 presents a study of a continuous network model. The model takes the form

$$\begin{aligned} \dot{m} &= -\mu\, m + \int_0^1 K(x-\bar{x}) H(p_d(\bar{x}))\, d\bar{x} \\ \dot{p} &= m - \mu\, p \end{aligned}$$

where $m = m(x,t)$, $p = p(x,t)$, $p_d(\bar{x}) = p(\bar{x}, t-T)$, H is a Hill function, and where $K(x-\bar{x})$ is a weighting function. We choose $K(x-\bar{x})$ in two different ways $K(x-\bar{x}) = 1$ and $K(x-\bar{x}) = e^{-|x-\bar{x}|}$ which we name uniform and exponential weighting, respectively. Both of these cases are studied by either theoretical or numerical analysis, and a detailed stability study of the steady states is given. Closed form expressions for the critical delay T_{cr} and associated frequency ω are found. Finally, confirmation of our results are presented by discretizing the continuous system into an N-dimensional system and showing that the discrete results in Chapter 5 approach the continuous results as $N \to \infty$.

BIOGRAPHICAL SKETCH

Anael Verdugo was born in Arizona on October 8th, 1979. When he was one year old, his parents moved back to Mexico, where he spent the first 19 years of his life. Upon finishing high school in 1999, there was no doubt that he would pursue a career in science, and so he came to the United States and enrolled in community college. There he found that his biggest barrier was language, and his biggest disappointment was that his mathematics and physics classes were not challenging. Anael knew he wanted to transfer to one of the top universities in the country, but since this was not going to be an easy task, he knew he had to give nothing less than his best efforts. Luckily, in May 2000, he received his acceptance letter from Caltech. That was one of the happiest days of his life.

Once at Caltech he was amazed to find out that his math and physics courses were very exciting (and demanding). Thus he got to spend more time learning math, physics, and biology. After three years, all the hard work paid off, and he graduated from Caltech in 2003 with a BS in Mathematics.

After he was accepted into Cornell University for a PhD program in Mathematics, he decided to start taking a few Applied Math courses. It was there where he met his current advisor Professor Richard Rand. Working with Prof Rand and learning dynamical systems has been an amazing experience for him. It did not take long for him to realize that he wanted to pursue a career in mathematical biology. It was then when he decided to transfer to the Center for Applied Mathematics and continue his career.

During his years at Cornell, Anael has been blessed by earning three important fellowships: NSF Graduate VIGRE fellowship (2003-2006), Colman Graduate fellowship (2006-2007), and the Dean's Diversity fellowship (2007-2008). These fellowships provided Anael with the time to work on several research

projects with his advisor. The outcome of these projects resulted in five journal articles and two refereed conference proceedings, all of which are fully realized in this dissertation.

After graduation day on May 24th 2009, Anael will start a postdoctoral appointment at the Department of Biological Sciences at Virginia Tech with Professor John Tyson. His plans afterwards are to find an academic tenure-track appointment and become a mathematical modeler of gene networks.

I dedicate this dissertation to my wife, Ninive, for all of her love and support.

ACKNOWLEDGEMENTS

There are many people I would like to thank for their help and guidance in finishing my thesis and getting my PhD. First, and most importantly, my friend and advisor Professor Richard Rand. His day-to-day example will remain a part of me throughout my academic career. His dedication to my progress was amazing: from answering emails at four in the morning, to giving me academic and personal advice all these years. His valuable guidance and infinite patience taught me the importance of being an educator. For all this and much more: Thank you Professor Rand!

I also want to thank Professors Steve Strogatz and Paul Steen for their encouragement and instruction. I am appreciative of their support and guidance during my candidacy years, especially during these last few months when their excellent advice helped me choose the best possible postdoctoral offer for my future career.

I also want to thank those who have given financial support: The Mathematics Department for supporting me through an NSF VIGRE Graduate Mathematics Fellowship during my first two years at Cornell, the Colman Foundation for a one-year fellowship during my third year at the Center for Applied Mathematics, and the Cornell Dean's Diversity program for a one semester fellowship.

Moreover, I am grateful to four very special women for being extremely helpful and supportive: Dolores Pendell, Donna Smith, Polly Marion, and Cindy Twardokus. You guys are the best!

On a more personal note, I would like to thank my friends: Ana & Gerardo and Francisco & Mary, who kept me sane and gave me time to think about other things. To my closest friends Manu & Fer for all their time and company: I will always have a lot of special memories from you guys.

And last but definitely not least, I want to thank my family. My wife, Ninive, who deserves a very special thanks for all her love and patience throughout these years. Her unwavering support made the completion of this dissertation possible: Thank you for being part of my life. Finally, to my parents: "Gracias padres por haberme dado las bases para ser un hombre de bien. Gracias por ser mis guias espirituales, por estar conmigo durante todos estos años, y por el infinito amor que siempre me han dado. Gran parte de lo soy y sere se los debo a ustedes."

TABLE OF CONTENTS

LIST OF TABLES

LIST OF FIGURES

CHAPTER 1

INTRODUCTION

Over the past few decades, mathematical modeling has been extensively used to understand biological phenomena. For most physical systems, it has been generally assumed that the behavior of the process depends only on the present state. Although the latter has been verified for a large class of physical phenomena, many other processes involve time lags or delays [72, 94, 97, 108, 116]. Thus, modern modeling techniques use delay differential equations (DDEs) as a powerful tool to capture the dynamics of these systems with delays [24, 54, 57, 58, 80, 88, 99]. Unfortunately, the use of DDEs brings mathematical complexity into their computational and theoretical study. Fortunately, over the past decade, rapid advances in analytical results, new software tools, and reliable numerical techniques have revived interest in DDEs [15, 16, 64, 85, 101, 119]. One of the main purposes of this thesis is to provide constructive numerical methods to analyze DDE models in the biological field of gene regulatory networks.

1.1 Motivation

The main motivation in designing accurate models of gene networks is to understand the underlying biological behavior and thus allow predictions of the network's dynamics. These predictions are then compared with experimental results and the model's accuracy is confirmed or a correction to the model is then needed [31, 33, 89, 103]. Experimental biology has provided formal methods for the modeling and simulation of gene network processes [4, 105, 107]. However, since most genetic systems involve multiple genes interconnected [106],

an intuitive understanding of their dynamics is hard to obtain [76]. Fortunately, powerful mathematical methods for modeling biochemical reactions have been developed in the past century, especially in the context of metabolic processes [104, 114].

Going back to early work by Goodwin [36] the end-product of a metabolic pathway (protein) may inhibit the expression of a gene coding site for an enzyme (mRNA) that catalyzes a reaction in the pathway. This gives rise to interesting dynamics involving a feedback mechanism of mRNA and protein concentrations. Although there are many formal methods to study gene networks [40, 46, 47, 57], the most popular is through the use of dynamical systems, nonlinear ordinary differential equations (ODEs), and delay differential equations (DDEs) [64, 68, 74, 92]. The differential equation approach captures the behavior of the concentrations of mRNA, proteins, and other molecules by the use of time-dependent variables [24, 93, 108]. In addition, ODE and DDE studies are complemented by simulation techniques to make behavioral predictions [54, 55], as well as modeling techniques to construct the model from experimental data and knowledge on cellular molecular circuitry [20, 47, 68, 76, 89].

In this thesis we analyze several of these feedback inhibition models with parameter-dependent DDEs. We will follow the standard dynamical system's approach, by finding first the steady state solutions, followed by analyzing their associated stability properties, and finally determining their possible bifurcations. As we will see, the first Hopf bifurcation is of particular importance for a DDE because it will tell us how the biological system exhibits periodic responses due to the delay. This will lead us to interesting results regarding the dependence of delay on the amplitude and frequency of oscillation.

1.2 Thesis Overview

The research presented in this thesis began with a beautiful DDE model proposed by Monk in [72]:

$$\dot{M} = \alpha_m \left(\frac{1}{1 + \left(\frac{P_d}{P_0}\right)^n} \right) - \mu_m M \tag{1.1}$$

$$\dot{P} = \alpha_p M - \mu_p P \tag{1.2}$$

where dots represent differentiation with respect to time t, and where M and P represent concentrations of mRNA and protein, respectively. The subscript d denotes a variable which is delayed by time T, that is $P_d = P(t-T)$, and the model constants are given as follows: α_m is the rate at which mRNA is transcribed in the absence of the associated protein, α_p is the rate at which the protein is produced from mRNA in the ribosome, μ_m and μ_p are the rates of degradation of mRNA and of protein, respectively, P_0 is a reference concentration of protein, and n is a parameter (Hill constant). The graphical representation of this model is given by Figure 1.1.

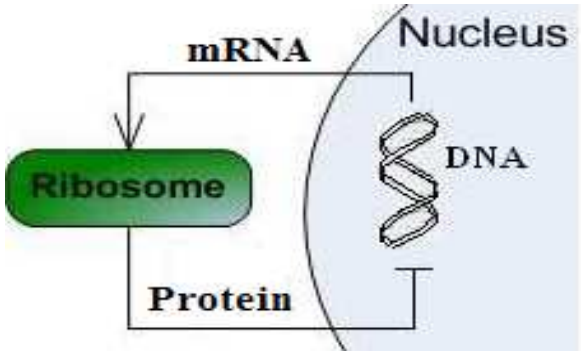

Figure 1.1: Feedback inhibition mechanism.

The biology of the feedback inhibition mechanism presented in Figure 1.1 may be described as follows: A gene is copied onto mRNA, which then diffuses out of the nucleus and attaches to a ribosome. The ribosome then reads the

mRNA and produces a protein, which then goes back into the nucleus where it represses the transcription of its own gene. From a dynamical systems perspective, this process may result in steady state equilibrium, where concentrations of messenger and protein are constant, or it may result in an oscillation.

The analysis of eqs.(1.1) and (1.2) begins with a study of its dynamical behavior when the delay is constant. Theoretical proof that this model exhibits oscillatory behavior of mRNA and protein expressions was found. Subsequently, we assumed that the delay depends on the concentration of mRNA, and is therefore state-dependent. Thus the study of this model is divided into three cases:

Case 1: Perturbation Methods with Constant Delay. Here we prove [108] that the nondelayed system T=0 exhibits a stable steady state and then found a critical delay $T = T_{cr}$ after which it becomes unstable due to a Hopf bifurcation. Explicit closed form expressions for the critical delay and frequency are found. Subsequently, nonlinear analysis (perturbations) on the full system yielded approximate expressions for the amplitude and frequency of oscillation.

Case 2: Center Manifold Reduction with Constant Delay. We reformulate eqs.(1.1) and (1.2) as an operator differential equation acting on function space, with the result that an infinite dimensional system was reduced to a two-dimensional invariant subspace where the limit cycle is born. This work extends our case 1 results by providing approximations of general motions, including the approach (or slow flow) to the periodic motion found previously [109].

Case 3: Perturbation Methods with State-Dependent Delay. This extends our results even further for state-dependent delays $T = T(p(t))$. Biologically, this implies that T depends on concentration of mRNA within the nucleus. Us-

ing linear stability analysis, we prove that the steady state becomes unstable and then use perturbations on the nonlinear system to find expressions for the amplitude and frequency of oscillation. Numerical analysis is used to confirm results [111].

The next step in this thesis is the natural extension of the single gene model (1.1)-(1.2) by considering multiple gene mRNA-protein units interconnected. See Figure 1.2.

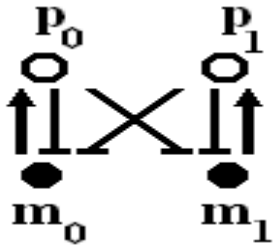

Figure 1.2: Multiple gene mRNA-protein units for N=2.

The biological motivation of this part comes from gene regulatory networks. In Figure 1.2, empty circles represent proteins coming back to the nucleus to inhibit production of mRNA (black circles). The system is modeled so that all proteins affect each mRNA production site. The model takes the form of a system of ODEs coupled to DDEs (see Chapter 5 for more details).

The final step in this thesis is the investigation of a *continuous* model of gene expression in which the protein product of a given gene not only represses its own mRNA production, but also represses the mRNA production of other nearby genes. Mathematically, we tag a given gene with a variable $x \in [0, 1]$, and generalize the system (1.1),(1.2) to be of the form:

$$\dot{m} = -\mu m + \int_0^1 K(x - \bar{x}) H(p_d(\bar{x}))\, d\bar{x} \tag{1.3}$$

$$\dot{p} = m - \mu p \tag{1.4}$$

where $m = m(x,t)$, $p = p(x,t)$, $p_d(\bar{x}) = p(\bar{x}, t-T)$, H is a Hill function, and $K(x-\bar{x})$ is a weighting function. A significant result in the study of eqs.(1.3) and (1.4) is that the steady state is not a constant but a function of location x. Stability analysis reveals that the steady state is stable (for T=0) and further analysis gives expressions for the critical value of delay when the network oscillates. We confirm our results by means of a numerical approximation for different N. Good agreement was found with the continuous counterpart as N became large [111].

1.3 Organization of the Thesis

The following provides a summary of how the chapters in this dissertation are organized.

Chapter 2 contains a friendly introduction to gene regulatory networks. It covers the history and biological background to some of the most relevant problems and discusses previous and current methods for analyzing them.

Chapter 3 is an introduction to the theory of delay-differential equations. The primary target of this chapter is to give a friendly introduction of the basic mathematical theory behind the rest of thesis. The approach is focused on giving the simplest possible explanations of the linear and nonlinear theory. Examples are presented throughout the chapter.

Chapter 4 looks at a single gene network. We present three different studies: (1) perturbation methods for constant delay, (2) center manifold reduction for constant delay, and (3) perturbation methods for state-dependent delay. Our studies entail linear and nonlinear analysis along with numerical results.

Chapter 5 presents a study of an N gene network system. This analysis is the natural extension of the single gene network, obtained by interconnecting multiple gene units. Both linear and nonlinear analyses are given and the stability of the steady state solutions and their bifurcations are analyzed.

Chapter 6 extends the discrete results from Chapter 5 to a continuous network. In this chapter we study the steady state solutions and the stability of two different models of a gene network with time delay. Both of these models are characterized by a system of two coupled equations: an ordinary differential equation and a delay differential-integral equation.

We conclude in **Chapter 7** by providing a summary of the thesis, giving final remarks on our investigations, and looking at some ideas for future work.

CHAPTER 2

AN INTRODUCTION TO GENE REGULATORY NETWORKS

2.1 Gene Regulation

One of the greatest mysteries in modern science is gene regulation. Finding a full description of how proteins within the cell regulate their own production or the production of other proteins is still lacking. The difficulty comes from finding the mechanisms that relate multiple biochemical processes inside the cell. Unfortunately, most cellular processes involve many different molecules interconnected. Thus the metabolism of a cell consists of many interlinked reactions, in which products of one reaction will affect the next. These reactions will form a metabolic network where interlinked molecules can cross-talk and affect different signaling cascades [6, 47, 105].

Gene regulation is mainly achieved by two cellular process: transcription and translation. Transcription is the first step in gene expression and it includes the identical replication of a gene into messenger RNA (mRNA). The second step is the translation process, where the information in the mRNA is translated into a protein with a specific amino acid sequence. The latter process is accomplished by a well-known protein-manufacturing machine called a ribosome. Once the protein is created, it unbinds from the ribosome and carries out its cellular function. From these processes mRNA and protein concentrations arise naturally as the main intracellular regulatory agents for gene expression. Thus, transcription and translation are the main processes by which a cell expresses the instructions encoded in its genes. See Figure 2.1.

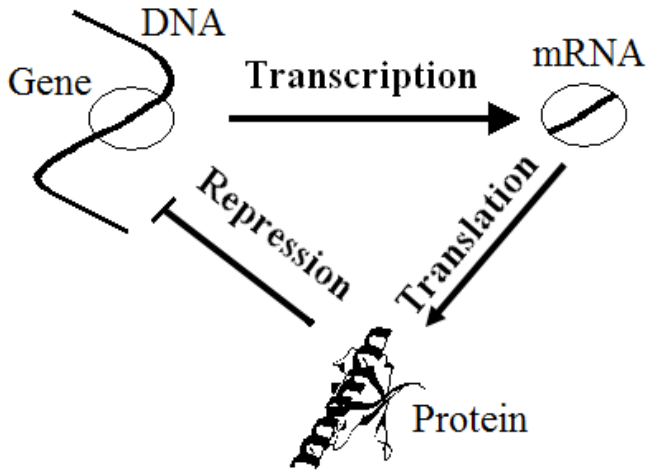

Figure 2.1: Feedback Mechanism. Transcription and translation are the main processes by which a cell expresses the instructions encoded in its genes.

There are several mechanisms that the cell uses to regulate the levels of mRNA and protein concentrations. An example is the cell's ability to increase or decrease the concentration of enzymes that degrade proteins, that is, by having more of these "protein killers" the cell can diminish the amount of proteins present at a certain time. Another important regulatory mechanism is the cell's capacity to turn on and off the transcription process of a specific gene. The latter can be accomplished by means of feedback inhibition, where the expression of a gene is regulated by its own protein product (or by other proteins). This feedback mechanism arises when the protein returns to the nucleus and stops the transcription of its own mRNA by binding to the gene's promoter site. Previous findings [62, 72] show that there are time delays associated with this feedback mechanism. These delays arise naturally as transcriptional delays (time it takes the gene to get copied into mRNA) and translational delays (time it takes the ribosome to translate mRNA into protein). Furthermore, recent studies have shown that it suffices to consider only the transcriptional time delay to have

an accurate dynamic model [62, 72, 108]. Some of these transcriptional delay models can be represented by the following pair of equations:

$$\frac{dm}{dt} = -\mu_m m(t) + H(p(t-T)) \tag{2.1}$$

$$\frac{dp}{dt} = \alpha_p m(t) - \mu_p p(t) \tag{2.2}$$

where the time dependent variables are the mRNA concentration, $m(t)$, and its associated protein concentration, $p(t)$, and where the constants μ_m and μ_p are the decay rates of the mRNA and protein molecules, α_p is the rate of production of new protein molecules per mRNA molecule, and $H(p(t-T))$ is a Hill function representing the rate of *delayed* production of new mRNA molecules. In this thesis we will assume that $H(p(t-T))$ is a decreasing function of the concentration of protein present at a previous time $p(t-T)$, where T represents the transcriptional time delay. Recent findings reveal how the dynamics of the system depends on the model parameters [72, 108, 109, 110].

It is important to point out that, although mRNA transcription factors are one of the best studied gene regulatory mechanisms, there are many other mechanisms of gene regulation that are not fully understood or (in some cases) have not been tackled [2, 26, 47, 61]. These include cell signaling, mRNA splicing, protein degradation, chromatin modifications, and other mechanisms of protein localization. Thus, although scientists have spent more than half a century studying mRNA transcriptional regulation [17, 72, 108], an important goal for future research would be to understand how the previous mechanisms affect or govern the dynamics of gene regulatory networks.

2.2 Mathematical Models of Gene Regulatory Networks

Understanding the interactions between genes and their protein products is an important part of experimental and theoretical biology. Recent experiments [1, 6, 26, 34, 40, 90] and theoretical techniques [9, 68, 84, 108, 109, 117] have been developed to understand the dynamics of gene regulatory networks. From a theoretical point of view, the gene network structure is an abstraction of the system's chemical dynamics, and it includes how protein products affect the expression of other genes and their associated proteins. If the network involves only a few genes then its dynamical behavior could be studied directly [30, 34]. On the other hand, if the network is formed of hundreds or thousands of genes then its experimental or theoretical study may be highly difficult [20, 74]. Nevertheless, research trends show that the study of these complex dynamical networks is a natural step in genomic research [104].

Several mathematical models of gene regulatory networks have been developed over the last couple of decades (for an extensive review see [47, 54, 92, 88, 93]). Some of the most common modeling techniques involve the use of graphs [18, 19, 58, 69], Boolean networks [16, 61, 78, 80], Bayesian networks [5, 31], Petri nets [3, 32, 66], reverse engineering methods [27, 99], and coupled differential equations (linear [55], nonlinear [24, 46, 71], partial [101], stochastic [8, 38, 85, 98, 119], and delayed [8, 25, 29, 108]). As explained above, here we are interested in models where the natural lags or delays play an important role in the system's dynamics [62, 72, 108, 109]. Since these delays arise naturally from transcription, translation, degradation, and other cellular processes, then they can be of the same order of the system's time scale, and thus taking them into account can potentially change the system's dynamics [59, 61, 80, 90, 104, 105, 108].

The study of gene regulatory networks started in the 1960's with Goodwin's oscillator model [36, 37], which consists of a negative feedback loop within a single gene expression pathway (see Figure 2.1). His theoretical studies validated several biochemical experiments which showed the presence of regulatory sequences in the proximity of genes. In modern days, however, other interesting (and more complex) gene regulatory models have been studied and validated with experiments. Some of these include the Hes1 model and the p53-Mdm2 model. The following sections give a brief overview of these interesting and important models.

2.2.1 The Goodwin Oscillator

One of the simplest models of an oscillator is the Goodwin oscillator [36, 37]. In a Goodwin oscillator a gene expresses a mRNA molecule that is then translated into a protein. The protein then acts as an inhibitor by creating another "metabolic species" (see Figure 2.2) which then binds to the gene's promoter site and decreases production of mRNA. Interestingly, the Goodwin model does not only exhibit oscillations, but it can correctly predict the response to stimuli such as temperature, protein concentrations, and even light intensity [87]. Thus, the applications of Goodwin's work were not only restricted to gene expression models. In fact, many biological phenomena that describe a feedback process can be roughly modeled by Goodwin's theoretical framework. Examples in our daily life include our heart beat, temperature, and even our sleeping habits.

Another important application of Goodwin's work is to the field of circadian rhythms. Since many physiological processes of living organisms are pe-

Chapter 4

THE DYNAMICS OF THE EPIGENETIC SYSTEM

The Control Circuits

Our primary concern in this chapter is to derive differential equations which describe the dynamic properties of a certain class of control mechanisms for macromolecular synthesis in cells. As we proceed with the argument, the limitations of a strictly classical analysis in terms of differential equations and integrals will become evident. The procedure will be to select an idealized model of a metabolic feed-back control cycle which, however, incorporates what are believed to be the essential features of the real system. The type of unit component which we will study is that shown in Fig. 1. L_i represents a genetic locus which synthesizes mRNA in quantities represented by the

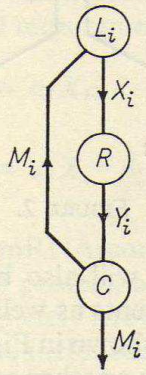

Figure 1.

variable X_i. This specific "signal" encounters a cellular structure R (a ribosome), where its activity results in the synthesis of a particular species of protein in quantities denoted by the variable Y_i. The protein then travels to some cellular locus, C, where it exerts an influence upon the metabolic state either by enzyme action or by some other means (we will usually assume that Y_i is an enzyme). The result of this activity by the protein is the generation of a metabolic species in quantity M_i, a fraction of which closes the control loop by returning to the genetic locus, L_i, where it is assumed to act as a repressor either alone or as a "co-repressor" coupled with another molecule, the "aporepressor". If a separate operator locus exists for the control of genetic activity at L_i then it is included for the purposes of the present discussion as part of the locus L_i itself.

23

Figure 2.2: Page 23, Chapter 4 in Goodwin's "Temporal Organization in Cells" [36].

riodic, then developing a theoretical framework was an important and remarkable achievement by Goodwin. Although he developed his framework for genetic systems, he was also aware that his work had many applications to the field of biological clocks (see page 135 in [36]). The latter is important since many interesting (and well studied) biological processes exhibit periodic behavior with periods of seconds, minutes, hours, and even days. Probably the most important processes are those that oscillate with a 24 hour period [91]. These 24 hour periodic rhythms were first observed by the French scientist Jean-Jacques d'Ortous in 1729, but is wasn't until 1959 that Franz Halberg [41] used the term "circadian rhythms," which comes from the Latin "circa" meaning "around" and "diem" meaning "day". This day-to-day periodicity has a profound importance in our lives and is responsible for many of our biological functions such as body temperature, sleeping habits, regulation of the heart beat, breathing, and even hormonal concentration changes [67] among others.

2.2.2 The Hes1 Network

The Hairy and Enhancer of Split 1 (aka HES1) is a human gene. The mRNA associated to HES1 is conveniently called hes1 mRNA (lowercase) and its protein product is called Hes1, which serves as a transcriptional repressor for the gene HES1. As described above in Section 2.2.1, the Hes1 network is another example of a genetic clock. It has been previously shown [72, 108] that the two hour oscillation period of this biological clock is driven by a time delay of about 15 minutes, which is associated to the transcription process. Thus, the Hes1 network is an ideal candidate for modeling the two hour oscillation dynamics with a system of delay differential equations. However, the two most interesting fea-

tures of Hes1 that make it an ideal candidate for mathematical modeling are: (1) hes1 mRNA and Hes1 protein have short half-lives of approximately 20 minutes [72], and (2) Hes1 protein binds to the Hes1 promoter and represses transcription. These two biological properties allow Hes1 protein to repress hes1 mRNA transcription, followed immediately by a rapid degradation of the Hes1 protein. The latter allows a "resetting" of the clock, by restarting the Hes1 transcription, translation, and repression processes, which is what drives the two hour oscillation. Thus, the importance of this model comes from it's biological simplicity and tractable mathematical model (see [72, 108, 118] for a full description of the math model).

2.2.3 The p53 Network

A topic of great current interest in cancer biology is how cells respond to DNA damage. The p53 protein is one of the main guardians that protect us against these damages in our DNA [102, 114]. For example, if we were to stay too long under the sun, p53 would soon know about it, and it would organize a mechanism to either repair the cell or kill it (if there is too much DNA damage). Fortunately for us, high concentrations of p53 are down regulated by its negative complement Mdm2 [20, 59, 60], and because our body needs finely tuned concentrations of these two antagonists, the cell's natural mechanisms regulate the concentrations of these two. After years of experimental research, molecular cell biologists have uncovered some of the basic (and wonderful) properties that govern p53 dynamics. However, there is still much work to be done, especially in terms of a quantitative 'systems' approach to the problem, including mathematical modeling and hypothesis testing.

Exploring the dynamical properties of the p53-Mdm2 network is a recent and important scientific endeavor. Developing mathematical models based on properties of molecular circuitry and using novel modeling methods to construct realistic versions of the p53 network is one of the main tasks that many mathematical biologists are currently working on. By using smaller and simpler modules [105] in the p53 signaling pathway and fitting experimental data, scientists are able to construct math models that capture the dynamics of the p53-Mdm2 network. Previous observations [59, 103] on p53 dynamics show oscillations in its expression due to the negative feedback between p53 and Mdm2. In a breakthrough study by Lahav et al [59] they found that cells emit discrete pulses of p53 with fixed height and duration. Their main results suggest that DNA damage activates p53 in a series of oscillations or pulses that continue until the cell is repaired or apoptosis (suicide) is triggered. However, recent findings [4] show that this feedback mechanism is insufficient to explain the oscillatory behavior of p53 dynamics. All of these results show that there is still much work to be done. This thesis contributes to such an endeavor, by providing a theoretical and numerical approach to studying these interesting models.

CHAPTER 3

AN INTRODUCTION TO DELAY DIFFERENTIAL EQUATIONS

3.1 Introduction

The historical development of delay differential equations (DDEs) dates back to the 1920's when Volterra [115] investigated the predator-prey model in a parasite population with delay (time it took the infection to manifest within the host). Unfortunately, the momentum on studying DDEs did not pick up until half a century later, when Bellman and Cooke wrote the now classical book "Differential Difference Equations" [7], which is now credited as the first formal study of DDEs. Subsequently, Jack Hale [42] pushed the study of DDEs to the present level of depth, but it wasn't until 1991 that Verduyn Lunel in collaboration with Hale wrote the current "introductory" text on DDEs [44].

The use of ordinary and partial differential equations have played an important role in the development of several scientific fields. However, it is becoming clear that some of the simplest models cannot capture the rich variety of dynamics observed in these systems. Introducing time lags or delays into the construction of some of these models is one possible approach of dealing with these complexities. So, why do we care about learning and studying DDEs? From an applications viewpoint, the use of delays in modeling many natural processes is an important area of applied mathematics. Like it or not, time delays occur very often in nature that to ignore them is to ignore reality. Thus DDE models are becoming more common, appearing in many branches of biological modeling: infectious disease dynamics [21, 22], ecology [100], circadian rhythms [91], epidemiology [23], tumor growth [113], and neural networks [12].

3.2 The Initial-Value Problem

Delay differential equations describe systems where the present state depends on a past value or history of the system. The theory of DDEs is a nontrivial generalization of the theory of ODEs. The generalization comes from the use of functional analysis tools for the study and understanding of the infinite dimensional spaces associated to DDEs. Unfortunately, most DDE results are too technical for the biology community and their usage is currently limited. This chapter serves as a friendly introduction to DDEs. We present step-by-step calculations with examples and basic theory. Some of our results lack mathematical rigorousness, but exemplify basic geometric and computational principles used for the study of delayed models.

The simplest linear DDE has the form

$$\dot{x}(t) = Ax(t) + Bx(t - T) \tag{3.1}$$

where A, B, T are constants with $T > 0$ and x scalar. One immediate question that arises by looking at Eq.(3.1) is the following: what is the initial-value problem for Eq.(3.1)? that is, what is the minimum amount of initial data that we need to specify in order for Eq.(3.1) to define a well-posed initial-value problem?

The most logical (and correct) answer to the question above is that we need to specify an *initial function* on the interval $[-T, 0]$. Just as an ODE needs a single point as initial condition, DDEs need a "history" function over the entire interval $[-T, 0]$. We refer to $\phi(t)$ as the initial condition function for Eq.(3.1). Notice that when $T = 0$ the DDE reduces to an ODE, and only one point ($t = 0$) is needed to specify an initial-value problem (IVP). Thus, we state the following theorem without proof (see [44] for a complete statement and a detailed proof):

Theorem 3.1 If ϕ is a given initial function on $[-T, 0]$, then there is a unique function $x(\phi)$ defined on $[-T, \infty]$ that coincides with ϕ on $[-T, 0]$ and satisfies Eq.(3.1) for $t \geq 0$.

Having defined the IVP for Eq.(3.1) we now consider the existence and uniqueness question. As explained in [44], the main ideas of existence and uniqueness for DDEs are a natural extension on the theory of ODEs, however, the notation involves complicated proofs and technical lemmas using advanced theory of functional analysis. Here we present a less rigorous (but friendlier) approach known as the *method of steps.*

The method of steps is a powerful technique where a DDE of the form (3.1) may be solved as a chain of coupled differential equations over successive intervals. The idea of the method of steps is to solve iteratively the initial function over each of these intervals and restart on the next interval (being sure to reevaluate the function from the right to find the appropriate constant). By reducing a DDE to a series of ODEs, the method of steps allows us to use well-established results for ODEs to *verify* existence and uniqueness of solutions for DDEs. A simple example will elucidate the method:

Example. Let $A = 0$, $B = -1$, and $\phi(t) = 1$ in Eq.(3.1). Then

$$\dot{x}(t) = -x(t-T) = -\phi(t) = -1 \quad \text{when } t \in [0, T] \tag{3.2}$$

which gives

$$x(t) = x_1(t) = -t + C_1 \quad \text{when } t \in [0, T] \tag{3.3}$$

and where we choose $C_1 = 1$ so that $\phi(T) = 1 = x(0)$. Notice that the solution found in Eq.(3.3) is only valid within the interval $t \in [0, T]$, which is why we denote the solution $x(t) = x_1(t)$ for $t \in [0, T]$. In general there will be a solution

$x_j(t)$ for any interval $[(j\text{-}1)T, jT]$. For this example the first three are given as

$$x_0(t) = 1 \ , \quad x_1(t) = -t + 1 \ , \quad x_2(t) = -\frac{t^2}{2} + t - 1 \tag{3.4}$$

for $T = 2$. The geometric representation of this example is provided in Figure 3.1 for $A = 0$, $B = -1$, $T = 2$, and $\phi(t) = 1$.

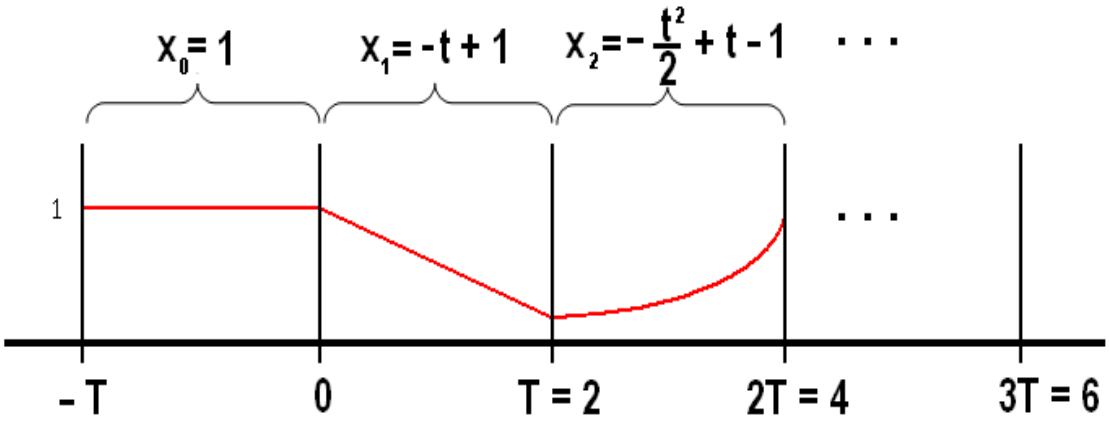

Figure 3.1: Geometric representation using the method of steps for $\dot{x} = -x(t-2)$ when the initial function is given by $\phi(t) = 1$.

3.3 The Characteristic Equation

The characteristic equation for a linear homogeneous constant coefficient DDE is obtained (as in the case for ODEs) by looking for nontrivial solutions of the form $x(t) = Ce^{\lambda t}$. As an example consider Eq.(3.1), which has a nontrivial solution of the form $Ce^{\lambda t}$ if and only if $\lambda - A - Be^{-\lambda T} = 0$. This shows that, contrary to ODEs (which have polynomial characteristic equations), DDEs have transcendental characteristic equations. The latter implies that the characteristic equation of a DDE has infinitely many roots, which yields an infinite family of linearly independent solutions to the DDE.

Continuing our previous example:

Example. If $A = 0$ and $B = -1$ in Eq.(3.1) then assuming $x(t) = Ce^{\lambda t}$ yields

$$\dot{x} \;=\; -x(t-T) \quad \Rightarrow \quad \lambda \;=\; -e^{-\lambda T}. \tag{3.5}$$

Notice when $T = 0$, Eq.(3.5) reduces to

$$\dot{x} \;=\; -x(t) \quad \Rightarrow \quad \lambda \;=\; -1 \tag{3.6}$$

which is the solution of the associated ODE. So, what happens to the the single root at $\lambda = -1$ after $T = \epsilon > 0$? By numerical simulations we can show that the root at $\lambda = -1$ "breaks" into a complex conjugate pair. See Figure 3.2.

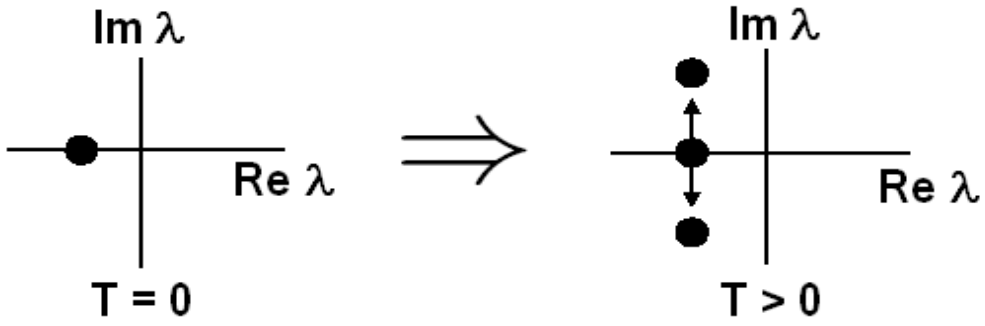

Figure 3.2: Roots of the characteristic equation when $T = 0$ and $T > 0$ for Eq.(3.1) when $A = 0$ and $B = -1$. Notice that $\lambda = -1$ breaks into a conjugate pair when $T > 0$.

From our previous example three interesting questions arise: (1) Can we determine the location in the complex plain of all roots λ when $T > 0$? (2) Can we determine if $\mathrm{Re}(\lambda)<0\ \forall\lambda$? (3) Can we show that the dynamics of the DDE converge to the dynamics of the ODE as $T \to 0$?

The answers to all three questions above are nontrivial. For question (1) several numerical methods [10, 112] have proven to be useful, but a general

theory is still not available. Questions (2) and (3) also lack a general proof for families of equations. Thus the common approach is to study each DDE in a case by case basis, just as is explained by Hale in [43] page 9. See Figure 3.3.

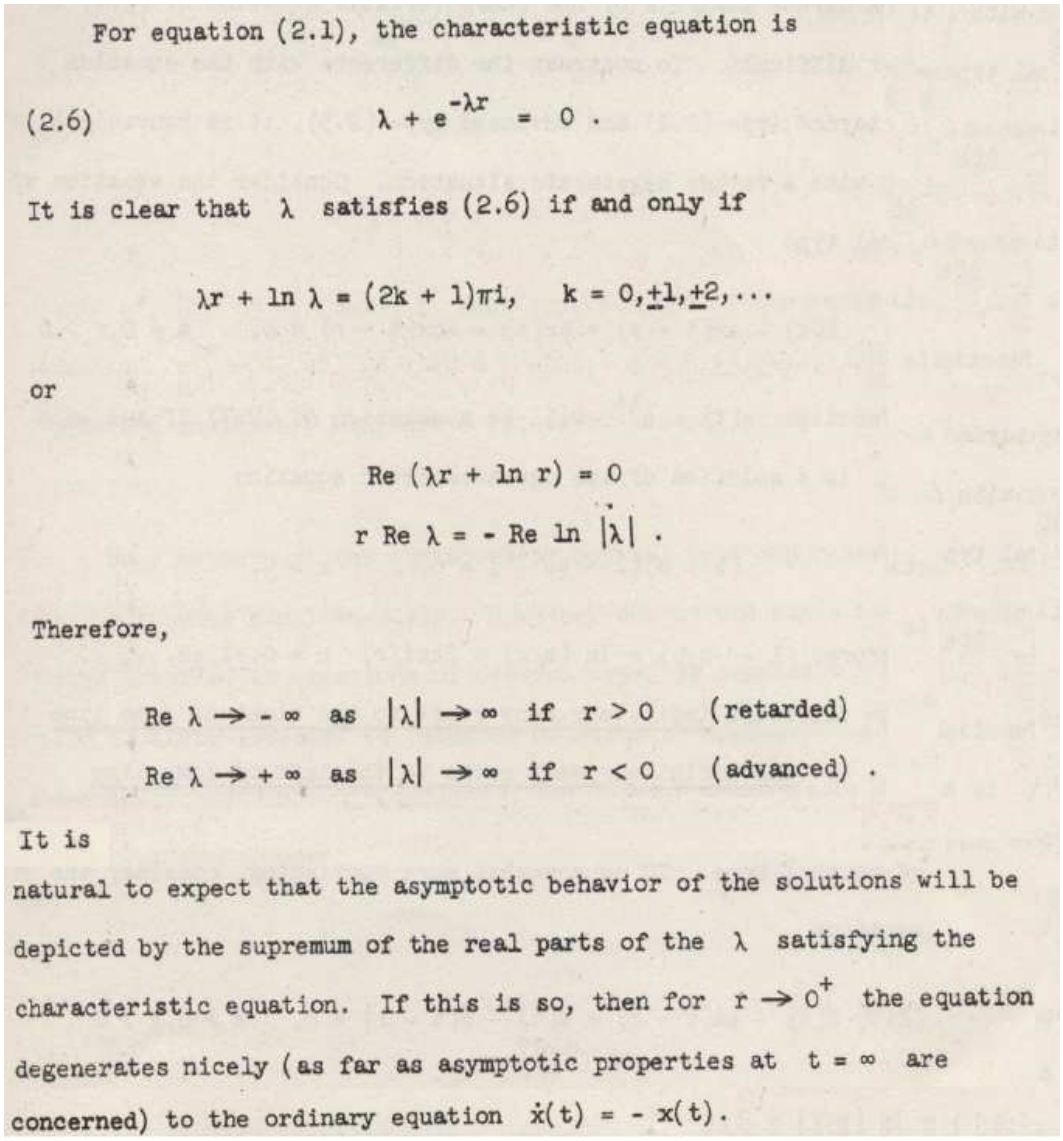

For equation (2.1), the characteristic equation is

$$\lambda + e^{-\lambda r} = 0 . \tag{2.6}$$

It is clear that λ satisfies (2.6) if and only if

$$\lambda r + \ln \lambda = (2k + 1)\pi i, \quad k = 0, \pm 1, \pm 2, \ldots$$

or

$$\operatorname{Re} (\lambda r + \ln r) = 0$$

$$r \operatorname{Re} \lambda = - \operatorname{Re} \ln |\lambda| .$$

Therefore,

$$\operatorname{Re} \lambda \to - \infty \text{ as } |\lambda| \to \infty \text{ if } r > 0 \quad \text{(retarded)}$$

$$\operatorname{Re} \lambda \to + \infty \text{ as } |\lambda| \to \infty \text{ if } r < 0 \quad \text{(advanced)} .$$

It is natural to expect that the asymptotic behavior of the solutions will be depicted by the supremum of the real parts of the λ satisfying the characteristic equation. If this is so, then for $r \to 0^+$ the equation degenerates nicely (as far as asymptotic properties at $t = \infty$ are concerned) to the ordinary equation $\dot{x}(t) = - x(t)$.

Figure 3.3: Page 9 of 'Functional Differential Equations' by Jack Hale [43].

Before we move on to the next section on stability, we first generalize Eq.(3.1) as follows:

Example. Suppose T_{1j} and T_{0k}, are finite constant delays so that Eq.(3.1) generalizes to the multiple delayed version

$$\dot{x}(t) \;=\; \sum_{j=1}^{p} C_j \dot{x}(t - T_{1j}) + \sum_{k=0}^{q} B_k x(t - T_{0k}) \tag{3.7}$$

where without loss of generality we assume

$$0 < T_{11} < \ldots < T_{1p} \tag{3.8}$$

$$0 = T_{00} < \ldots < T_{0q} \tag{3.9}$$

$$C_j \in \mathbb{R} \;\; (j = 1, \ldots, p)\,, \;\; \text{and} \;\; B_k \in \mathbb{R} \;\; (k = 0, \ldots, q) \tag{3.10}$$

Then the characteristic function D is given by

$$D(\lambda) \;=\; \lambda - \lambda \sum_{j=1}^{p} C_j e^{-T_{1j}\lambda} - \sum_{k=0}^{q} B_k e^{-T_{0j}\lambda} \tag{3.11}$$

Notice that the latter example can be extended to C_j and B_k of the form of $n \times n$ matrices and integrals. For a complete treatment on the subject we refer the reader to Stepan's "Retarded Dynamical Systems: Stability and Characteristics Functions" [95]. The main results when C_j and B_k are integrals (better known as bounded variations) are given in Figure 3.4. Notice that the terms NFDE and RFDE refer to neutral functional differential equations and retarded functional differential equations, respectively. By definition NFDEs describe a system where the rate of change of the state, $\dot{x}(t)$, depends on the past state of the system, $x(t - T)$ and on its own past rate of change, $\dot{x}(t - T)$. Thus if any $C_j \neq 0$ then Eq.(3.7) is an NFDE. On the other hand, RFDEs are only defined by the past state of the system, $x(t - T)$. This would be the case when all $C_j = 0$ in Eq.(3.7).

The theory of NFDEs is more complicated than that of the RFDEs. However, the linear autonomous NFDEs have also a simple form:

$$\dot{x}(t) = \int_{-\infty}^{0} [d\eta_1(\theta)]\dot{x}(t+\theta) + \int_{-\infty}^{0} [d\eta_0(\theta)]x(t+\theta) \tag{1.8}$$

where η_0 and η_1 are $n \times n$ matrices of functions of bounded variation. Its characteristic function D is defined by

$$D(\lambda) = \det\left(\lambda I - \lambda \int_{-\infty}^{0} e^{\lambda\vartheta} d\eta_1(\theta) - \int_{-\infty}^{0} e^{\lambda\theta} d\eta_0(\theta)\right). \tag{1.9}$$

Figure 3.4: Page 5 of "Retarded Dynamical Systems" by Gabor Stepan. NFDEs describe a system where the rate of change of the state, $\dot{x}(t)$, depends on the past state of the system, $x(t-T)$, and on its own past rate of change, $\dot{x}(t-T)$. RFDEs are only defined by the past state of the system, $x(t-T)$.

3.4 Stability and Critical Delays

As in the case for ODEs, linear stability analysis for DDEs is also determined by the roots of the characteristic equation. As seen in our previous section, the characteristic equation of a DDE is, in general, a transcendental equation, and hence has infinitely many roots. In this section we discuss stability properties of DDEs and their relationship to the main bifurcation parameter: the delay, T.

It is well known from dynamical systems theory that several stability criterion can be defined for ODEs. Similarly, for DDEs a few are also known and they include: Lyapunov's criterion, Pontryagin criterion, Yesipovich-Svirskii criterion, delay-decomposition criterion, Chebotarev criterion, d-subdivision method, Nyquist criterion, and many others (see [95] for an extensive overview). Here we motivate a formal definition of stability by following Stepan's criterion in [95]:

Definition. The trivial solution of Eq.(3.1) is exponentially asymptotically stable if there exists a scalar $\epsilon > 0$ such that $\mathrm{Re}(\lambda_k) \leq -\epsilon$ for all the zeros λ_k of the corresponding characteristic equation.

An interesting feature of DDEs is that the delay, T, is the main bifurcation parameter in the study of the roots of the characteristic equation. Being the roots functions of the delay, the stability conditions for DDEs are usually defined in terms of the eigenvalue with maximum real part: $\lambda_{\max} = \lambda_{\max}(T)$. This implies that if the system is originally stable for $T = 0$ (where all $\mathrm{Re}(\lambda_k) < 0$), then there may exist a critical value of the delay, $T = T_{cr}$, when the first root (or complex conjugates) cross the imaginary axis, giving thus $\mathrm{Re}(\lambda_{\max}) = 0$. We continue our example used earlier to clarify the latter.

Example. We start by numerically integrating Eq.(3.1) above for $A = 0$ and $B = -1$. We use Matlab's dde23 and obtain Figure 3.5 as a result. The system is originally stable when T is small, oscillates when $T = \pi/2$, and becomes unstable when $T > \pi/2$. The expression for T_{cr} can be easily found by setting $\lambda = i\omega$ into the characteristic equation (3.5):

$$\lambda + e^{-\lambda T} = 0 \quad \Leftrightarrow \quad i\omega + e^{-i\omega T_{cr}} = 0 \tag{3.12}$$

$$\Leftrightarrow \quad \cos \omega T_{cr} = 0\,, \quad \omega - \sin \omega T_{cr} = 0 \tag{3.13}$$

$$\Leftrightarrow \quad \omega = 1\,, \quad T_{cr} = \frac{\pi}{2} \tag{3.14}$$

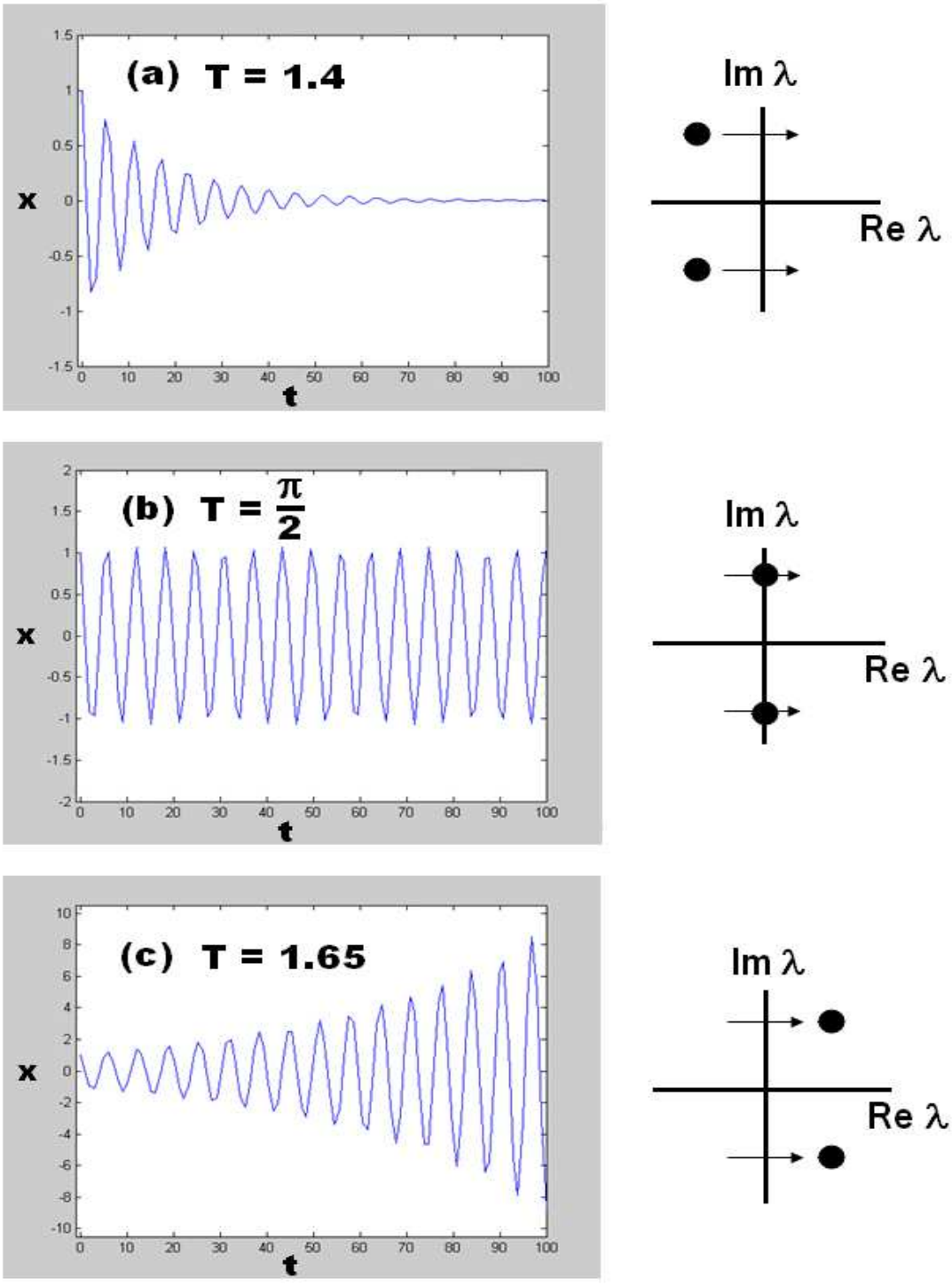

Figure 3.5: Numerical integration using Matlab's dde23 of $\dot{x} = -x(t-T)$ for (a) $T = 1.4$, (b) $T = \pi/2$, and (c) $T = 1.65$

3.5 Nonlinear Investigations

The fundamental problem in the analysis of a nonlinear DDE is to find the appropriate bifurcation conditions for the stability of the trivial solution of the associated linear system. If the relevant steady states of the original nonlinear DDE are non trivial, then we may Taylor expand them about the equilibrium solution to obtain a first order approximation (also known as the *linear variational equations*). In this section we deal with the simplest possible situation, and choose examples where only trivial solutions are studied. We point out, however, that we can always find the associated linear variational equations if the steady states were non trivial.

There are many nonlinear results in the literature for DDEs. For an extensive summary we refer the reader to [28, 42, 43, 44, 95]. In this thesis however, we will deal with mainly two nonlinear theorems: (1) the Hopf bifurcation theorem, and (2) the center manifold theorem. We point out that for DDEs with constant delays most of the nonlinear results and theorems extend naturally from regular ODE theory. However, although the "ideas" are the same, the notation and theory is highly technical. For the curious reader, we present theorems (1) and (2) here from Diekmann et al [28]. See Figures 3.6 and 3.7 respectively.

In the following sections we deal with three nonlinear DDEs. All three exhibit a Hopf bifurcation scenario in which an equilibrium point changes its stability due to a change in parameters, giving rise to the birth of a periodic motion called a limit cycle. The most familiar setting in which this scenario occurs is the

(1) Hopf bifurcation theorem

Theorem 2.7. (*Hopf bifurcation for RFDE.*) *Assume* (Hζ1-Hζ3) and (Hg1-Hg2). *Then there exist* C^{k-1}*-functions* $\epsilon \mapsto \mu^*(\epsilon)$, $\epsilon \mapsto \rho^*(\epsilon)$ *and* $\epsilon \mapsto \omega^*(\epsilon)$, *with values in* $\mathbb{R}$ *and a mapping* $\epsilon \mapsto \psi(\epsilon)$ *taking values in* W $(\subset X_0)$, *defined for* ϵ *sufficiently small, such that the solution of* (2.6) *with initial condition* $\varphi(\epsilon) = C_1(\rho^*(\epsilon)(\phi + \overline{\phi} + \psi(\epsilon)), \mu^*(\epsilon))$ *is* $\frac{2\pi}{\omega^*(\epsilon)}$*-periodic. Moreover,* $\mu^*(\epsilon)$ *and* $\omega^*(\epsilon)$ *are even in* ϵ, $\mu^*(0) = \mu_0$, $\omega^*(0) = \omega_0$ *and if* $x(t)$ *is any small periodic solution of this equation with* μ *close to* μ_0 *and period close to* $\frac{2\pi}{\omega_0}$, *then* $\mu = \mu^*(\epsilon)$ *for some* ϵ *and there exists* $\sigma \in [0, 2\pi/\omega^*(\epsilon))$ *such that* $x(\theta + \sigma) = C_1(\rho^*(\epsilon)(\phi + \overline{\phi} + \psi(\epsilon)), \mu^*(\epsilon))(\theta), \theta \in [-h, 0]$. *Finally,* $\rho^*(\epsilon) = \epsilon + o(\epsilon)$ *and* $\psi(\epsilon) = o(1)$ *as* $\epsilon \to 0$.

where

Hg1 g is a C^k-smooth mapping, $k \geq 2$, from $X \times \mathbb{R}$ into $\mathbb{R}^n$,

Hg2 $g(0, \mu) = 0$ and $D_1 g(0, \mu) = 0$ for all $\mu \in \mathbb{R}$,

Hζ1 the mapping $(\mu, \varphi) \mapsto \int_0^h d\zeta(\theta, \mu)\varphi(-\theta)$ from $\mathbb{R} \times X$ into $\mathbb{R}^n$ is C^k-smooth, $k \geq 2$.

Hζ2 $z = \pm i\omega_0$ are simple roots of $\det \Delta(z, \mu_0) = 0$ and no other root belongs to $i\omega_0\mathbb{Z}$,

Hζ3 $\mathrm{Re}\,(q \cdot D_2\Delta(i\omega_0, \mu_0)p) \neq 0$.

Figure 3.6: "Delay equations: functional-, complex-, and nonlinear analysis" by Diekmann et al. [28]

(2) Center manifold theorem

$$u(t) = T(t-s)u(s) + \int_s^t T^{\odot *}(t-\tau)R(u(\tau))\,d\tau, \quad -\infty < s \leq t < \infty \tag{1.2}$$

Theorem 5.3. (*Center manifold: invariance and relation to bounded orbits.*)

(i) $\mathcal{W}_c$ *is locally positively invariant in the sense that if* $\varphi \in \mathcal{W}_c$ *and the solution of* (1.2) *with* $u(0) = \varphi$, $\Sigma(t, \varphi)$ *satisfies* $||\Sigma(t, \varphi)|| < \delta$ *for* $t \in [0, T]$, *then* $\Sigma(T, \varphi) \in \mathcal{W}_c$.

(ii) $\mathcal{W}_c$ *contains all solutions of* (1.2) *which are defined on* $\mathbb{R}$ *and have their norm bounded above by* δ.

(iii) *The origin is contained in* $\mathcal{W}_c$: $\mathcal{C}(0) = 0$.

Figure 3.7: "Delay equations: functional-, complex-, and nonlinear analysis" by Diekmann et al. [28]

phase plane of a pair of first order ODEs (see for example [39, 82]):

$$\frac{dx}{dt} = -y + \mu x + a_1 x^2 + a_2 xy + a_3 y^2 + b_1 x^3 + b_2 x^2 y + b_3 x y^2 + b_4 y^3 \quad (3.15)$$

$$\frac{dy}{dt} = x + \mu y + c_1 x^2 + c_2 xy + c_3 y^2 + d_1 x^3 + d_2 x^2 y + d_3 x y^2 + d_4 y^3 \quad (3.16)$$

As μ passes through zero, a limit cycle is generically born. It can be written in the approximate form:

$$x = A\cos\omega t, \qquad y = A\sin\omega t \quad (3.17)$$

where $\omega = 1 + O(\mu)$, and where the amplitude A is given by the Hopf bifurcation formula:

$$A^2 = \frac{-8}{S}\,\mu \quad (3.18)$$

where

$$S = 3d_4 + d_2 + 3b_1 + b_3 + 2a_3c_3 + a_2(a_1 + a_3) - 2a_1c_1 - c_2(c_1 + c_3) \quad (3.19)$$

In Eq.(3.18), A is real so that $A^2 > 0$, which means that μ must have the opposite sign as S.

In the following sections we present a comparable formula for a class of first order nonlinear constant coefficient DDEs. We start by presenting the linear analysis followed by the nonlinear investigations.

3.6 Example 1:

$$\dot{x} = \alpha x + \beta x_d + a_1 x^2 + a_2 x x_d + a_3 x_d^2 + b_1 x^3 + b_2 x^2 x_d + b_3 x x_d^2 + b_4 x_d^3$$

3.6.1 Linear Analysis: Stability and Critical Delays

We start this section by introducing the following first order nonlinear constant coefficient DDE with quadratic and cubic nonlinearities:

$$\frac{dx}{dt} = \alpha x + \beta x_d + a_1 x^2 + a_2 x x_d + a_3 x_d^2 + b_1 x^3 + b_2 x^2 x_d + b_3 x x_d^2 + b_4 x_d^3 \tag{3.20}$$

where $x = x(t)$ and $x_d = x(t - T)$. Here T is the delay. Associated with (3.20) is the linear DDE

$$\frac{dx}{dt} = \alpha x + \beta x_d \tag{3.21}$$

We assume that (3.21) has a critical delay T_{cr} for which it exhibits a pair of pure imaginary eigenvalues $\pm\omega i$ corresponding to the solution

$$x = c_1 \cos \omega t + c_2 \sin \omega t \tag{3.22}$$

Then for values of delay T which lie close to T_{cr},

$$T = T_{cr} + \mu, \tag{3.23}$$

the nonlinear Eq.(3.20) may exhibit a periodic solution which can be written in the approximate form:

$$x = A \cos \omega t \tag{3.24}$$

The critical delay, T_{cr}, may be obtained by substituting Eq.(3.24) into Eq.(3.21). We equate to zero coefficients of $\sin(\omega t)$ and $\cos(\omega t)$, and obtain the following two equations:

$$\beta \sin(\omega \mathrm{T_{cr}}) = -\omega, \qquad \beta \cos(\omega \mathrm{T_{cr}}) = -\alpha \tag{3.25}$$

Squaring and adding these gives

$$\omega = \sqrt{\beta^2 - \alpha^2} \tag{3.26}$$

Substituting (3.26) into the second of (3.25), we obtain the desired relationship between T_{cr} and α and β:

$$T_{cr} = \frac{\arccos\left(\frac{-\alpha}{\beta}\right)}{\sqrt{\beta^2 - \alpha^2}} \tag{3.27}$$

or equivalently

$$T_{cr} = \frac{\arctan\left(\frac{\alpha}{\sqrt{\beta^2 - \alpha^2}}\right)}{\sqrt{\beta^2 - \alpha^2}} \tag{3.28}$$

3.6.2 Nonlinear Analysis: Lindstedt's Method

For the nonlinear analysis we use Lindstedt's method. See [75, 81] for an introduction on Lindstedt's method. We begin by introducing a small parameter ϵ via the scaling

$$x = \epsilon u \tag{3.29}$$

The detuning μ of Eq.(3.23) is scaled like ϵ^2:

$$T = T_{cr} + \mu = T_{cr} + \epsilon^2 \hat{\mu} \tag{3.30}$$

Next we stretch time by replacing the independent variable t by τ, where

$$\tau = \Omega t \tag{3.31}$$

This results in the following form of Eq.(3.20):

$$\Omega \frac{du}{d\tau} = \alpha u + \beta u_d + \epsilon(a_1 u^2 + a_2 u u_d + a_3 u_d^2) + \epsilon^2(b_1 u^3 + b_2 u^2 u_d + b_3 u u_d^2 + b_4 u_d^3) \tag{3.32}$$

where $u_d = u(\tau - \Omega T)$. We expand Ω in a power series in ϵ, omitting the $O(\epsilon)$ term for convenience, since it turns out to be zero:

$$\Omega = \omega + \epsilon^2 k_2 + \cdots \tag{3.33}$$

Next we expand the delay term u_d:

$$\begin{aligned} u_d = u(\tau - \Omega T) &= u(\tau - (\omega + \epsilon^2 k_2 + \cdots)(T_{cr} + \epsilon^2 \hat{\mu})) && (3.34)\\ &= u(\tau - \omega T_{cr} - \epsilon^2 (k_2 T_{cr} + \omega \hat{\mu}) + \cdots) && (3.35)\\ &= u(\tau - \omega T_{cr}) - \epsilon^2 (k_2 T_{cr} + \omega \hat{\mu})\, u'(\tau - \omega T_{cr}) + O(\epsilon^3) && (3.36) \end{aligned}$$

Finally we expand $u(\tau)$ in a power series in ϵ:

$$u(\tau) = u_0(\tau) + \epsilon u_1(\tau) + \epsilon^2 u_2(\tau) + \cdots \tag{3.37}$$

Substituting and collecting terms, we find:

$$\begin{aligned} \omega \frac{du_0}{d\tau} - \alpha u_0(\tau) - \beta u_0(\tau - \omega T_{cr}) &= 0 && (3.38)\\ \omega \frac{du_1}{d\tau} - \alpha u_1(\tau) - \beta u_1(\tau - \omega T_{cr}) &= a_1 u_0(\tau)^2 + a_2 u_0(\tau) u_0(\tau - \omega T_{cr}) && \\ & \quad + a_3 u_0(\tau - \omega T_{cr})^2 && (3.39)\\ \omega \frac{du_2}{d\tau} - \alpha u_2(\tau) - \beta u_2(\tau - \omega T_{cr}) &= \cdots && (3.40) \end{aligned}$$

where $\cdots$ stands for terms in u_0 and u_1, omitted here for brevity. We take the solution of the u_0 equation as (cf. Eq.(3.22) above):

$$u_0(\tau) = \hat{A} \cos(\tau) \tag{3.41}$$

We substitute (3.41) into (3.39) and obtain the following expression for u_1:

$$u_1(\tau) = m_1 \sin(2\tau) + m_2 \cos(2\tau) + m_3 \tag{3.42}$$

where m_1 is given by the equation:

$$m_1 = -\frac{\hat{A}^2\ (2\,a_3\beta + a_2\beta - 2\,a_1\beta - 2\,a_3\,\alpha)\ \sqrt{\beta^2 - \alpha^2}}{2\beta\ (\beta + \alpha)\ (5\beta - 4\,\alpha)} \tag{3.43}$$

and where m_2 and m_3 are given by similar equations, omitted here for brevity. In deriving (3.43), ω has been replaced by $\sqrt{\beta^2 - \alpha^2}$ as in Eq.(3.26).

Next the expressions for u_0 and u_1, Eqs.(3.41),(3.42), are substituted into the u_2 equation, Eq.(3.40), and, after trigonometric simplifications have been performed, the coefficients of the resonant terms, $\sin\tau$ and $\cos\tau$, are equated to zero. This results in the following equation for A^2:

$$A^2 = \frac{P}{Q}\,\mu \tag{3.44}$$

where

$$P = 4\beta^3\ (\beta - \alpha)\ (\beta + \alpha)^2\ (-5\beta + 4\alpha) \tag{3.45}$$

and where $Q = Q_0 + Q_1 T_{cr}$ is given by

$$\begin{aligned} Q_0 \;=\; & 5\,b_3\beta^5 + 15\,b_1\beta^5 - 15\,\alpha\,b_4\beta^4 + \alpha\,b_3\beta^4 - 15\,\alpha\,b_2\beta^4 + 3\,\alpha\,b_1\beta^4 - 4\,{a_3}^2\beta^4 \\ & -9\,a_2\,a_3\beta^4 - 18\,a_1\,a_3\beta^4 - {a_2}^2\beta^4 - 9\,a_1\,a_2\beta^4 - 18\,{a_1}^2\beta^4 - 3\,\alpha^2\,b_4\beta^3 \\ & +6\,\alpha^2\,b_3\beta^3 - 3\,\alpha^2\,b_2\beta^3 - 12\,\alpha^2\,b_1\beta^3 + 26\,{a_3}^2\,\alpha\beta^3 + 19\,a_2\,a_3\,\alpha\beta^3 \\ & +30\,a_1\,a_3\,\alpha\beta^3 + 11\,{a_2}^2\,\alpha\beta^3 + 33\,a_1\,a_2\,\alpha\beta^3 + 12\,{a_1}^2\,\alpha\beta^3 + 12\,\alpha^3\,b_4\beta^2 \\ & +2\,\alpha^3\,b_3\beta^2 + 12\,\alpha^3\,b_2\beta^2 - 8\,{a_3}^2\,\alpha^2\beta^2 - 32\,a_2\,a_3\,\alpha^2\beta^2 - 12\,a_1\,a_3\,\alpha^2\beta^2 \\ & -14\,{a_2}^2\,\alpha^2\beta^2 - 18\,a_1\,a_2\,\alpha^2\beta^2 - 8\,\alpha^4\,b_3\beta - 8\,{a_3}^2\,\alpha^3\beta + 8\,a_2\,a_3\,\alpha^3\beta \\ & +4\,{a_2}^2\,\alpha^3\beta + 8\,a_2\,a_3\,\alpha^4 \end{aligned} \tag{3.46}$$

and

$$
\begin{aligned}
Q_1 \;=\;& 15\,b_4\beta^6 + 5\,b_2\beta^6 + 3\,\alpha\,b_4\beta^5 - 15\,\alpha\,b_3\beta^5 + \alpha\,b_2\beta^5 \\
& -15\,\alpha\,b_1\beta^5 - 22\,{a_3}^2\beta^5 - 7\,a_2\,a_3\beta^5 - 14\,a_1\,a_3\beta^5 - 3\,{a_2}^2\beta^5 \\
& -7\,a_1\,a_2\beta^5 - 4\,{a_1}^2\beta^5 - 12\,\alpha^2\,b_4\beta^4 - 3\,\alpha^2\,b_3\beta^4 + 6\,\alpha^2\,b_2\beta^4 \\
& -3\,\alpha^2\,b_1\beta^4 + 12\,{a_3}^2\,\alpha\beta^4 + 37\,a_2\,a_3\,\alpha\beta^4 + 30\,a_1\,a_3\,\alpha\beta^4 \\
& +7\,{a_2}^2\,\alpha\beta^4 + 19\,a_1\,a_2\,\alpha\beta^4 + 18\,{a_1}^2\,\alpha\beta^4 + 12\,\alpha^3\,b_3\beta^3 \\
& +2\,\alpha^3\,b_2\beta^3 + 12\,\alpha^3\,b_1\beta^3 + 4\,{a_3}^2\,\alpha^2\beta^3 - 20\,a_2\,a_3\,\alpha^2\beta^3 \\
& -16\,a_1\,a_3\,\alpha^2\beta^3 - 12\,{a_2}^2\,\alpha^2\beta^3 - 26\,a_1\,a_2\,\alpha^2\beta^3 - 8\,{a_1}^2\,\alpha^2\beta^3 \\
& -8\,\alpha^4\,b_2\beta^2 - 4\,a_2\,a_3\,\alpha^3\beta^2 + 8\,{a_2}^2\,\alpha^3\beta^2 + 8\,a_1\,a_2\,\alpha^3\beta^2
\end{aligned}
\tag{3.47}
$$

In Eq.(3.44), A is real so that $A^2 > 0$, which means that μ must have the same sign as $\frac{P}{Q}$. Also, note that $A = \epsilon\hat{A}$ from Eqs.(3.24),(3.29),(3.41), and $\mu = \epsilon^2\hat{\mu}$ from Eq.(3.30). Thus, the perturbation method gives $\hat{A}^2$ as a function of $\hat{\mu}$, but multiplication by ϵ^2 converts to a relation between A^2 and μ.

We point out that Eq.(3.44) is the Hopf bifurcation formula for first order DDEs. Although the idea of using Lindstedt's method on bifurcation problems for DDEs goes back to a 1980 paper by Casal and Freedman [13], their work provided the algorithm but not the Hopf bifurcation formula. Thus our computational study [83] was the first to provide such formula, and it is hoped that having a general expression for the Hopf bifurcation will be a convenience for researchers in the field of DDEs.

3.7 Example 2

As an example, we consider the following DDE:

$$\frac{dx}{dt} = -x - 2x_d - xx_d - x^3 \tag{3.48}$$

This corresponds to the following parameter assignment in Eq.(3.20):

$$\alpha = -1,\ \beta = -2,\ a_1 = a_3 = b_2 = b_3 = b_4 = 0,\ a_2 = b_1 = -1 \tag{3.49}$$

The associated linearized equation (3.21) is stable for zero delay. As the delay T is increased, the origin first becomes unstable when $T = T_{cr}$, where Eq.(3.27) gives that

$$T_{cr} = \frac{\arccos\left(\frac{-1}{2}\right)}{\sqrt{3}} = \frac{2\pi}{3\sqrt{3}} \tag{3.50}$$

Substituting (3.49) and (3.50) into (3.44)-(3.47), we obtain:

$$A^2 = \frac{648\mu}{40\sqrt{3}\pi + 171} = 1.667\mu \tag{3.51}$$

where we have set

$$T = T_{cr} + \mu = \frac{2\pi}{3\sqrt{3}} + \mu = 1.2092 + \mu \tag{3.52}$$

Thus the origin is stable for $\mu < 0$ and unstable for $\mu > 0$. In order for A^2 in (3.51) to be positive, we require that $\mu > 0$. Therefore the limit cycle is born out of an unstable equilibrium point. Since the stability of the limit cycle must be the opposite of the stability of the equilibrium point from which it is born, we may conclude that the limit cycle is stable and that we have a *supercritical* Hopf. This result is in agreement with numerical integration of Eq.(3.48).

3.8 Example 3

As a second example, we consider the case in which the quantity Q in Eqs.(3.44)-(3.47) is zero. In the context of the ODE system (3.15),(3.16) this case corresponds to S=0 in Eq.(3.18) and has been discussed in [39], Section 7.1. To generate such an example for the DDE (3.20), we embed the previous example in a one-parameter family of DDE's:

$$\frac{dx}{dt} = -x - 2x_d - xx_d - \lambda x^3 \tag{3.53}$$

and we choose λ so that Q=0 in Eq.(3.44). This leads to the following critical value of λ:

$$\lambda = \lambda_{cr} = \frac{4\pi + 3\sqrt{3}}{18(2\pi + 3\sqrt{3})} = 0.0859 \tag{3.54}$$

Since this choice for λ leads to Q=0, Eq.(3.44) obviously cannot be used to find the limit cycle amplitude A. Instead we use Lindstedt's method, maintaining terms of $O(\epsilon^4)$. The correct scalings in this case turn out to be (cf.Eqs.(3.30) and (3.33)):

$$T = T_{cr} + \mu = \frac{2\pi}{3\sqrt{3}} + \epsilon^4\hat{\mu} \tag{3.55}$$

$$\Omega = \omega + \epsilon^2 k_2 + \epsilon^4 k_4 + \cdots \tag{3.56}$$

We find that the limit cycle amplitude A satisfies the equation:

$$A^4 = -\Gamma\mu \tag{3.57}$$

where we omit the closed form expression for Γ and give instead its approximate value, Γ=620.477.

The analysis of this example has assumed that the parameter λ exactly takes on the critical value given in Eq.(3.54). Let us consider a more robust model which allows λ to be detuned:

$$\lambda = \lambda_{cr} + \Lambda = \frac{4\pi + 3\sqrt{3}}{18(2\pi + 3\sqrt{3})} + \epsilon^2 \hat{\Lambda} \tag{3.58}$$

Using Lindstedt's method we obtain for this case the following equation on A:

$$A^4 + \sigma\Lambda A^2 + \Gamma\mu = 0 \tag{3.59}$$

where we omit the closed form expression for σ and give instead its approximate value, σ=342.689. Eq.(3.59) can have 0,1, or 2 positive real roots for A, each of which is a limit cycle in the original system. Thus the number of limit cycles which are born in the Hopf bifurcation depends on the detuning coefficients Λ and μ. Elementary use of the quadratic formula and the requirement that A^2 be both real and positive gives the following results: If $\mu < 0$ then there is one limit cycle. If $\mu > 0$ and $\sigma\Lambda < -2\sqrt{\Gamma\mu}$ then there are two limit cycles. If $\mu > 0$ and $\sigma\Lambda > -2\sqrt{\Gamma\mu}$ then there are no limit cycles.

3.9 Discussion

This chapter presents some of the basic linear and nonlinear properties of DDEs. In example 1 we found an explicit formula for determining the radius of a limit cycle which is born in a Hopf bifurcation in a class of first order constant coefficient DDEs. The derivation is accomplished using Lindstedt's perturbation method. Example 2 is a particular case of example 1 (with a user friendly DDE) which is used to exhibit the usefulness of Eqs.(3.44)-(3.47). Example 3 presents an example where Eq.(3.44) cannot be used to determine the radius of the limit cycle. By including higher order terms and rescaling the system, we were able to present the new regions where the limit cycle exists.

The idea of using Lindstedt's method on bifurcation problems for DDEs goes back to a 1980 paper by Casal and Freedman [13]. That work provided the algorithm but not the Hopf bifurcation formula. It is hoped that having a general expression for the Hopf bifurcation, as in Eqs.(3.44)-(3.47), will be a convenience for researchers in the field of DDEs.

Another interesting feature about Lindstedt's method is that although it is a formal perturbation method, i.e., lacking a proof of convergence, we will see in the following chapters that it gives the same results as the center manifold approach (which is difficult to understand but has a much more rigorous mathematical foundation). The center manifold approach has been described in many places, for example [45, 11, 95, 56, 81], but it has not become widely used due to its complicated and highly technical computational nature. Thus the main advantage of the Hopf calculation using Lindstedt's method is that it is simpler to understand and easier to execute than the center manifold approach.

CHAPTER 4

SINGLE GENE MODEL

4.1 Introduction

This chapter deals with a beautiful mathematical model of gene expression. The model was first studied by Monk in [72], where he gives some very interesting biological consequences and compares his numerical findings with previous experimental results. The main motivation to study this particular model, comes from its connection to the fields of delay differential equations and gene networks.

We start by explaining the biology behind the model: A gene, i.e. a section of the DNA molecule, is copied (*transcribed*) onto messenger RNA (mRNA), which diffuses out of the nucleus of the cell into the cytoplasm, where it enters a subcellular structure called a ribosome. The genetic code is then read by the ribosome, which yields a final product in the form of a protein (this process is called *translation*). For this particular model, the protein then diffuses back into the nucleus where it represses the transcription of its own gene.

Dynamically speaking, this process may result in a steady state equilibrium, in which the concentrations of mRNA and protein are constant, or it may result in an oscillation. Oscillations in biological systems with delay have been dealt with previously [64, 65, 70]. Mahaffy [64] studied a system in which concentrations of mRNA and cell repressor are analyzed by varying several parameters, such as diffusivity and cell radii. Delay is introduced into the system and the model is linearized to find stability changes and associated critical delays

which give rise to Hopf bifurcations. In a later study, Mahaffy et al [65] investigated a transport mechanism in cells to obtain nutrients. Their model examined how the change in diffusivities and cell radii caused biochemical oscillatory responses in the concentrations of the nutrients. Their model was reduced to a system of DDEs and stability analysis was used to show that the system can undergo Hopf bifurcations for certain parameter values. In a more recent study, Mocek et al [70] studied biochemical systems with delay. They approximated the DDE system with an ODE system by means of characterizing critical delays.

In all of the above studies, the presence of Hopf bifurcations was indicated by the existence of a periodic solution of the associated linearized system. Thus, although they present interesting numerical results, in this chapter we go beyond the linearized equations by considering nonlinear terms in our analysis. By taking into account nonlinear effects we were able to predict the stability, amplitude, and frequency of the resulting limit cycle, and show that the transition between equilibrium and oscillation is a Hopf bifurcation.

The model takes the form of two equations, one an ordinary differential equation (ODE) and the other a delayed differential equation (DDE). The delay is due to an observed time lag in the transcription process. The time dependent variables are $M(t)$, which represents the concentration of mRNA, and $P(t)$, which represents the concentration of the associated protein repressor:

$$\dot{M} = \alpha_m \left(\frac{1}{1 + \left(\frac{P}{P_0}\right)^n} \right) - \mu_m M \tag{4.1}$$

$$\dot{P} = \alpha_p M - \mu_p P \tag{4.2}$$

where dots represent differentiation with respect to time t, and where the model constants are given as in [72]: α_m is the rate at which mRNA is transcribed in the absence of the associated protein, α_p is the rate at which the protein is produced

from mRNA in the ribosome, μ_m and μ_p are the rates of degradation of mRNA and of protein, respectively, P_0 is a reference concentration of protein, and n is a parameter.

As stated above, and confirmed by laboratory experiments, it has been observed that the dynamics of the gene copying process sometimes results in a steady state equilibrium and others in an oscillation. However, it is easy to see that the system (4.1) and (4.2) cannot support oscillations, as follows: Differentiating (4.2) and substituting (4.1) into the result gives the second order equation:

$$\ddot{P} + (\mu_m + \mu_p)\dot{P} + F(P) \;=\; 0 \tag{4.3}$$

where

$$F(P) \;=\; \mu_m\mu_p P - \frac{\alpha_m\alpha_p}{1 + \left(\frac{P}{P_0}\right)^n} \tag{4.4}$$

Eq.(4.3) is a linearly damped oscillator with nonlinear conservative restoring force F and as such cannot oscillate.

A natural question arises as to how the model (4.1)-(4.2) can be changed to be more realistic so that it will oscillate. One possibility involves coupling a series of such systems together. For example, Elowitz and Leibler [30] have shown that three such systems (a "repressilator") can be coupled in such a way as to exhibit a periodic motion. Another approach involves introducing delay into the model.

Sources of the delay include the time required for transcription and translation to occur (see Chapter 2). Monk [72] states that transcription has an average delay time of about 10-20 min while translation delays are about 1-3 min. He

very cleverly posits the following delayed version of Eqs.(4.1), (4.2):

$$\dot{M} = \alpha_m \left(\frac{1}{1 + \left(\frac{P_d}{P_0}\right)^n} \right) - \mu_m M \tag{4.5}$$

$$\dot{P} = \alpha_p M - \mu_p P \tag{4.6}$$

where the subscript d denotes a variable which is delayed by time T, that is, $P_d = P(t - T)$. In [73] it is shown that (4.5),(4.6) are equivalent to a system which contains both transcriptional and translational delays.

4.2 Stability of Equilibrium

We begin by rescaling Eqs.(4.1) and (4.2). We set $m = \frac{M}{\alpha_m}$, $p = \frac{P}{\alpha_m \alpha_p}$, and $p_0 = \frac{P_0}{\alpha_m \alpha_p}$, giving:

$$\dot{m} = \frac{1}{1 + \left(\frac{p_d}{p_0}\right)^n} - \mu m \tag{4.7}$$

$$\dot{p} = m - \mu p \tag{4.8}$$

Equilibrium points, (m^*, p^*), for (4.7) and (4.8) are found by setting $\dot{m} = 0$ and $\dot{p} = 0$

$$\mu m^* = \frac{1}{1 + \left(\frac{p^*}{p_0}\right)^n} \tag{4.9}$$

$$m^* = \mu p^* \tag{4.10}$$

Eliminating m^* from Eqs. (4.9) and (4.10), we obtain an equation on p^*:

$$(p^*)^{n+1} + p_0^n p^* - \frac{p_0^n}{\mu^2} = 0. \tag{4.11}$$

Next we define ξ and η to be deviations from equilibrium: ξ=$\xi(t)$=$m(t)$-m^*, η=$\eta(t)$=$p(t)$-p^*, and η_d=$\eta(t$-$T)$. This results in the nonlinear system:

$$\dot{\xi} = \frac{1}{1 + \left(\frac{\eta_d + p^*}{p_0}\right)^n} - \mu(m^* + \xi) \tag{4.12}$$

$$\dot{\eta} = \xi - \mu\eta \tag{4.13}$$

Expanding for small values of η_d, eq.(4.12) becomes:

$$\dot{\xi} = -\mu\xi - K\,\eta_d + H_2\,\eta_d^2 + H_3\,\eta_d^3 + \cdots \tag{4.14}$$

where K, H_2 and H_3 depend on p^*, p_0, and n as follows:

$$K = \frac{n\beta}{p^*(1+\beta)^2}, \quad \text{where} \quad \beta = \left(\frac{p^*}{p_0}\right)^n \tag{4.15}$$

$$H_2 = \frac{\beta\, n\, (\beta\, n - n + \beta + 1)}{2\,(\beta+1)^3\; p^{*2}} \tag{4.16}$$

$$H_3 = -\frac{\beta\, n\left(\beta^2\, n^2 - 4\,\beta\, n^2 + n^2 + 3\,\beta^2\, n - 3\, n + 2\,\beta^2 + 4\,\beta + 2\right)}{6\,(\beta+1)^4\; p^{*3}} \tag{4.17}$$

Next we analyze the linearized system coming from Eqs.(4.14) and (4.13):

$$\dot{\xi} = -\mu\,\xi - K\,\eta_d \tag{4.18}$$

$$\dot{\eta} = \xi - \mu\,\eta \tag{4.19}$$

Stability analysis of Eqs. (4.18) and (4.19) shows that for T=0 (no delay), the equilibrium point (m^*, p^*) is a stable spiral. Increasing the delay, T, in the linear system (4.18)-(4.19), will yield a critical delay, T_{cr}, such that for $T>T_{cr}$, (m^*, p^*) will be unstable, giving rise to a Hopf bifurcation. For $T=T_{cr}$ the system (4.18)-(4.19) will exhibit a pair of pure imaginary eigenvalues $\pm\omega i$ corresponding to the solution

$$\xi(t) = B\cos(\omega t + \phi) \tag{4.20}$$

$$\eta(t) = A\cos\omega t \tag{4.21}$$

where A and B are the amplitudes of the $\eta(t)$ and $\xi(t)$ oscillations, and where ϕ is a phase angle. Note that we have chosen the phase of $\eta(t)$ to be zero without loss of generality. Then for values of delay T close to T_{cr},

$$T = T_{cr} + \Delta \tag{4.22}$$

the nonlinear system (4.7)-(4.8) is expected to exhibit a periodic solution (a limit cycle) which can be written in the approximate form of Eqs.(4.20) and (4.21). Substituting Eqs.(4.20) and (4.21) into Eqs.(4.18) and (4.19) and solving for ω and T_{cr} we obtain

$$\omega = \sqrt{K-\mu^2} \tag{4.23}$$

$$T_{cr} = \frac{\arctan\left(\frac{2\mu\sqrt{K-\mu^2}}{K-2\mu^2}\right)}{\sqrt{K-\mu^2}} \tag{4.24}$$

where we have used the trig identities

$$\sin(\omega T_{cr}) = -\frac{2\mu\sqrt{K-\mu^2}}{K} \tag{4.25}$$

$$\cos(\omega T_{cr}) = \frac{2\mu^2}{K} - 1 \tag{4.26}$$

4.3 Lindstedt's Method

In this section we will use Lindstedt's perturbation method [81, 108] on Eqs.(4.14) and (4.13) to find an approximate expressions for the limit cycle amplitude and frequency of oscillation. We begin by changing the first order system into a second order DDE. This results in the following form

$$\ddot{\eta} + 2\mu\dot{\eta} + \mu^2\eta = -K\eta_d + H_2\eta_d^2 + H_3\eta_d^3 + \cdots \tag{4.27}$$

where K, H_2 and H_3 are defined by Eqs.(4.15)-(4.17). Next we introduce a small parameter ϵ via the scaling

$$\eta = \epsilon u \tag{4.28}$$

The detuning Δ of Eq. (4.22) is scaled like ϵ^2, $\Delta = \epsilon^2\delta$:

$$T = T_{cr} + \Delta = T_{cr} + \epsilon^2\delta \tag{4.29}$$

Next we stretch time by replacing the independent variable t by τ, where

$$\tau = \Omega\, t \tag{4.30}$$

and substitute Eqs.(4.28) and (4.30) into Eq.(4.27) to get

$$\Omega^2 \frac{d^2u}{d\tau^2} + 2\,\mu\,\Omega \frac{du}{d\tau} + \mu^2\, u = -K\, u_d + \epsilon\, H_2\, u_d^2 + \epsilon^2\, H_3\, u_d^3 \tag{4.31}$$

where $u_d = u(\tau - \Omega\, T)$. We expand Ω in a power series in ϵ, omitting the $O(\epsilon)$ for convenience, since it turns out to be zero:

$$\Omega = \omega + \epsilon^2 k_2 + \ldots \tag{4.32}$$

Next we expand the delay term u_d for small ϵ

$$\begin{aligned} u_d = u(\tau - \Omega T) &= u(\tau - (\omega + \epsilon^2 k_2 + \ldots)(T_{cr} + \epsilon^2 \delta)) && (4.33)\\ &= u(\tau - \omega T_{cr} - \epsilon^2 (k_2 T_{cr} + \omega\delta) + \ldots) && (4.34)\\ &= u(\tau - \omega T_{cr}) - \epsilon^2 (k_2 T_{cr} + \omega\delta) u'(\tau - \omega T_{cr}) + O(\epsilon^3) && (4.35) \end{aligned}$$

and expand $u(\tau)$ in a power series in ϵ:

$$u(\tau) = u_0(\tau) + \epsilon u_1(\tau) + \epsilon^2 u_2(\tau) + \ldots \tag{4.36}$$

Substituting Eqs.(4.32)-(4.36) into (4.31) and collecting ϵ-like terms gives

$$\begin{aligned} \omega^2 \frac{d^2u_0}{d\tau^2} + 2\mu\omega \frac{du_0}{d\tau} + K u_0(\tau - \omega T_{cr}) + \mu^2 u_0 &= 0 && (4.37)\\ \omega^2 \frac{d^2u_1}{d\tau^2} + 2\mu\omega \frac{du_1}{d\tau} + K u_1(\tau - \omega T_{cr}) + \mu^2 u_1 &= H_2 u_0^2(\tau - \omega T_{cr}) && (4.38)\\ \omega^2 \frac{d^2u_2}{d\tau^2} + 2\mu\omega \frac{du_2}{d\tau} + K u_2(\tau - \omega T_{cr}) + \mu^2 u_2 &= \ldots && (4.39) \end{aligned}$$

where $\ldots$ stands for terms in u_0 and u_1, omitted here for brevity. We take the solution of the u_0 equation as:

$$u_0(\tau) = \hat{A} \cos\tau \tag{4.40}$$

where from Eqs.(4.21) and (4.28) we know $A = \hat{A}\epsilon$. Next we substitute (4.40) into (4.38) and obtain the following expression for u_1:

$$u_1(\tau) = m_1 \sin 2\tau + m_2 \cos 2\tau + m_3 \tag{4.41}$$

where m_1 is given by the equation:

$$m_1 = -\frac{2\,\hat{A}^2\,H_2\,\mu\,\sqrt{K-\mu^2}\,\left(\mu^2-K\right)\left(2\,\mu^2-3\,K\right)}{K\,\left(16\,\mu^6-39\,K\,\mu^4+18\,K^2\,\mu^2+9\,K^3\right)} \tag{4.42}$$

and where m_2 and m_3 are given by similar equations, omitted here for brevity. We substitute Eqs.(4.40) and (4.41) into (4.39), and, after trigonometric simplifications have been performed, we equate to zero the coefficients of the resonant terms $\sin\tau$ and $\cos\tau$. This yields the amplitude, A, of the limit cycle that was born in the Hopf bifurcation:

$$A^2 = \frac{P}{Q}\,\Delta \tag{4.43}$$

where

$$P = -8\,K^2\,\left(\mu^2-K\right)\left(\mu^2+K\right)\left(16\,\mu^6-39\,K\,\mu^4+18\,K^2\,\mu^2+9\,K^3\right) \tag{4.44}$$

$$Q = Q_0\,T_{cr} + Q_1 \tag{4.45}$$

and

$$\begin{aligned} Q_0 = {} & 48\,\mathrm{H}_3\,K^2\,\mu^8+16\,{\mathrm{H}_2}^2\,K\,\mu^8-69\,\mathrm{H}_3\,K^3\,\mu^6+32\,{\mathrm{H}_2}^2\,K^2\,\mu^6-63\,\mathrm{H}_3\,K^4\,\mu^4 \\ & -162\,{\mathrm{H}_2}^2\,K^3\,\mu^4+81\,\mathrm{H}_3\,K^5\,\mu^2+108\,{\mathrm{H}_2}^2\,K^4\,\mu^2+27\,\mathrm{H}_3\,K^6+30\,{\mathrm{H}_2}^2\,K^5 \end{aligned} \tag{4.46}$$

$$\begin{aligned} Q_1 = {} & 96\,\mathrm{H}_3\,K\,\mu^9+64\,{\mathrm{H}_2}^2\,\mu^9-138\,\mathrm{H}_3\,K^2\,\mu^7-16\,{\mathrm{H}_2}^2\,K\,\mu^7-126\,\mathrm{H}_3\,K^3\,\mu^5 \\ & -308\,{\mathrm{H}_2}^2\,K^2\,\mu^5+162\,\mathrm{H}_3\,K^4\,\mu^3+296\,{\mathrm{H}_2}^2\,K^3\,\mu^3+54\,\mathrm{H}_3\,K^5\,\mu+12\,{\mathrm{H}_2}^2\,K^4\,\mu \end{aligned} \tag{4.47}$$

Eq. (4.45) depends on μ, K, H_2, H_3, and T_{cr}. By using Eq. (4.24) we may express (4.45) as a function of μ, K, H_2, and H_3 only. Removal of secular terms also yields

a value for the frequency shift k_2, where, from Eq.(4.32), we have $\Omega = \omega + \epsilon^2 k_2$:

$$k_2 = -\frac{R}{Q}\,\delta \tag{4.48}$$

where Q is given by (4.45) and

$$R = \sqrt{K - \mu^2}\; Q_0 \tag{4.49}$$

An expression for the amplitude B of the periodic solution for $\xi(t)$ (see Eq.(4.20)) may be obtained directly from Eq.(4.13) by writing $\xi = \dot{\eta} + \mu\eta$, where $\eta \sim A\cos\omega t$. We find:

$$B = \sqrt{K}A \tag{4.50}$$

where K and A are given as in (4.15) and (4.43) respectively.

4.3.1 Numerical Example

Using the same parameter values as in [72]

$$\mu = 0.03/\text{min}\,,\;\; p_0 = 100\,,\;\; n = 5 \tag{4.51}$$

we obtain

$$p^* = 145.9158\,,\;\; m^* = 4.3774 \tag{4.52}$$

$$K = 3.9089 \times 10^{-3}\,,\;\; H_2 = 6.2778 \times 10^{-5}\,,\;\; H_3 = -6.4101 \times 10^{-7} \tag{4.53}$$

$$T_{cr} = 18.2470\,,\;\; w = 5.4854 \times 10^{-2}\,,\;\; \frac{2\pi}{w} = 114.5432 \tag{4.54}$$

Here the delay T_{cr} and the response period $2\pi/\omega$ are given in minutes. Substituting (4.52)-(4.54) into (4.43)-(4.50) yields the following equations:

$$A = 27.0215\;\sqrt{\Delta} \tag{4.55}$$

$$k_2 = -2.4512 \times 10^{-3}\;\delta \tag{4.56}$$

$$B = 1.6894\;\sqrt{\Delta} \tag{4.57}$$

Note that since Eq. (4.55) requires $\Delta > 0$ for the limit cycle to exist, and since we saw in Eqs. (4.18) and (4.19) that the origin is unstable for $T > T_{cr}$, i.e. for $\Delta > 0$, we may conclude that the Hopf bifurcation is supercritical, i.e., the limit cycle is stable.

We may also multiply Eq.(4.56) by ϵ^2 and substitute it into (4.32) to find

$$\Omega = 5.4854 \times 10^{-2} - 2.4512 \times 10^{-3} \Delta \tag{4.58}$$

where $\Delta = T - T_{cr} = T - 18.2470$. Plotting the period, $\frac{2\pi}{\Omega}$, against the delay, T, yields the graph shown in Figure 4.1. These results are in agreement with those obtained by numerical integration of the original Eqs.(4.1) and (4.2) and with those presented in [72].

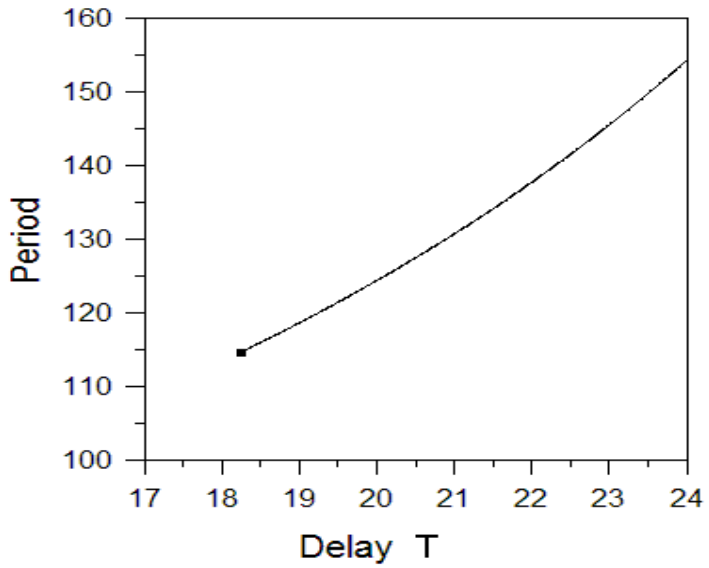

Figure 4.1: Period of oscillation, $\frac{2\pi}{\Omega}$, plotted as a function of delay T, where Ω is given by Eq.(4.58). The initiation of oscillation at $T = T_{cr} = 18.2470$ is due to a supercritical Hopf bifurcation, and is marked in the figure with a dot.

4.3.2 Effect of Changing Parameters

An advantage of the closed form approximate solutions presented in the previous analysis is that the effect of changes in parameters may be easily studied. In this section we present a few results obtained from our solution.

The equilibrium concentration p^* is determined by solving Eq.(4.11) for given values of μ, p_0 and n. Figure 4.2 shows p^* displayed as a function of μ for p_0= 10, 50, 100 and 200. Here and in the following plots we follow [72] and take $n = 5$.

We note from Eq.(4.24) that the quantity $K - 2\mu^2$ must be non-negative in order that $T_{cr} > 0$, that is in order that parameters corresponding to the Hopf bifurcation occur in a *delay* equation (if $T_{cr} < 0$ then we would have a *future* equation, which is physically unreasonable). Figure 4.3 shows that this condition restricts the values of degradation rate μ for a given value of reference concentration p_0. For values of μ which are greater than this critical value $\mu_{critical}$, the system will not exhibit a Hopf bifurcation and no oscillation will result.

From Eq.(4.43) we see that the amplitude A of protein oscillation is the product of $\sqrt{\frac{P}{Q}}$ and $\sqrt{\Delta}$. Figure 4.4 displays $\sqrt{\frac{P}{Q}}$ as a function of μ for p_0= 10, 50, 100 and 200 and for n=5. Note that the maximum permissible value of μ depends on p_0 as shown in Figure 4.3.

Eqs.(4.32),(4.48),(4.49),(4.23) and (4.29) give that $\Omega = \omega(1 - \frac{Q_0}{Q}\Delta)$ where Ω is the frequency of oscillation for delay $T = T_{cr} + \Delta$, and ω is the frequency of oscillation for delay $T = T_{cr}$. Figure 4.5 displays $\frac{Q_0}{Q}$ as a function of μ for p_0= 10, 50, 100 and 200 and for n=5. Note again that the maximum permissible value of μ depends on p_0 as shown in Figure 4.3.

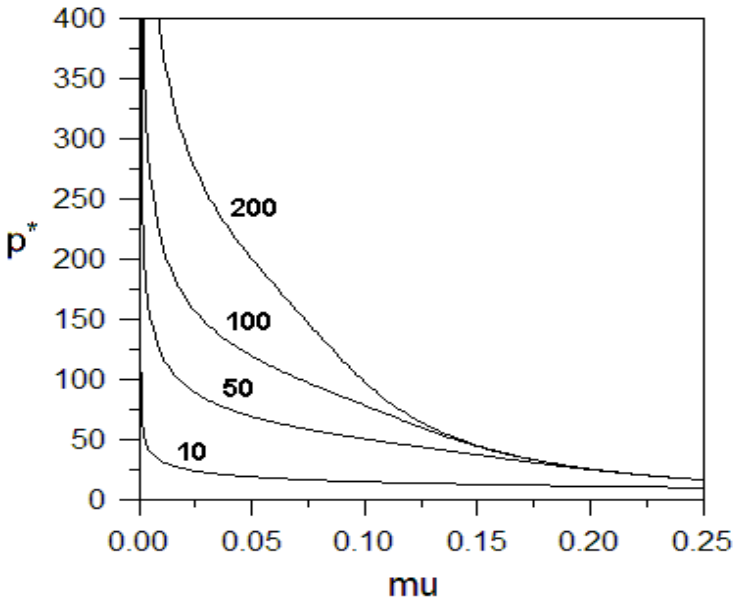

Figure 4.2: The equilibrium concentration p^* displayed as a function of μ for p_0= 10, 50, 100 and 200 and for n=5.

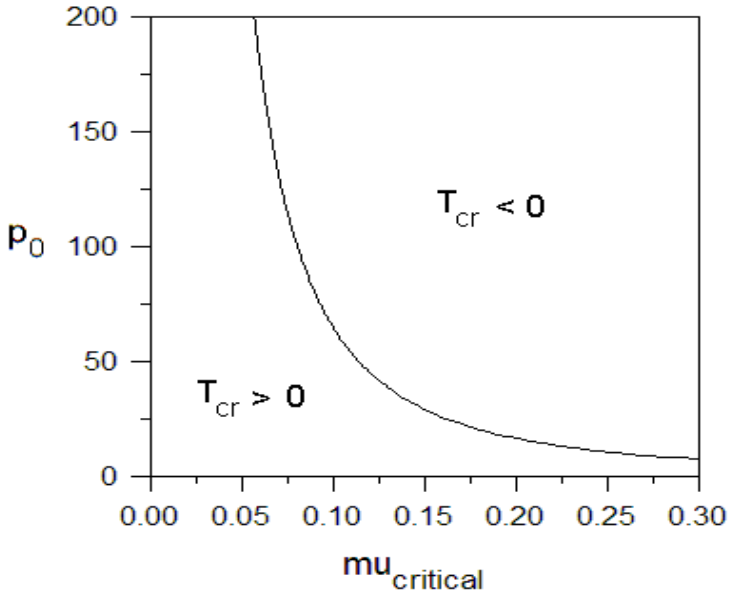

Figure 4.3: Values of degradation rate μ which are greater than $\mu_{critical}$ correspond to negative values of T_{cr} and will prevent the system from oscillating. Here $\mu_{critical}$ is shown to depend on the reference concentration p_0.

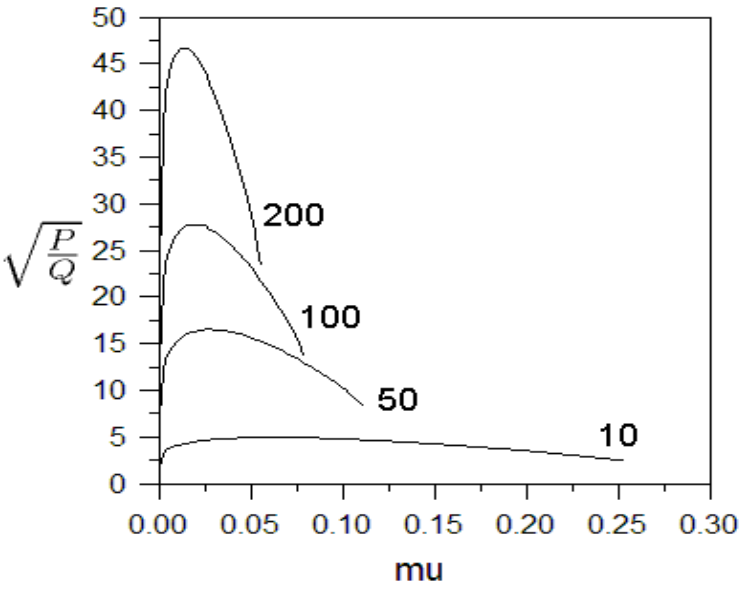

Figure 4.4: Eq.(4.43) shows that the amplitude A of protein oscillation is the product of $\sqrt{\frac{P}{Q}}$ and $\sqrt{\Delta}$. Here $\sqrt{\frac{P}{Q}}$ is displayed as a function of μ for p_0= 10, 50, 100 and 200 and for n=5.

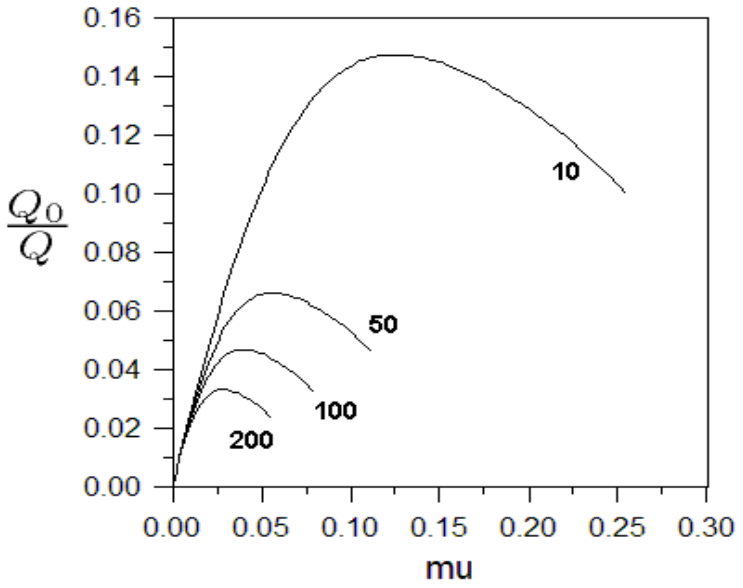

Figure 4.5: Our solution gives that $\Omega = \omega(1-\frac{Q_0}{Q}\Delta)$ where Ω is the frequency of oscillation for delay $T = T_{cr} + \Delta$ and ω is the frequency of oscillation for delay $T = T_{cr}$. Here $\frac{Q_0}{Q}$ is displayed as a function of μ for p_0= 10, 50, 100 and 200 and for n=5.

4.4 Center Manifold Analysis

The present section complements the previous by providing a center manifold analysis (CMA). The advantage of the CMA is two-fold. First, it can be used, together with an asymptotic method such as averaging, to provide approximations of general motions, including the *approach* to a periodic motion, in contrast to Lindstedt's method, which approximates only the periodic motion itself. Second, the CMA is based on theorems [14] which place the results on a valid mathematical basis, in contrast to the strictly formal asymptotic analysis of Lindstedt's method.

The idea of the CMA is to reduce the DDE system, which is infinite dimensional, to a two dimensional system by projecting the original dynamics onto the eigenvectors corresponding to purely imaginary eigenvalues. The center manifold is a two dimensional surface which is tangent to a two dimensional plane (called the center subspace) which is generated by those two eigenvectors (see Figure 4.6). The center manifold theorem (not proved here, cf.Figure 3.7 in [28]) guarantees the existence of a *curved* two dimensional subspace (the center manifold) which is tangent to the *flat* center subspace spanned by the eigenvectors corresponding to those eigenvalues with zero real part. All solutions starting sufficiently close to the equilibrium point will tend asymptotically towards the center manifold. The stability of the equilibrium point in the full nonlinear equations will be the same as its stability in the flow on the center manifold. Also, any bifurcations which occur in the neighborhood of the equilibrium point on the center manifold are guaranteed to also occur in the full nonlinear system. In particular, if a limit cycle is born on the center manifold, then it will also be born in the full system.

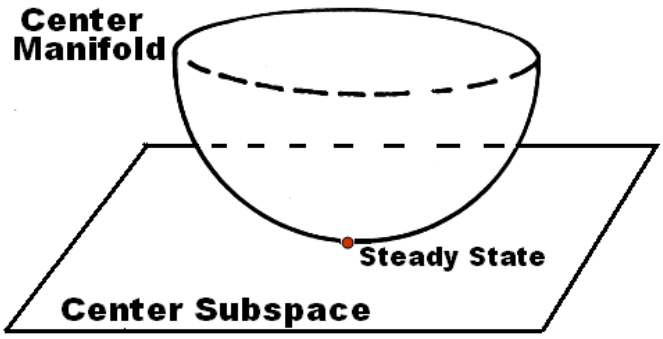

Figure 4.6: Geometric representation of the center manifold and center subspace.

In order to accomplish the above, the DDE is reformulated as an evolution equation on a function space. The idea here is that the initial condition for the DDE consists of a function defined on $-T \leq t \leq 0$. As t increases from zero we may consider the piece of the solution lying in the time interval $[-T + t, t]$ as having evolved from the initial condition function. In order to avoid confusion, the variable θ is used to identify a point in the interval $[-T, 0]$, whereupon $x(t + \theta)$ will represent the piece of the solution which has evolved from the initial condition function at time t. See Figure 4.7. Thus from the point of view of the function space, t is a parameter, and it is θ which is the independent variable. To emphasize this, we write:

$$x_t(\theta) = x(t + \theta) \tag{4.59}$$

Before we begin the center manifold analysis, we transform the DDE system given by (4.13) and (4.14) into an operator differential equation which acts on a function space consisting of continuously differentiable functions on $[-T, 0]$ (for an extensive overview see [45, 95, 11, 56, 77, 81]):

$$\dot{x}_t = Ax_t + F(x_t) \tag{4.60}$$

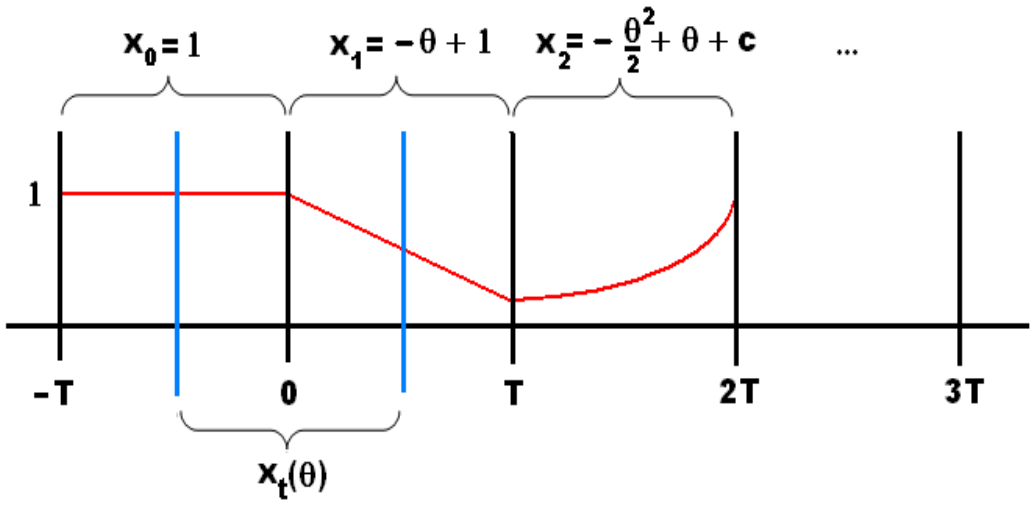

Figure 4.7: Notice that now $\theta \in [-T, 0]$ is considered as the independent variable. From the point of view of the function space t is a parameter.

where the column vector x_t, the linear operator A, and the nonlinear operator F are defined as follows:

$$x_t(\theta) = \begin{pmatrix} \xi_t \\ \eta_t \end{pmatrix}(\theta) \tag{4.61}$$

$$Ax_t(\theta) = \begin{cases} \frac{d}{d\theta}x_t(\theta), & \theta \in [-T_{cr}, 0) \\ Lx_t(0) + Mx_t(-T_{cr}), & \theta = 0 \end{cases} \tag{4.62}$$

$$F(x_t)(\theta) = \begin{cases} 0, & \theta \in [-T_{cr}, 0) \\ f\Big(x_t(0), x_t(-T_{cr})\Big), & \theta = 0 \end{cases} \tag{4.63}$$

The matrix L in Eq.(4.62) is associated with the linear nondelayed terms of Eqs.(4.13) and (4.14). Similarly M is associated with the linear delayed terms. In Eq.(4.63) f is associated with the nonlinear terms of (4.13)-(4.14). Thus for this system L, M, and f become

$$L = \begin{pmatrix} -\mu & 0 \\ 1 & -\mu \end{pmatrix} \tag{4.64}$$

$$M = \begin{pmatrix} 0 & -K \\ 0 & 0 \end{pmatrix} \tag{4.65}$$

$$f\Big(x_t(0), x_t(-T_{cr})\Big) = \begin{pmatrix} H_2\eta_t(-T_{cr})^2 + H_3\eta_t(-T_{cr})^3 \\ 0 \end{pmatrix} \tag{4.66}$$

Note that the original DDE system (4.13)-(4.14) appears as a boundary condition at $\theta = 0$. The flow on the rest of the interval is based on the identity $\frac{\partial x_t(\theta)}{\partial t} = \frac{\partial x_t(\theta)}{\partial \theta}$, which follows from Eq.(4.59).

The last piece of information we need is T_{cr}. As before, T_{cr} represents the value of the delay T such that the characteristic equation of (4.13)-(4.14) has a pair of pure imaginary roots $\pm i\omega$. From our previous linear stability in Section 4.2 we have that Eqs.(4.24),(4.23) give the critical delay and critical frequency:

$$\begin{aligned} T_{cr} &= \frac{\arctan\left(\frac{2\mu\sqrt{K-\mu^2}}{K-2\mu^2}\right)}{\sqrt{K-\mu^2}} \\ \omega &= \sqrt{K-\mu^2} \end{aligned}$$

4.4.1 Local Approximation

The center manifold reduction is based on the idea of writing the solution x_t as the sum of vectors lying in the center subspace spanned by the eigenvectors s_1 and s_2 corresponding to the eigenvalues $\pm i\omega$, and the rest of the solution, w, which does not lie in the center subspace. See Figure 4.8.

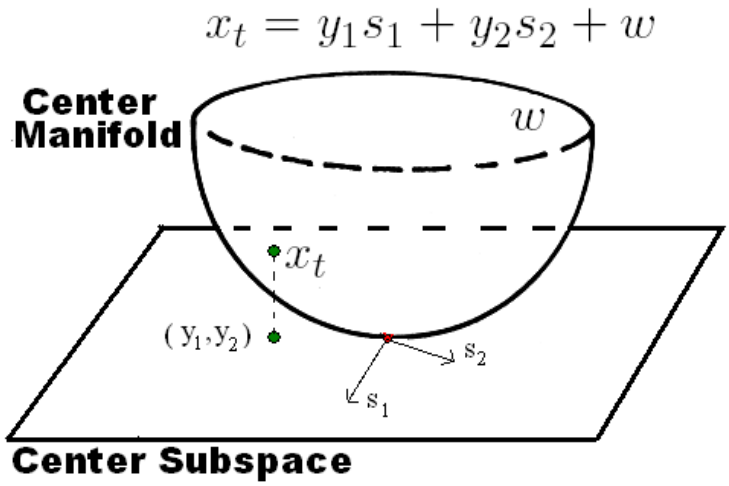

Figure 4.8: Geometric representation of the center manifold, w, with eigenvectors s_1 and s_2, and two-dimensional projection y_1-y_2 of the solution x_t onto the center subspace.

Mathematically this is expressed as follows:

$$x_t = y_1 s_1 + y_2 s_2 + w \tag{4.67}$$

The eigenvectors s_1 and s_2 corresponding to the eigenvalues $\pm i\omega$ are calculated as the solution of the four-dimensional first order boundary value problem

$$\frac{d}{d\theta} s_1(\theta) = -\omega s_2(\theta) \tag{4.68}$$

$$\frac{d}{d\theta} s_2(\theta) = \omega s_1(\theta) \tag{4.69}$$

$$L s_1(0) + M s_1(-T_{cr}) = -\omega s_2(0) \tag{4.70}$$

$$L s_2(0) + M s_2(-T_{cr}) = \omega s_1(0) \tag{4.71}$$

Substituting Eqs.(4.64)-(4.66) and (4.23)-(4.26) into (4.68)-(4.71) yields

$$s_1(\theta) = \begin{pmatrix} b\omega + a\mu \\ a \end{pmatrix} \cos(\omega\theta) + \begin{pmatrix} b\mu - a\omega \\ b \end{pmatrix} \sin(\omega\theta) \tag{4.72}$$

$$s_2(\theta) = -\begin{pmatrix} b\mu - a\omega \\ b \end{pmatrix} \cos(\omega\theta) + \begin{pmatrix} b\omega + a\mu \\ a \end{pmatrix} \sin(\omega\theta) \tag{4.73}$$

To simplify the latter equations, and without loss of generality, we take $a = 1$ and $b = 0$. Thus Eqs.(4.72) and (4.73) become

$$s_1(\theta) = \begin{pmatrix} \mu \\ 1 \end{pmatrix} \cos(\omega\theta) - \begin{pmatrix} \omega \\ 0 \end{pmatrix} \sin(\omega\theta) \tag{4.74}$$

$$s_2(\theta) = \begin{pmatrix} \omega \\ 0 \end{pmatrix} \cos(\omega\theta) + \begin{pmatrix} \mu \\ 1 \end{pmatrix} \sin(\omega\theta) \tag{4.75}$$

In order to find the equations on $y_1(t)$ and $y_2(t)$, we need to project $x_t(\theta)$ onto the center subspace. In this system, projections are accomplished by means of a bilinear form [56]:

$$< v, u >= v^*(0)u(0) + \int_{-T_{cr}}^{0} v^*(\theta + T_{cr})Mu(\theta)d\theta \tag{4.76}$$

where $u(\theta)$ lies in the original function space, i.e. the space of continuously differentiable functions defined on $[-T_{cr}, 0]$, and where $v(\theta)$ lies in the adjoint function space of continuously differentiable functions defined on $[0, T_{cr}]$.

To project onto the center subspace, we first need to find the adjoint eigenvectors: n_1 and n_2. These are determined from a similar boundary value problem as above

$$-\frac{d}{d\theta}n_1(\theta) = \omega n_2(\theta) \tag{4.77}$$

$$-\frac{d}{d\theta}n_2(\theta) = -\omega n_1(\theta) \tag{4.78}$$

$$L^*n_1(0) + M^*n_1(T_{cr}) = \omega n_2(0) \tag{4.79}$$

$$L^*n_2(0) + M^*n_2(T_{cr}) = -\omega n_1(0) \tag{4.80}$$

where L^* and M^* are the transposed matrices. We proceed as before and obtain

$$n_1(\theta) = \begin{pmatrix} c \\ c\mu + d\omega \end{pmatrix} \cos(\omega\theta) - \begin{pmatrix} d \\ d\mu - c\omega \end{pmatrix} \sin(\omega\theta) \tag{4.81}$$

$$n_2(\theta) = \begin{pmatrix} d \\ d\mu - c\omega \end{pmatrix} \cos(\omega\theta) + \begin{pmatrix} c \\ c\mu + d\omega \end{pmatrix} \sin(\omega\theta) \tag{4.82}$$

Now we find the constants c and d by taking into account the conditions of orthonormality:

$$< n_i, s_j >= \begin{cases} 0, & \text{if } i \neq j \\ 1, & \text{if } i = j \end{cases} \tag{4.83}$$

where, from Eq.(4.76),

$$< n_i, s_j >= n_i^*(0) s_j(0) + \int_{-T_{cr}}^{0} n_i^*(\theta + T_{cr}) M s_j(\theta) d\theta \tag{4.84}$$

The calculation yields

$$n_1(\theta) = v_1 \cos(\omega\theta) - v_2 \sin(\omega\theta) \tag{4.85}$$

$$n_2(\theta) = v_2 \cos(\omega\theta) + v_1 \sin(\omega\theta) \tag{4.86}$$

where

$$v_1 = \frac{2}{K C_0} \begin{pmatrix} 2\mu^2 T_{cr} - K T_{cr} + 2\mu \\ \mu K T_{cr} + 2K \end{pmatrix} \tag{4.87}$$

$$v_2 = \frac{2}{K C_0} \begin{pmatrix} 2\ (\mu T_{cr} + 1)\ \omega \\ K T_{cr}\, \omega \end{pmatrix} \tag{4.88}$$

$$C_0 = K T_{cr}^2 + 4\mu T_{cr} + 4 \tag{4.89}$$

Next we define the time dependent scalars

$$y_1(t) = < n_1, x_t > \tag{4.90}$$

$$y_2(t) = < n_2, x_t > \tag{4.91}$$

where y_1 and y_2 are the coordinates of x_t in the s_1 and s_2 directions, respectively. Differentiating Eqs.(4.90) and (4.91) we obtain (cf. [81])

$$\dot{y}_1 = \omega y_2 + h(y_1, y_2) \tag{4.92}$$

$$\dot{y}_2 = -\omega y_1 + g(y_1, y_2) \tag{4.93}$$

where we let

$$h(y_1, y_2) = n_1^*(0)\ f(x_t(0), x_t(-T_{cr})) \tag{4.94}$$

$$g(y_1, y_2) = n_2^*(0)\ f(x_t(0), x_t(-T_{cr})) \tag{4.95}$$

The next step is to look for an approximate expression for the center manifold, which is tangent to the y_1-y_2 plane at the origin (see Figure 4.8), and which may be written in the following truncated form by neglecting third and higher order terms (see Eq.(4.67)):

$$w(y_1, y_2)(\theta) = m_1(\theta)y_1^2 + m_2(\theta)y_1y_2 + m_3(\theta)y_2^2 \tag{4.96}$$

where the unknown vectors m_1, m_2, and m_3 will be calculated by equating the *time*-derivative of Eq.(4.96)

$$\dot{w} = -\omega m_2 y_1^2 + 2\omega(m_1 - m_3)y_1y_2 + \omega m_2 y_2^2 \tag{4.97}$$

and the *time*-derivative of Eq.(4.67)

$$\dot{w} = \dot{x}_t - \dot{y}_1 s_1 - \dot{y}_2 s_2 \tag{4.98}$$

$$= Ax_t + F(x_t) - < n_1, \dot{x}_t > s_1 - < n_2, \dot{x}_t > s_2 \tag{4.99}$$

$$= Aw + F(x_t) - < n_1, Fx_t > s_1(\theta) - < n_2, Fx_t > s_2(\theta) \tag{4.100}$$

Before finding the m_i's we calculate the nonlinear term $< n_1, Fx_t >$ (see Eq.(4.76)):

$$< n_1, Fx_t > = n_1^*(0)\ f(x_t(0), x_t(-T_{cr})) \tag{4.101}$$

$$= v_1^* \begin{pmatrix} H_2\eta(-T_{cr})^2 + H_3\eta(-T_{cr})^3 \\ 0 \end{pmatrix} \tag{4.102}$$

$$= \frac{2H_2}{KC_0}\Big(2\mu^2 T_{cr} - KT_{cr} + 2\mu\Big)\Big(s_{12}(-T_{cr})y_1 + s_{22}(-T_{cr})y_2\Big)^2 + \text{h.o.t.} \tag{4.103}$$

$$\approx C_1(2\mu^2 - K)^2 y_1^2 + 4\mu\,\omega\, C_1(2\mu^2 - K)y_1y_2 - 4C_1\mu^2(\mu^2 - K)y_2^2 \tag{4.104}$$

where

$$\eta(-T_{cr}) = y_1 s_{12}(-T_{cr}) + y_2 s_{22}(-T_{cr}) + w_2(-T_{cr}) \tag{4.105}$$

and

$$C_1 = \frac{2H_2(2\mu^2 T_{cr} - KT_{cr} + 2\mu)}{K^3 C_0} \tag{4.106}$$

In Eq.(4.105), s_{12} represents the second entry of the vector s_1, and w_2 represents the second entry of the vector w, and so on. Similarly,

$$< n_2, Fx_t > \approx C_2(2\mu^2 - K)^2 y_1^2 + 4\mu\,\omega\, C_2(2\mu^2 - K)y_1y_2 - 4C_2\mu^2(\mu^2 - K)y_2^2 \tag{4.107}$$

where

$$C_2 = \frac{4\omega H_2(\mu T_{cr} + 1)}{K^3 C_0} \tag{4.108}$$

Now we equate Eqs.(4.97) and (4.100), substitute the expressions for A, F, s_1, s_2, n_1, and n_2, and set the coefficients of y_1^2, y_1y_2, and y_2^2 to zero to obtain the following six-dimensional first order boundary value problem:

$$m_1' - (\mu^2 - \omega^2)^2(C_1 s_1 + C_2 s_2) = -\omega m_2 \tag{4.109}$$

$$m_2' - 4\mu\,\omega\,(\mu^2 - \omega^2)(C_1 s_1 + C_2 s_2) = 2\omega(m_1 - m_3) \tag{4.110}$$

$$m_3' - 4\omega^2\mu^2(C_1 s_1 + C_2 s_2) = \omega m_2 \tag{4.111}$$

$$Lm_1(0) + Mm_1(-T_{cr}) - (\mu^2 - \omega^2)^2(C_1 s_1(0) + C_2 s_2(0) + C_3\hat{e}) = -\omega m_2(0) \tag{4.112}$$

$$Lm_2(0) + Mm_2(-T_{cr}) - 4\mu\omega(\mu^2 - \omega^2)(C_1 s_1(0) + C_2 s_2(0) + C_3\hat{e}) = 2\omega(m_1(0) - m_3(0)) \tag{4.113}$$

$$Lm_3(0) + Mm_3(-T_{cr}) - 4\omega^2\mu^2(C_1 s_1(0) + C_2 s_2(0) + C_3\hat{e}) = \omega m_2(0) \tag{4.114}$$

where

$$C_3 = -\frac{H_2}{K^2} \tag{4.115}$$

$$\hat{e} = \begin{pmatrix} 1 \\ 0 \end{pmatrix} \tag{4.116}$$

The solution to the BVP problem (4.109)-(4.114) is:

$$m_1(\theta) = u_{11}\sin 2\omega\theta + u_{12}\cos 2\omega\theta + u_{13}\sin\omega\theta + u_{14}\cos\omega\theta + u_{15} \tag{4.117}$$

$$m_2(\theta) = u_{21}\sin 2\omega\theta + u_{22}\cos 2\omega\theta + u_{23}\sin\omega\theta + u_{24}\cos\omega\theta + u_{25} \tag{4.118}$$

$$m_3(\theta) = u_{31}\sin 2\omega\theta + u_{32}\cos 2\omega\theta + u_{33}\sin\omega\theta + u_{34}\cos\omega\theta + u_{35} \tag{4.119}$$

where the u_{ij}'s are given by Eqs.(4.123)-(4.132) and

$$C_4 = \frac{H_2}{K(16\mu^6 - 39K\mu^4 + 18K^2\mu^2 + 9K^3)} \tag{4.120}$$

$$C_5 = \frac{2H_2}{3C_0K^2} \tag{4.121}$$

$$C_6 = \frac{H_2}{2(\mu^2 + K)} \tag{4.122}$$

$$u_{11} = -\frac{1}{2}u_{22} = -u_{31} = C_4 \begin{pmatrix} -\omega(12\mu^6 - 34K\mu^4 + 27K^2\mu^2 - 3K^3) \\ 2\omega^3\mu(2\mu^2 - 3K) \end{pmatrix} \tag{4.123}$$

$$u_{12} = \frac{1}{2}u_{21} = -u_{32} = \frac{C_4}{2} \begin{pmatrix} \mu(24\mu^6 - 80K\mu^4 + 85K^2\mu^2 - 27K^3) \\ 8\mu^6 - 24K\mu^4 + 21K^2\mu^2 - 3K^3 \end{pmatrix} \tag{4.124}$$

$$u_{13} = \frac{C_5}{K\omega} \begin{pmatrix} K(4\mu^5 T_{cr} - 8K\mu^3 T_{cr} + 5K^2\mu T_{cr} - 8\mu^4 + 8K\mu^2 + 2K^2) \\ 8\mu^6 T_{cr} - 12K\mu^4 T_{cr} + 6K^2\mu^2 T_{cr} - K^3 T_{cr} + 8\mu^5 - 16K\mu^3 + 10K^2\mu \end{pmatrix} \tag{4.125}$$

$$u_{14} = -\frac{C_5}{K} \begin{pmatrix} K(4\mu^4 T_{cr} + K^2 T_{cr} + 16\mu^3 - 8K\mu) \\ 2(4\mu^5 T_{cr} - 4K\mu^3 T_{cr} + 3K^2\mu T_{cr} + 4\mu^4 + K^2) \end{pmatrix} \tag{4.126}$$

$$u_{15} = u_{35} = C_6 \begin{pmatrix} \mu \\ 1 \end{pmatrix} \tag{4.127}$$

$$u_{23} = \frac{2C_5}{K} \begin{pmatrix} K(4\mu^4 T_{cr} - 6K\mu^2 T_{cr} + K^2 T_{cr} - 8\mu^3 + 4K\mu) \\ 2(4\mu^5 T_{cr} - 4K\mu^3 T_{cr} + 4\mu^4 - 6K\mu^2 + K^2) \end{pmatrix} \tag{4.128}$$

$$u_{24} = \frac{2C_5}{K\omega} \begin{pmatrix} K(4\mu^5 T_{cr} - 2K\mu^3 T_{cr} - K^2\mu T_{cr} + 16\mu^4 - 16K\mu^2 + 2K^2) \\ 8\mu^6 T_{cr} - 12K\mu^4 T_{cr} + 6K^2\mu^2 T_{cr} - K^3 T_{cr} + 8\mu^5 - 4K\mu^3 - 2K^2\mu \end{pmatrix} \tag{4.129}$$

$$u_{25} = \begin{pmatrix} 0 \\ 0 \end{pmatrix} \tag{4.130}$$

$$u_{33} = -\frac{2C_5}{K\omega} \begin{pmatrix} K(2\mu^5 T_{cr} - 4K\mu^3 T_{cr} + K^2\mu T_{cr} - 4\mu^4 + 4K\mu^2 - 2K^2) \\ 4\mu^6 T_{cr} - 6K\mu^4 T_{cr} + K^3 T_{cr} + 4\mu^5 - 8K\mu^3 + 2K^2\mu \end{pmatrix} \tag{4.131}$$

$$u_{34} = \frac{2C_5}{K} \begin{pmatrix} K(2\mu^4 T_{cr} - K^2 T_{cr} + 8\mu^3 - 4K\mu) \\ 2(2\mu^5 T_{cr} - 2K\mu^3 T_{cr} + 2\mu^4 - K^2) \end{pmatrix} \tag{4.132}$$

The flow on the center manifold is given by Eqs.(4.92) and (4.93), where we can now evaluate the expressions for $h(y_1, y_2)$ and $g(y_1, y_2)$ given in Eqs.(4.94) and (4.95) as follows:

$$h(y_1, y_2) = \frac{C_1 K^2}{H_2}\left(H_2\,\eta(-T_{cr})^2 + H_3\,\eta(-T_{cr})^3\right) \tag{4.133}$$

$$g(y_1, y_2) = \frac{C_2 K^2}{H_2}\left(H_2\,\eta(-T_{cr})^2 + H_3\,\eta(-T_{cr})^3\right) \tag{4.134}$$

where $\eta(-T_{cr})$ is given by Eq.(4.105). Note that $\eta(-T_{cr})$ involves our expression for the center manifold, Eq.(4.96), which in turn uses the expressions (4.117)-(4.122) and (4.123)-(4.132).

4.4.2 Averaging

The foregoing computation has permitted us to replace the infinite dimensional DDE problem (4.13)-(4.14) by the two dimensional flow (4.92)-(4.93), where $h(y_1, y_2)$ and $g(y_1, y_2)$ are known and involve quadratic and cubic terms in y_1 and y_2 (to the order of truncation to which we have been working). This two dimensional system can be treated by traditional methods such as averaging, two variable expansion, or normal forms [39, 81]. The results can be most conveniently stated in terms of polar coordinates:

$$y_1 = r\cos\theta \tag{4.135}$$

$$y_2 = r\sin\theta \tag{4.136}$$

By means of a near-identity transformation, the flow (4.92)-(4.93) on the center manifold may be shown to give the following approximate equations on r and θ:

$$\frac{dr}{dt} = Qr^3 + O(r^5), \qquad \frac{d\theta}{dt} = \omega + O(r^2) \tag{4.137}$$

We refer the reader to pp.154-156 in [39] where it is shown that Q is given by the following expression:

$$16Q = h_{111}+h_{122}+g_{112}+g_{222}-\frac{1}{\omega}\Big(h_{12}(h_{11}+h_{22})-g_{12}(g_{11}+g_{22})-h_{11}g_{11}+h_{22}g_{22}\Big) \quad (4.138)$$

where the subscript i represents a partial derivative with respect to y_i, and where all terms are to be evaluated at y_1=y_2=0.

For the functions h and g in Eqs.(4.133) and (4.134), we obtain

$$Q = -\frac{2\omega^2}{C_0 P}\left(Q_0 T_{cr} + Q_1\right) \quad (4.139)$$

where P, Q_0, and Q_1 are defined as follows:

$$P = -8K^2\left(\mu^2-K\right)\left(\mu^2+K\right)\left(16\mu^6-39K\mu^4+18K^2\mu^2+9K^3\right) \quad (4.140)$$

$$\begin{aligned} Q_0 = {} & 48\,\mathrm{H}_3 K^2\mu^8 + 16\,\mathrm{H}_2{}^2 K\mu^8 - 69\,\mathrm{H}_3 K^3\mu^6 + 32\,\mathrm{H}_2{}^2 K^2\mu^6 - 63\,\mathrm{H}_3 K^4\mu^4 \\ & -162\,\mathrm{H}_2{}^2 K^3\mu^4 + 81\,\mathrm{H}_3 K^5\mu^2 + 108\,\mathrm{H}_2{}^2 K^4\mu^2 + 27\,\mathrm{H}_3 K^6 + 30\,\mathrm{H}_2{}^2 K^5 \end{aligned} \quad (4.141)$$

$$\begin{aligned} Q_1 = {} & 96\,\mathrm{H}_3 K\mu^9 + 64\,\mathrm{H}_2{}^2\mu^9 - 138\,\mathrm{H}_3 K^2\mu^7 - 16\,\mathrm{H}_2{}^2 K\mu^7 - 126\,\mathrm{H}_3 K^3\mu^5 \\ & -308\,\mathrm{H}_2{}^2 K^2\mu^5 + 162\,\mathrm{H}_3 K^4\mu^3 + 296\,\mathrm{H}_2{}^2 K^3\mu^3 + 54\,\mathrm{H}_3 K^5\mu + 12\,\mathrm{H}_2{}^2 K^4\mu \end{aligned} \quad (4.142)$$

The importance of the result (4.139) is that, from (4.137), the sign of Q determines the stability of the origin.

4.4.3 Unfolding the Center

In this section we use the center manifold computation to approximate the amplitude of a periodic motion (a limit cycle) which is born as parameters change

in the neighborhood of a center (i.e. in a Hopf bifurcation). The idea is to compute the real part of the eigenvalues of the linear system due to a small change in delay off of the critical delay T_{cr}. Let

$$T = T_{cr} + \Delta, \qquad |\Delta| << T_{cr} \tag{4.143}$$

and suppose the resulting eigenvalues are $\lambda = R \pm i\Omega$, where R and Ω have the approximate expressions $R = R_1\Delta$ and $\Omega = \omega + \omega_1\Delta$. Then Eqs.(4.92)-(4.93) will take the approximate form

$$\dot{y}_1 = Ry_1 + \Omega y_2 + h(y_1, y_2) \tag{4.144}$$

$$\dot{y}_2 = Ry_2 - \Omega y_1 + g(y_1, y_2) \tag{4.145}$$

and Eq.(4.137) will be replaced by the approximation

$$\frac{dr}{dt} = Rr + Qr^3 + O(r^5), \qquad \frac{d\theta}{dt} = \Omega + O(r^2) \tag{4.146}$$

where the first of (4.146) gives the limit cycle amplitude r as

$$r^2 = -\frac{R}{Q} \tag{4.147}$$

In the case of the linearization of the system (4.13)-(4.14), we have

$$\dot{\xi} = -\mu\,\xi - K\,\eta_d \tag{4.148}$$

$$\dot{\eta} = \xi - \mu\,\eta \tag{4.149}$$

which has solutions of the form

$$\xi = B\,e^{\lambda t} \tag{4.150}$$

$$\eta = A\,e^{\lambda t} \tag{4.151}$$

Setting $\lambda = R \pm i\Omega$, we find

$$(R+\mu)^2 - \Omega^2 = -K\,e^{-RT}\cos(\Omega T) \tag{4.152}$$

$$2\,\Omega\,(R+\mu) = K\,e^{-RT}\sin(\Omega T) \tag{4.153}$$

Substituting Eq.(4.143) into (4.152),(4.153) and linearizing for small Δ, we obtain

$$R = \frac{2\omega^2}{KT_{cr}^2 + 4\mu T_{cr} + 4}\,\Delta \tag{4.154}$$

$$\Omega = \omega - \frac{\omega(2\mu + KT_{cr})}{KT_{cr}^2 + 4\mu T_{cr} + 4}\,\Delta \tag{4.155}$$

Finally, by substituting (4.154) and (4.139) into (4.147), we obtain the following approximation for the limit cycle amplitude r:

$$r^2 = \frac{P}{Q_0 T_{cr} + Q_1}\,\Delta \tag{4.156}$$

which agrees with the comparable result obtained in Section 4.3 by Lindstedt's method.

We point out that r found in Eq.(4.156) is equal to A found in Eq.(4.43). This can be confirmed by noticing that y_1 and y_2 are the coordinates of x_t in the s_1 and s_2 directions (see eqs.(4.90)-(4.91)). Thus small ξ and η implies small y_1 and y_2. This shows that the infinite dimensional center manifold, w, can be neglected for small y_1 and y_2 (see eq.(4.96)). Hence by eqs.(4.61), (4.67), (4.74), and (4.75) we obtain

$$\begin{pmatrix} \xi(t) \\ \eta(t) \end{pmatrix} = \begin{pmatrix} \mu \\ 1 \end{pmatrix} y_1 + \begin{pmatrix} \omega_0 \\ 0 \end{pmatrix} y_2 \tag{4.157}$$

Since the system (4.148)-(4.149) is linear, then the solution can be expressed as

$$\xi(t) = B\cos(\omega_1 t + \phi) \tag{4.158}$$

$$\eta(t) = A\cos\omega_1 t \tag{4.159}$$

where A and B are the amplitudes of the $\eta(t)$ and $\xi(t)$ oscillations, and where ϕ is a phase angle (see Eqs.(4.20) and (4.21) in Section 4.2). Substituting Eqs.(4.135), (4.136) and (4.158), (4.159) into (4.157) yields

$$B\cos(\omega_1 t + \phi) = \mu r\cos\omega_1 t + \omega_0 r\sin\omega_1 t \tag{4.160}$$

$$A\cos\omega_1 t = r\cos\omega_1 t \tag{4.161}$$

Eq.(4.161) yields r=A and by eq.(4.156) we confirm Eq.(4.43) in Section 4.3. In addition, by expanding eq.(4.160) we obtain

$$B\cos(\omega_1 t)\cos\phi - B\sin(\omega_1 t)\sin\phi = \mu r\cos(\omega_1 t) + \omega_0 r\sin(\omega_1 t) \tag{4.162}$$

where by equating to zero the coefficients of the $\sin(\omega_1 t)$ and $\cos(\omega_1 t)$ terms in eq.(4.162), solving for $\sin^2\phi$ and $\cos^2\phi$, and adding these we obtain

$$B^2 = (\mu^2 + \omega_0^2)\, r^2 \tag{4.163}$$

Since r=A for small y_1, y_2 and by Eq.(4.23) we conclude that B= $\sqrt{K}A$. The latter confirms Eq.(4.50) in Section 4.3.

The study presented in this section extends Section's 4.3 Lindstedt's method analysis. The significance of these calculations is to provide approximations of general motions, including the *approach* to a periodic motion, given by Eqs.(4.92) and (4.93). The latter is a generalization of Lindstedt's method, which gives Eq.(4.36), and thus approximates only the periodic motion itself.

In particular, the work in Section 4.3 based on Lindstedt's method was unable to determine the stability of the origin at the bifurcation value $T = T_{cr}$. Using the same parameter values as in Section 4.3.1 we find that (where $\mu = 0.03$):

$$K = 3.9089 \times 10^{-3} \tag{4.164}$$

$$H_2 = 6.2778 \times 10^{-5} \tag{4.165}$$

$$H_3 = -6.4101 \times 10^{-7} \tag{4.166}$$

using which we compute from Eq.(4.139) that $Q = -1.100 \times 10^{-6}$, which implies that the zero solution is asymptotically stable for T=T_{cr}.

4.4.4 Summary

Due to the challenging technical nature of the previous analysis, we provide a summary of the steps taken in our study. The first step involves reformulating the original DDE problem (4.5)-(4.6) as an operator differential equation (4.60), followed by a cumbersome computational reduction of the infinite dimensional system to one of two dimensions (4.92)-(4.93). The second step is to choose the delay T so that the linearized system possesses a pair of pure imaginary eigenvalues. The center manifold theorem then guarantees that there exists a curved two dimensional manifold which is tangent to the subspace spanned by the eigenvectors corresponding to those eigenvalues with zero real part (see Figure 4.8).

The third step is to solve for the eigenvectors s_1 and s_2, Eqs.(4.74)-(4.75), which span a linear center subspace with coordinates y_1 and y_2. Then we look for the curved center manifold, $w(y_1, y_2)$, which is tangent to the y_1-y_2 plane at the origin, in the form of a truncated power series, Eq.(4.96). The coefficients m_1, m_2 and m_3 of this series are 2-vectors which satisfy the ODE's (4.109)-(4.111) with the boundary conditions (4.112)-(4.114). The resulting expressions for the m_i's, Eqs.(4.117)-(4.119), were then used to allow the original nonlinear system to be projected onto the center manifold, giving a two dimensional flow on the y_1-y_2 phase plane, Eqs.(4.92)-(4.93).

The final step was to use averaging on the familiar form of Eqs.(4.92)-(4.93). This allowed us to get the normal form equation (4.137), from which the stability of the origin could be determined from the sign of Q. Moreover, by detuning the delay T from the Hopf bifurcation value T_{cr}, we were able to generalize the normal form (4.146), yielding the amplitude of the resulting limit cycle (4.156).

4.5 State Dependent Delay

As seen in previous chapters, we now fully understand oscillations in the system (4.5), (4.6) when the delay is constant. In this section we extend our previous results to include delays which are state dependent, that is, where the delay T depends on m, the concentration of mRNA. This effect is important in systems where the mechanisms which transport the mRNA from the nucleus to the cytoplasm become saturated. The previous argument motivates the use of state-dependent delays, and it might be validated by the fact that the expression of many genes is estimated by measurement of the cellular concentration of mRNA. Thus, in this chapter, we assume that the transcriptional delay will increase with the concentration of mRNA. This leads us to propose the following form for the state-dependent delay:

$$T = T_0 + \bar{c}M \tag{4.167}$$

where T_0 and $\bar{c}$ are parameters, and where M=$M(t)$ is the concentration of mRNA.

4.5.1 Linear Analysis

We start by rescaling Eqs.(4.5)-(4.6) by setting $m = \frac{M}{\alpha_m}$, $p = \frac{P}{\alpha_m \alpha_p}$, and $p_0 = \frac{P_0}{\alpha_m \alpha_p}$:

$$\dot{m} = \frac{1}{1 + \left(\frac{p_d}{p_0}\right)^n} - \mu m \tag{4.168}$$

$$\dot{p} = m - \mu p \tag{4.169}$$

Notice that Eq.(4.168) differs from Eq.(4.5) in that p_d is given by

$$p_d = p(t - T) = p(t - T_0 - \bar{c}M) = p(t - T_0 - cm) \tag{4.170}$$

where $c = \bar{c}\alpha_m$.

Equilibrium points, (m^*, p^*), for (4.168) and (4.169) are found by setting $\dot{m} = 0$ and $\dot{p} = 0$

$$\mu m^* = \frac{1}{1 + \left(\frac{p^*}{p_0}\right)^n} \tag{4.171}$$

$$m^* = \mu p^* \tag{4.172}$$

Solving Eqs.(4.171) and (4.172) for p^* we get

$$(p^*)^{n+1} + p_0^n p^* - \frac{p_0^n}{\mu^2} = 0. \tag{4.173}$$

Next we define ξ and η to be deviations from equilibrium: ξ=$\xi(t)$=$m(t)$-m^*, η=$\eta(t)$=$p(t)$-p^*, and η_d=$\eta(t$-$T)$. This results in the nonlinear system:

$$\dot{\xi} = \frac{1}{1 + \left(\frac{\eta_d + p^*}{p_0}\right)^n} - \mu(m^* + \xi) \tag{4.174}$$

$$\dot{\eta} = \xi - \mu\eta \tag{4.175}$$

Expanding for small values of η_d, Eq.(4.174) becomes:

$$\dot{\xi} = -\mu\xi - K\,\eta_d + H_2\,\eta_d^2 + H_3\,\eta_d^3 + \cdots \tag{4.176}$$

where K, H_2 and H_3 depend on p^*, p_0, and n as in Eqs.(4.15)-(4.17).

Next we analyze the associated linear system coming from Eqs.(4.175) and (4.176):

$$\dot{\xi} = -\mu\,\xi - K\,\eta_d \tag{4.177}$$

$$\dot{\eta} = \xi - \mu\,\eta \tag{4.178}$$

Although Eq.(4.177) would be linear for constant delay, it is nonlinear for a state-dependent delay due to the term η_d:

$$\eta_d = \eta(t - T_0 - cm) = \eta(t - T_0 - cm^* - c\,\xi) \tag{4.179}$$

where m^* is the equilibrium value of m, related to the protein equilibrium p^* by Eq.(4.172). In order to linearize eq.(4.177), we must develop η_d in Eq.(4.179) in a Taylor series for small values of ξ and η. We obtain

$$\eta_d \;=\; \eta(t - T_0 - cm^*) \;+\; \text{nonlinear terms} \tag{4.180}$$

Thus the stability of the equilibrium point (m^*, p^*) will be determined by the linearized system:

$$\dot{\xi} \;=\; -\mu\,\xi - K\,\eta(t - T_0 - cm^*) \tag{4.181}$$

$$\dot{\eta} \;=\; \xi - \mu\,\eta \tag{4.182}$$

As seen in Section 4.2, stability analysis of Eqs.(4.181) and (4.182) shows that for $T = T_0 + cm^* = 0$ (no delay), the equilibrium point (m^*, p^*) is a stable spiral. Increasing the delay, T, in the linear system (4.181)-(4.182) will yield a critical delay, T_{cr}, such that for $T>T_{cr}$, (m^*, p^*) will be unstable, giving rise to a Hopf bifurcation. Thus, for $T = T_0 + cm^* = T_{cr}$ the system (4.181),(4.182) will exhibit a pair of pure imaginary eigenvalues $\pm\omega i$ corresponding to the solution

$$\xi(t) \;=\; B\cos(\omega t + \phi) \tag{4.183}$$

$$\eta(t) \;=\; A\cos\omega t \tag{4.184}$$

where A and B are the amplitudes of the $\eta(t)$ and $\xi(t)$ oscillations, and where ϕ is a phase angle. Note that we have chosen the phase of $\eta(t)$ to be zero without loss of generality. Then for values of delay T close to T_{cr},

$$T = T_{cr} + \Delta + c\,\xi \tag{4.185}$$

the nonlinear system (4.168)-(4.169) is expected to exhibit a periodic solution (a limit cycle) which can be written in the approximate form of Eqs.(4.183), (4.184). Substituting Eqs.(4.183) and (4.184) into Eqs.(4.181) and (4.182) and solving for ω and T_{cr} we obtain Eqs.(4.23) and (4.24) respectively.

4.5.2 Lindstedt's Method

According to Stepan and Insperger [52, 53], linearized constant DDEs govern the stability of an equilibrium solution of a state dependent delay equation (SDDE). In this section we provide a new approach in understanding the non-linear dynamics of an SDDE. We will use Lindstedt's perturbation method to investigate periodic solutions to the system (4.168),(4.169) in the case that the delay depends on the state of the system as given by Eq.(4.167). We will follow Section 4.3 for our analysis.

We begin by changing the first order system into a second order SDDE. This results in the following form

$$\ddot{\eta} + 2\,\mu\,\dot{\eta} + \mu^2\,\eta = -K\,\eta_d + H_2\,\eta_d^2 + H_3\,\eta_d^3 + \cdots \tag{4.186}$$

where K, H_2 and H_3 are defined by Eqs.(4.15)-(4.17) and where η_d is given by Eq.(4.179). We eliminate the appearance of ξ in the expression for the delay in Eq.(4.179) by using Eq.(4.178) and obtain:

$$\xi = \dot{\eta} + \mu\,\eta \tag{4.187}$$

Next we introduce a small parameter ϵ via the scaling

$$\eta = \epsilon u. \tag{4.188}$$

Since the detuning Δ of Eq.(4.185) is scaled like ϵ^2 then using Eq.(4.188) yields

$$\begin{aligned} T &= T_{cr} + \Delta + c\,\xi && (4.189)\\ &= T_{cr} + \Delta + c(\dot{\eta} + \mu\,\eta) && (4.190)\\ &= T_{cr} + \epsilon^2\delta + c\epsilon(\dot{u} + \mu\,u) && (4.191) \end{aligned}$$

Next we stretch time by replacing the independent variable t by τ, where

$$\tau = \Omega\,t \tag{4.192}$$

Substituting Eqs.(4.188) and (4.192) into Eq.(4.186) results in the following:

$$\Omega^2 \frac{d^2u}{d\tau^2} + 2\mu\Omega\frac{du}{d\tau} + \mu^2 u = -K u_d + \epsilon H_2 u_d^2 + \epsilon^2 H_3 u_d^3 \tag{4.193}$$

where $u_d = u(\tau - \Omega T)$.

Next we expand Ω and u_d in a power series in ϵ. We start by expanding Ω, omitting the $O(\epsilon)$ for convenience, since it turns out to be zero:

$$\Omega = \omega + \epsilon^2 k_2 + \ldots \tag{4.194}$$

then we expand the delay term u_d:

$$\begin{aligned}
u_d &= u(\tau - \Omega T) && (4.195)\\
&= u(\tau - \Omega(T_{cr} + \epsilon^2\delta + c\,\epsilon(\Omega u'(\tau) + \mu u(\tau)))) && (4.196)\\
&= u(\tau - \omega T_{cr}) + \\
&\quad \epsilon[-c\,\omega(\omega u'(\tau) + \mu u(\tau))\,u'(\tau - \omega T_{cr})] + \\
&\quad \epsilon^2[\frac{1}{2}c^2\omega^2(\omega u'(\tau) + \mu u(\tau))^2\,u''(\tau - \omega T_{cr}) \\
&\quad -(\delta\omega + k_2 T_{cr})u'(\tau - \omega T_{cr})] + O(\epsilon^3) && (4.197)
\end{aligned}$$

where primes represent differentiation with respect to τ. Now we expand $u(\tau)$ in a power series in ϵ:

$$u(\tau) = u_0(\tau) + \epsilon u_1(\tau) + \epsilon^2 u_2(\tau) + \ldots \tag{4.198}$$

By substituting Eqs.(4.191), (4.194), (4.197), and (4.198) into (4.193) and collecting terms, we obtain three equations on u_0, u_1 and u_2. Each of these involves the same linear differential-delay operator L:

$$L f \equiv \omega^2\frac{d^2 f}{d\tau^2} + 2\mu\omega\frac{df}{d\tau} + K f(\tau - \omega T_{cr}) + \mu^2 f \tag{4.199}$$

and they are given by

$$
\begin{aligned}
L\,u_0 &= 0 && (4.200)\\
L\,u_1 &= H_2\,u_0^2(\tau-\omega T_{cr}) + \\
&\quad cK\omega(\omega u_0'(\tau)+\mu u_0(\tau))\,u_0'(\tau-\omega T_{cr}) && (4.201)\\
L\,u_2 &= \ldots && (4.202)
\end{aligned}
$$

where $\ldots$ stands for terms in u_0 and u_1, omitted here for brevity. We take the solution of the u_0 equation as:

$$u_0(\tau) = \hat{A}\cos\tau \tag{4.203}$$

where from Eqs.(4.184) and (4.188) we know $A = \hat{A}\epsilon$. Next we substitute (4.203) into (4.201) and obtain the following expression for u_1:

$$u_1(\tau) = m_1\sin 2\tau + m_2\cos 2\tau + m_3 \tag{4.204}$$

where m_1 is given by the equation:

$$m_1 = \frac{\hat{A}^2\,\mu\,\sqrt{K-\mu^2}\;\Phi}{2\,K\;(16\,\mu^6 - 39\,K\,\mu^4 + 18\,K^2\,\mu^2 + 9\,K^3)} \tag{4.205}$$

and where

$$\Phi \;=\; 4cK^2\mu^4 - 8H_2\mu^4 - 11cK^3\mu^2 + 20H_2K\mu^2 + 9cK^4 - 12H_2K^2 \tag{4.206}$$

As in Section 4.3, m_2 and m_3 are omitted here for brevity. We substitute Eqs.(4.203) and (4.204) into (4.202), and, after trigonometric simplifications have been performed, we equate to zero the coefficients of the resonant terms $\sin\tau$ and $\cos\tau$. This yields the amplitude, A, of the limit cycle that was born in the Hopf bifurcation:

$$A^2 \;=\; \frac{P}{Q}\,\Delta \tag{4.207}$$

where

$$P = 16K^2\left(\mu^4 - K^2\right) \times \left(16\mu^6 - 39K\mu^4 + 18K^2\mu^2 + 9K^3\right) \tag{4.208}$$

$$Q = Q_0\, T_{cr} + Q_1 \tag{4.209}$$

and

$$\begin{aligned} Q_0 = {} & 32\,c^2\,K^3\,\mu^{12} - 62\,c^2\,K^4\,\mu^{10} \\ & + \left(7\,c^2\,K^5 + 140\,c\,H_2\,K^3 - 96\,H_3\,K^2 - 32\,H_2^2\,K\right)\mu^8 \\ & + \left(20\,c^2\,K^6 - 428\,c\,H_2\,K^4 + 138\,H_3\,K^3 - 64\,H_2^2\,K^2\right)\mu^6 \\ & + \left(-6\,c^2\,K^7 + 396\,c\,H_2\,K^5 + 126\,H_3\,K^4 + 324\,H_2^2\,K^3\right)\mu^4 \\ & + \left(42\,c^2\,K^8 - 84\,c\,H_2\,K^6 - 162\,H_3\,K^5 - 216\,H_2^2\,K^4\right)\mu^2 \\ & - 33\,c^2\,K^9 - 24\,c\,H_2\,K^7 - 54\,H_3\,K^6 - 60\,H_2^2\,K^5 \end{aligned} \tag{4.210}$$

$$\begin{aligned} Q_1 = {} & 96\,c^2\,K^3\,\mu^{11} \\ & + \left(-354\,c^2\,K^4 + 48\,c\,H_2\,K^2 - 192\,H_3\,K - 128\,H_2^2\right)\mu^9 \\ & + \left(560\,c^2\,K^5 - 172\,c\,H_2\,K^3 + 276\,H_3\,K^2 + 32\,H_2^2\,K\right)\mu^7 \\ & + \left(-556\,c^2\,K^6 + 308\,c\,H_2\,K^4 + 252\,H_3\,K^3 + 616\,H_2^2\,K^2\right)\mu^5 \\ & + \left(368\,c^2\,K^7 - 340\,c\,H_2\,K^5 - 324\,H_3\,K^4 - 592\,H_2^2\,K^3\right)\mu^3 \\ & + \left(-114\,c^2\,K^8 + 156\,c\,H_2\,K^6 - 108\,H_3\,K^5 - 24\,H_2^2\,K^4\right)\mu \end{aligned} \tag{4.211}$$

Eq.(4.209) depends on μ, K, H_2, H_3, and T_{cr}. By using Eq.(4.24) we may express Eq.(4.209) as a function of μ, K, H_2, and H_3 only.

Removal of secular terms also yields a value for the frequency shift k_2 (cf. Eq.(4.194) above):

$$k_2 = -\frac{R}{Q}\,\delta \tag{4.212}$$

where Q is given by (4.209) and

$$R = \sqrt{K - \mu^2}\; Q_0 \tag{4.213}$$

An expression for the amplitude B of the periodic solution for $\xi(t)$ (see Eq.(4.183)) may be obtained directly from Eq.(4.175) by writing

$$\xi = \dot{\eta} + \mu\,\eta \ , \qquad \text{where } \ \eta \sim A\cos\omega t \tag{4.214}$$

This gives

$$B = \sqrt{K}A \tag{4.215}$$

where K and A are given as in (4.15) and (4.207) respectively.

4.5.3 Numerical Example

Using the same parameter values as in Section 4.3.1 we have

$$\mu = 0.03/\text{min}\,, \ p_0 = 100\,, \ n = 5 \tag{4.216}$$

which gives

$$p^* = 145.9158\,, \ m^* = 4.3774 \tag{4.217}$$

$$K = 3.9089\times 10^{-3}\,, \ H_2 = 6.2778\times 10^{-5}\,, \ H_3 = -6.4101\times 10^{-7} \tag{4.218}$$

$$T_{cr} = 18.2470\,, \ \omega = 5.4854\times 10^{-2}\,, \ \frac{2\pi}{\omega} = 114.5432 \tag{4.219}$$

Here the delay T_{cr} and the response period $2\pi/\omega$ are given in minutes. Substituting (4.216)-(4.219) into (4.207)-(4.215) yields the following equations:

$$A = \frac{27.0203}{\sqrt{0.0544\,c^2 - 0.05656\,c + 1.0}}\ \sqrt{\Delta} \tag{4.220}$$

$$k_2 = \frac{-8.39065\cdot 10^{-5}\,c^2 - 4.00072\cdot 10^{-4}\,c - 0.00245}{0.0544\,c^2 - 0.05656\,c + 1.0}\,\delta \tag{4.221}$$

Note that since Eq.(4.220) requires $\Delta > 0$ for the limit cycle to exist, and since we saw in Eqs.(4.181) and (4.182) that the origin is unstable for $T > T_{cr}$, i.e. for $\Delta > 0$, we may conclude that the Hopf bifurcation is supercritical, i.e., the limit cycle is stable.

Figure 4.9 shows a plot of p versus t for $c = 1$ and $\Delta = 0.16$ in which the results of the perturbation theory are compared to those of numerical simulation in Matlab using the function ddesd.

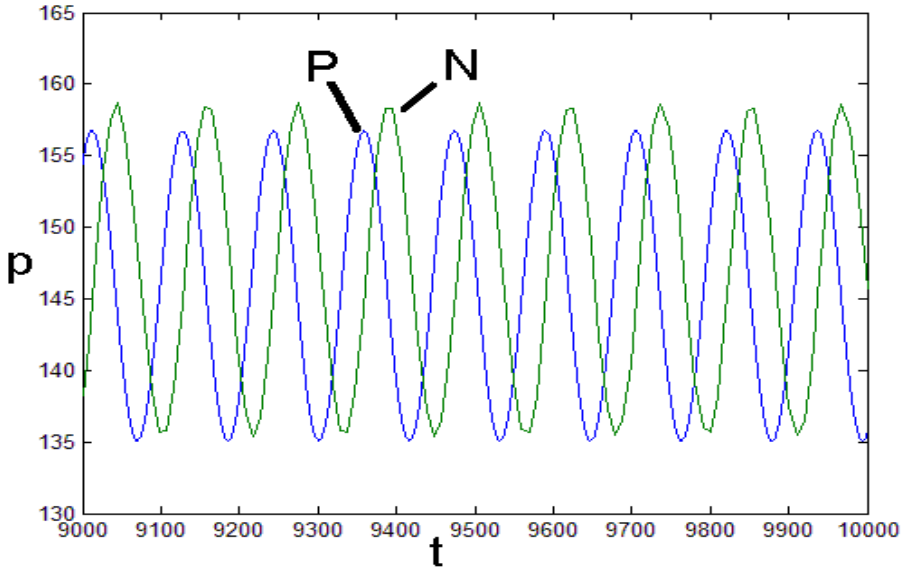

Figure 4.9: Comparison of perturbation results (P) with those of numerical integration (N) for c=1 and Δ=0.16. The perturbation solution is $p(t)$=145.91+10.82 cos(0.05438t). Since the system is autonomous, the phase of the steady state solution is arbitrary, which accounts for the difference in phase between the displayed solutions.

4.6 Conclusions

In this chapter we analyze a single gene-mRNA-protein model of gene transcription and protein synthesis which has been previously presented in the biological literature [72]. The model takes the form of an ODE (ordinary differential equation) coupled to a DDE (delay differential equation), the state variables being concentrations of messenger RNA and protein. Section 4.2 provides a linear stability analysis and gives a critical time delay beyond which a periodic motion is born in a Hopf bifurcation. In Sections 4.3 and 4.4 we analyzed the model when the delay is constant, and in Section 4.5 when the delay depends on the state of the system.

The biological literature [20, 62, 72, 108] shows that long time behavior of gene expression dynamics can consist of both stable equilibrium as well as periodic behavior. In this chapter we have shown that the transition between these states is due to a Hopf bifurcation. Our nonlinear analysis provides approximate expressions for the amplitude and frequency of the resulting limit cycle as a function of the model parameters. In the case of constant delay, Figure 4.3 shows that the Hopf bifurcation may not occur if the rates of degradation μ are too large. Also, inspection of Figure 4.4 shows that for a given detuning Δ off of the Hopf bifurcation, the amplitude of the oscillation depends on both p_0 and μ. We see that increasing p_0 for a fixed value of μ causes an increase in amplitude. However, for a fixed value of p_0, the amplitude is largest for a certain optimal value of μ. Figure 4.5 shows a similar behavior regarding the period of the oscillation. For a fixed value of p_0 we see that the quantity $\frac{Q_0}{Q}$ achieves a maximum for a certain optimal value of μ. In this case the peak values of $\frac{Q_0}{Q}$ correspond to minimal values of frequency Ω and thus to maximal values for the period.

In Section 4.4 we use center manifold theory to analyze the same gene-mRNA-protein model given by Eqs.(4.5) and (4.6). The highly technical analysis involves reformulating the problem as an operator differential equation followed by a cumbersome computational reduction of the infinite dimensional system into one of two dimensions. As explained in Section 4.4, in order to accomplish such reduction, the delay T is chosen so that the linearized system possesses a pair of pure imaginary eigenvalues as well as an infinite number of eigenvalues with negative real parts. The center manifold theorem then guarantees that there exists a curved two dimensional subspace center manifold which is tangent to the subspace spanned by the eigenvectors corresponding to those eigenvalues with zero real part, and which is invariant under the flow generated by the nonlinear equations. The center manifold analysis extends the study in Section 4.3 by providing approximations of general motions, including the *approach* to a periodic motion. The center manifold reduction is thus a more powerful method compared to Lindstedt's method, which approximates only the periodic motion itself. In particular, we were able to show that the origin is asymptotically stable for the critical (bifurcation) value of the delay parameter.

In Section 4.5 we investigated the effect of state-dependency on delay by using a perturbation method valid in the neighborhood of a Hopf bifurcation. We showed how Lindstedt's method can be used to deal with state-dependent delays. Figure 4.9 shows that the resulting approximate expressions for amplitude and frequency of the steady state oscillation are in good agreement with those obtained by numerical integration. On the other hand, Eqs.(4.220) and (4.221) show that the effect of c on amplitude and frequency is small for O(1) values of c.

A final thought on Lindstedt's method is that although it is a formal perturbation method, that is, lacking a proof of convergence, our experience is that it gives the same results as the center manifold approach. However, as was seen in Section 4.4, the center manifold procedure is much more complicated than the Hopf calculation. Stepan refers to the center manifold calculation as "long and tedious" ([95], p.112), and Campbell refers to it as "algebraically daunting" ([11], p.642). In [81], Chapter 14, 2 pages are spent explaining the application of Lindstedt's method to DDE's, whereas 10 pages are required for explanation of the center manifold approach. Thus the main advantage of using Lindstedt's method is that it is simpler to understand and easier to execute than the center manifold reduction.

CHAPTER 5

MULTIPLE GENE NETWORK MODEL

5.1 Introduction

Understanding the interactions between genes and their protein products is an important part of experimental and theoretical biology. Recent experiments [34, 90] and theoretical techniques [68, 108, 109] have been developed to understand the dynamics of gene regulatory networks. From a theoretical point of view, the gene network structure is an abstraction of the system's chemical dynamics, and it includes how protein products affect the expression of other genes and their associated proteins. If the network involves only a few genes then its dynamical behavior could be studied directly [30, 34]. On the other hand, if the network is formed of hundreds or thousands of genes then its experimental or theoretical study may be highly difficult [20, 74]. Nevertheless, research trends show that the study of these networks is the next in genomic research.

Several mathematical models of gene regulatory networks have been developed over the last couple of decades (for an extensive review see [47, 54, 88]). Some of the most common modeling techniques involve the use of graphs [58, 69], Boolean networks [16, 78, 80], Bayesian networks [31], Petri nets [32, 66], reverse engineering methods [99], and coupled differential equations (linear [55], nonlinear [24, 46, 71], partial [101], stochastic [38, 85, 119], and delayed [8, 29, 108]). Here we are interested in models where the natural lags or delays play an important role in the system's dynamics [62, 72, 108, 109]. As explained in Chapter 2, these delays arise naturally from transcription, translation, degradation, and other cellular processes.

Transcription and translation are the main processes by which a cell expresses the instructions encoded in its genes. Transcription is the first step in gene expression and it includes the identical replication of a gene into messenger RNA (mRNA). The second step is the translation process, where the information in the mRNA is translated into a protein with a specific amino acid sequence. The latter process is accomplished by a well-known protein-manufacturing machine called a ribosome. Once the protein is created, it unbinds from the ribosome and carries out its cellular function. From these processes mRNA and protein concentrations arise naturally as the main intracellular regulatory agents for gene expression (see Figure 5.1).

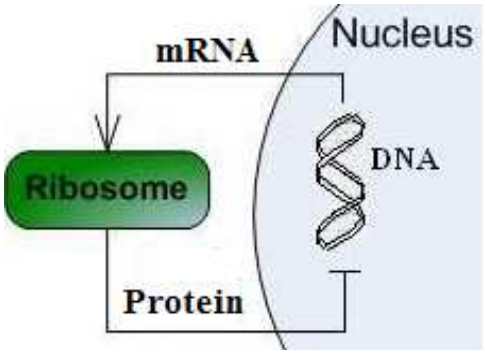

Figure 5.1: Feedback inhibition mechanism. The gene is copied onto mRNA, which then attaches to a ribosome and a protein is produced. The protein then diffuses back into the nucleus where it represses the transcription of its own gene.

There are several mechanisms that the cell uses to regulate the levels of mRNA and protein concentrations. An example is the cell's ability to increase or decrease the concentration of enzymes that degrade proteins (agents that destroy proteins). Another important regulatory mechanism is the cell's capacity to turn on and off the transcription process of a specific gene. The latter can be accomplished by means of feedback inhibition, where the expression of a gene is regulated by its own protein product. This feedback mechanism arises when

the protein product returns to the nucleus and stops the transcription of its own mRNA by binding to the gene's promoter site. Previous findings [62, 72] show that there are time delays associated with this feedback mechanism. These delays arise naturally as transcriptional delays (time it takes the gene to get copied into mRNA) and translational delays (time it takes the ribosome to translate mRNA into protein). Furthermore, recent studies [72] have shown that it suffices to consider only the transcriptional time delay to have an accurate dynamic model [62, 108]. These transcriptional delay models can be represented by the following pair of equations:

$$\frac{dM}{dt} = -\mu_M M(t) + H(P(t-T)) \tag{5.1}$$

$$\frac{dP}{dt} = \alpha_P M(t) - \mu_P P(t) \tag{5.2}$$

where the time dependent variables are the mRNA concentration, $M(t)$, and its associated protein concentration, $P(t)$, and where the constants μ_M and μ_P are the decay rates of the mRNA and protein molecules, α_P is the rate of production of new protein molecules per mRNA molecule, and $H(P(t-T))$ is a Hill function representing the rate of *delayed* production of new mRNA molecules. We assume that $H(P(t-T))$ is a decreasing function of the concentration of protein present at a previous time $P(t-T)$, where T represents the transcriptional time delay.

In this chapter we will study the dynamics of two different models of a gene network with time delay. Both of these models are characterized by a system of coupled ODEs and DDEs. The first model considers uniform weighting, where each ribosome produces a given quantity of protein which is then shared equally amongst all gene sites, that is, the protein produced will repress equally (with equal strength) the production of all other mRNAs. The second model

is characterized by an exponential weighting, where each protein product is shared unequally, with nearby gene sites being repressed to a greater extent than more distant genes. Both of these cases exhibit a steady state, which is stable when there is no delay. Linear analysis then reveals that a critical delay exists, where the steady state becomes unstable. Closed form expressions for the critical delay T_{cr} and associated frequency ω are thus found. We then present some nonlinear analysis results for both cases.

5.2 Geometric Representation and Hill Function Dependence

We start this section by defining a more compact geometric notation for the single gene model given by Figure 5.1. The left hand side of Figure 5.2 represents the same gene-mRNA-protein feedback loop as in Figure 5.1. Similarly, the right hand side, represents the same phenomena, but in a more compact notation. The black dot on the right side represents mRNA production and the empty dot represents protein production. Since mRNA activates protein production, which then represses mRNA, then the arrow (↑) represents activation and the perpendicular symbol (⊥) represents repression.

By normalizing Eqs.(5.1) and (5.2) (m=M/α_M, p=$P/\alpha_M\alpha_P$, and μ_P=μ_M=μ) we obtain the expressions that govern the dynamics of the single gene system

$$\frac{dm}{dt} = -\mu m + H(p(t-T)) \tag{5.3}$$

$$\frac{dp}{dt} = m - \mu p \tag{5.4}$$

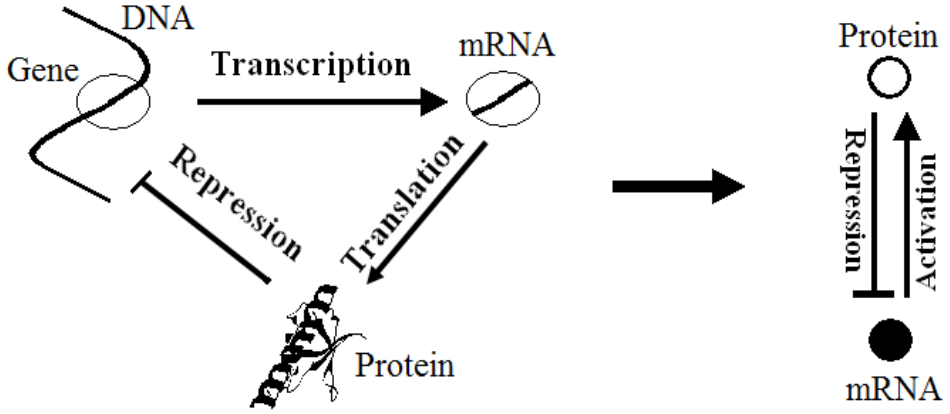

Figure 5.2: Compact notation for the mRNA-protein feedback loop for the single gene. Both sides represent the same gene-mRNA-protein feedback loop. The black dot on the right side represents mRNA production and the empty dot represents protein production. Here the arrow (↑) represents activation and the perpendicular symbol (⊥) represents repression.

Notice that the repression effect of the protein is captured by the Hill function. In other words, the production of mRNA, $\dot{m}$, depends on how *strong* is the repression effect of the protein which is given by $H(p(t-T))$. For the rest of this thesis we will use the previous compact notation for the mRNA-protein system. See Figure 5.3.

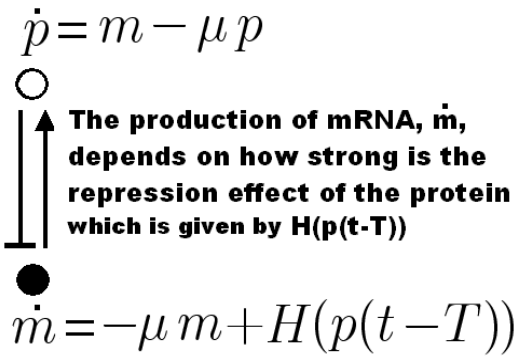

Figure 5.3: mRNA-protein feedback with associated differential equations.

5.2.1 Two Gene Network

We now extend the single mRNA-protein system given by Figure 5.3 to a system of two mRNA's with associated proteins. This may be geometrically viewed as in Figure 5.4.

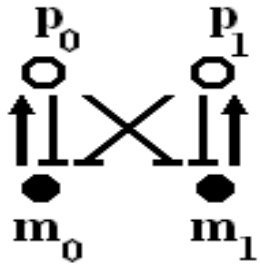

Figure 5.4: Geometric representation of the two gene network system. The protein product of the first gene, p_0, represses its own mRNA production, m_0, and the mRNA production of the second gene, m_1. Similarly for the second gene.

In this two gene system, the protein product of the first gene, p_0, not only represses its own mRNA production, but it also represses the mRNA production of the second gene. In a similar way, the protein product of the second gene also affects the first. The differential equation model of this two gene network is given as follows

$$\frac{dm_i}{dt} = -\mu m_i + \sum_{j=0}^{1} G_{ij} H\left(p_j(t-T)\right) \tag{5.5}$$

$$\frac{dp_i}{dt} = m_i - \mu p_i \tag{5.6}$$

where $i = 0, 1$ and where we have assumed for simplicity that the constants are the same for both genes. There are a couple of interesting features about this model of two coupled gene units:

First, notice that the only coupling between the two different gene units is through the mRNA repression. Since the effect of repression is captured by the Hill func-

tion, then the *total* mRNA repressive effect on the *i*th gene will be given by the sum of both Hill functions. This accounts for the sum on the RHS of Eq.(5.5).

The second interesting feature is the appearance of the G_{ij}'s inside the sum in Eq.(5.5). The biological meaning of these constants is related to the *strength* of the protein repression effect of one gene over another. Suppose, for example, that the effect of repression of gene zero is very strong over gene one, then G_{10} will be large. Similarly, if gene one (see Figure 5.4) had a very weak repression effect over gene zero, then G_{01} would be small.

According to the two gene model given by Eqs.(5.5) and (5.6) we may consider two different biological scenarios:

Case 1 (Uniform weighting): We characterize this case by the choice G_{ij}=1/2. Here each ribosome produces a given quantity of protein which is then shared equally amongst the other two gene promoter sites (hence G_{ij}=1/2). For the Hill function we choose the following equation (cf.Eq.(4.1)):

$$H(p_j(t-T)) \;=\; \frac{1}{1+\left(\frac{p_j(t-T)}{p_{0j}}\right)^n} \tag{5.7}$$

where p_{0j} is a reference concentration of protein p_j and n is the Hill coefficient. The resulting system from Eqs.(5.5)-(5.6) is of the form

$$\frac{dm_i}{dt} \;=\; -\mu\, m_i \;+\; \frac{1}{2}\sum_{j=0}^{1}\frac{1}{1+\left(\frac{p_j(t-T)}{p_{0j}}\right)^n} \tag{5.8}$$

$$\frac{dp_i}{dt} \;=\; m_i - \mu\, p_i \tag{5.9}$$

Case 2 (Exponential weighting): We characterize this case by the choice G_{ij}=$e^{-|i-j|}$. Here each protein product is shared unequally, with nearby gene promoter sites being repressed to a greater extent than more distant ones. For mathematical

simplicity we choose the Hill function of the form

$$H(p_j(t-T)) \;=\; 1 - p_j(t-T) + \alpha p_j^3(t-T) \tag{5.10}$$

which may be thought as an expansion of Eq.(5.7). The resulting system from Eqs.(5.5)-(5.6) is of the form

$$\frac{dm_i}{dt} \;=\; -\mu\, m_i \;+\; \sum_{j=0}^{1} e^{-|i-j|}\left(1 - p_j(t-T) + \alpha\, p_j^3(t-T)\right) \tag{5.11}$$

$$\frac{dp_i}{dt} \;=\; m_i - \mu\, p_i \tag{5.12}$$

5.2.2 Multiple Gene Network

The previous arguments may be generalized for a multiple gene network with N+1 gene units. The decision to use N+1 gene units (instead of N) comes from labeling genes from zero to N (which gives a total of N+1 genes). This will be convenient in Chapter 6 when we further generalize this argument to a continuous network. The generalization of Figure 5.4 is given by Figure 5.5.

The N+1 gene network translates into a (2N+2)-dimensional system of coupled DDEs (cf.(5.5)-(5.6)) as follows

$$\frac{dm_i}{dt} \;=\; -\mu\, m_i \;+\; \sum_{j=0}^{N} G_{ij}\, H\left(p_j(t-T)\right) \tag{5.13}$$

$$\frac{dp_i}{dt} \;=\; m_i - \mu\, p_i \tag{5.14}$$

where $i = 0, 1, 2, \ldots, N$.

As explained previously, we may consider two different biological scenarios: uniform and exponential weighting. Both of these extend naturally from the equations presented earlier as follows:

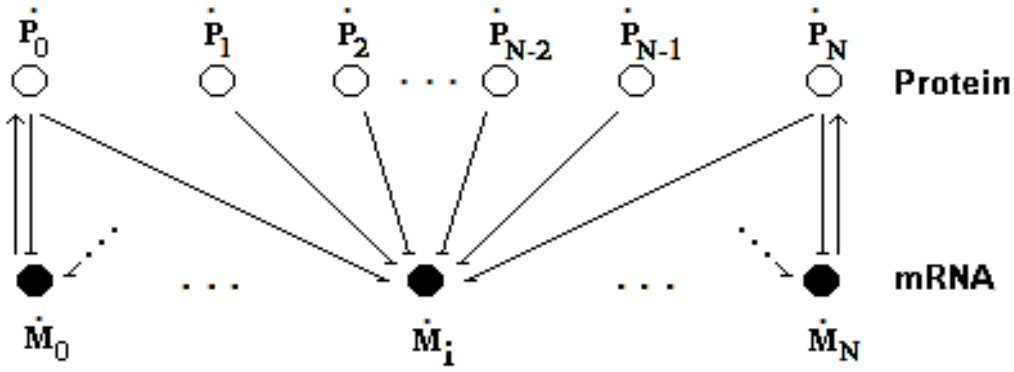

Figure 5.5: Geometric representation for the N+1 coupled system.

Case 1 (Uniform weighting): We choose G_{ij}=$\frac{1}{N+1}$ and a Hill function as in Eq.(5.7) (for $i = 0, 1, 2, \ldots, N$) giving thus the following system of equations:

$$\frac{dm_i}{dt} = -\mu\, m_i + \frac{1}{N+1}\sum_{j=0}^{N}\frac{1}{1+\left(\frac{p_j(t-T)}{p_{0j}}\right)^n} \tag{5.15}$$

$$\frac{dp_i}{dt} = m_i - \mu\, p_i \tag{5.16}$$

Case 2 (Exponential weighting): Here we choose G_{ij}=exp$\left(-\frac{|i-j|}{N}\right)$ and a Hill function of the form in Eq.(5.10) with a resulting system of the form

$$\frac{dm_i}{dt} = -\mu\, m_i + \frac{1}{N}\sum_{j=0}^{N} e^{-|i-j|/N}\left(1 - p_j(t-T) + \alpha\, p_j^3(t-T)\right) \tag{5.17}$$

$$\frac{dp_i}{dt} = m_i - \mu\, p_i \tag{5.18}$$

for $i = 0, 1, 2, \ldots, N$.

5.3 Uniform Weighting: Multiple Gene Network

5.3.1 Linear Analysis

To start the analysis we set $\dot{m}_i = \dot{p}_i = 0$ in Eqs.(5.15), (5.16) and find the equilibrium point $(m_0^*, \ldots, m_N^*, p_0^*, \ldots, p_N^*)$, which satisfies the following equations

$$\mu\, m_i^* = \frac{1}{N+1} \sum_{j=0}^{N} \frac{1}{1 + \left(\frac{p_j^*}{p_{j0}}\right)^n} \tag{5.19}$$

$$m_i^* = \mu\, p_i^* \tag{5.20}$$

We eliminate the m_i^*'s by substituting Eq.(5.20) into (5.19) and obtain

$$\mu^2\, p_i^* = \frac{1}{N+1} \sum_{j=0}^{N} \frac{1}{1 + \left(\frac{p_j^*}{p_{j0}}\right)^n} \tag{5.21}$$

Since Eq.(5.21) holds for any i=0, 1, … N, then the sum on the RHS will be constant and thus p_i^*=p^* will always be an equilibrium solution. Also, from Eq.(5.20) we have m_i^*=m^*=μp^*. Thus, using Eq.(5.21), the algebraic equation on p^* for the steady state $(\mu p^*, \ldots, \mu p^*, p^*, \ldots, p^*)$ will be given by

$$\mu^2\, p^* - \frac{1}{N+1} \sum_{j=0}^{N} \frac{p_{j0}^n}{p_{j0}^n + p^{*\,n}} = 0 \tag{5.22}$$

which can be multiplied by the product $(p_{00}^n + p^{*\,n})(p_{10}^n + p^{*\,n}) \cdots (p_{N0}^n + p^{*\,n})$, and thus be made into a polynomial of degree $n(N+1)+1$. The latter may then be solved numerically.

Next we define ξ_i and η_i to be deviations from equilibrium: $\xi_i = m_i - m^*$, $\eta_i = p_i - p^*$. Substituting the latter into (5.15) and (5.16) yields

$$\dot{\xi}_i = -\mu(\xi_i + m^*) + \frac{1}{N+1} \sum_{j=0}^{N} \frac{1}{1 + \left(\frac{\eta_{jd} + p^*}{p_{j0}}\right)^n} \tag{5.23}$$

$$\dot{\eta}_i = \xi_i - \mu\eta_i \tag{5.24}$$

Expanding for small η_{jd} Eq.(5.23) becomes

$$\dot{\xi}_i = -\mu\xi_i + \frac{1}{N+1}\left(\sum_{j=0}^{N} K_{j1}\eta_{jd} + \sum_{j=0}^{N} K_{j2}\eta_{jd}^2 + \sum_{j=0}^{N} K_{j3}\eta_{jd}^3 + \ldots\right) \tag{5.25}$$

where the Taylor coefficients, K_{ji}, are given as follows

$$K_{j1} = -\frac{n\beta_j}{(1+\beta_j)^2\, p^*}, \quad \text{where} \quad \beta_j = \left(\frac{p^*}{p_{j0}}\right)^n \tag{5.26}$$

$$K_{j2} = \frac{n\beta_j\left(\beta_j n - n + \beta_j + 1\right)}{2\left(1+\beta_j\right)^3\, p^{*2}} \tag{5.27}$$

$$K_{j3} = -\frac{n\beta_j\left(\beta_j^2 n^2 - 4\beta_j n^2 + n^2 + 3\beta_j^2 n - 3n + 2\beta_j^2 + 4\beta_j + 2\right)}{6\left(1+\beta_j\right)^4\, p^{*3}} \tag{5.28}$$

Now we prove that the steady state is stable when $T = 0$ (no delay) by considering the (2N+2)-dimensional linearized system coming from Eqs.(5.24)-(5.25):

$$\dot{\xi}_i = -\mu\xi_i + \frac{1}{N+1}\sum_{j=0}^{N} K_{j1}\eta_{jd} \tag{5.29}$$

$$\dot{\eta}_i = \xi_i - \mu\eta_i \tag{5.30}$$

Using linear analysis [81, 96] the system (5.29)-(5.30) has the following (2N+2) × (2N+2) Jacobian at the origin:

$$J = \begin{pmatrix} M & K \\ I & M \end{pmatrix} \tag{5.31}$$

where I is the (N+1)×(N+1) identity matrix, $M = -\mu I$, and

$$K = \frac{1}{N+1}\begin{pmatrix} K_{01} & K_{11} & \ldots & K_{N-1\,1} & K_{N1} \\ K_{01} & K_{11} & \ldots & K_{N-1\,1} & K_{N1} \\ \vdots & & \ldots & & \vdots \\ K_{01} & K_{11} & \ldots & K_{N-1\,1} & K_{N1} \\ K_{01} & K_{11} & \ldots & K_{N-1\,1} & K_{N1} \end{pmatrix}_{(N+1)\times(N+1)} \tag{5.32}$$

To find the eigenvalues, λ, of the Jacobian, J, we use basic properties of the determinant function on block matrices:

$$\det\begin{pmatrix} M-\lambda I & K \\ I & M-\lambda I \end{pmatrix} = \det((M-\lambda I)^2 - K) \tag{5.33}$$

$$= \det\left((\mu+\lambda)^2 I - K\right) \tag{5.34}$$

and equate to zero

$$\det((\mu+\lambda)^2 I - K) = (\lambda+\mu)^{2N+2} \det\left(\frac{1}{(\lambda+\mu)^2}K - I\right) = 0 \tag{5.35}$$

Using Eq.(5.38) (derived in the claim below) on the last equality of Eq.(5.35) we conclude that the eigenvalues are

$$\left\{-\mu\,, \quad -\mu \pm \sqrt{\frac{1}{N+1}\sum_{j=0}^{N} K_{j1}}\right\} \tag{5.36}$$

where $\mu>0$ and since $K_{j1}<0\ \forall j$ then the square root term in Eq.(5.36) will be imaginary and thus $\mathrm{Re}(\lambda)<0$ for all λ. The latter shows that the origin is stable for $T = 0$ (no delay).

Claim: If A_n is a square matrix of the form

$$A_n = \begin{pmatrix} a_1 & a_2 & \dots & a_{n-1} & a_n \\ a_1 & a_2 & \dots & a_{n-1} & a_n \\ \vdots & & \ddots & & \vdots \\ a_1 & a_2 & \dots & a_{n-1} & a_n \\ a_1 & a_2 & \dots & a_{n-1} & a_n \end{pmatrix}_{n\times n} \tag{5.37}$$

then the following holds

$$\det(kA_n - I) = (-1)^{n+1}\left[k\sum_{j=1}^{n} a_j - 1\right] \tag{5.38}$$

Proof: We use induction on n. For n=1 the claim holds true. To prove the inductive step we assume Eq.(5.38) holds for n and consider its n+1 version:

$$|kA_{n+1} - I| = \left| k \begin{pmatrix} & & & a_{n+1} \\ & A_n & & a_{n+1} \\ & & & \vdots \\ a_1 & a_2 & \dots & a_{n+1} \end{pmatrix} - I \right| = \left\| \begin{pmatrix} ka_1 - 1 & ka_2 & \dots & ka_{n+1} \\ ka_1 & ka_2 - 1 & \dots & ka_{n+1} \\ \vdots & & \ddots & \vdots \\ ka_1 & ka_2 & \dots & ka_{n+1} - 1 \end{pmatrix} \right|$$

Multiplying the last row by $h = -ka_{n+1}/(ka_{n+1} - 1)$ and adding it to the rest of the above n rows we obtain the following equivalent matrix

$$\left\| \begin{pmatrix} ka_1(h+1) - 1 & ka_2(h+1) & \dots & ka_n(h+1) & 0 \\ ka_1(h+1) & ka_2(h+1) - 1 & \dots & ka_n(h+1) & 0 \\ \vdots & \vdots & \ddots & \vdots & \vdots \\ ka_1(h+1) & ka_2(h+1) & \dots & ka_n(h+1) - 1 & 0 \\ ka_1 & ka_2 & \dots & ka_n & ka_{n+1} - 1 \end{pmatrix} \right| \tag{5.39}$$

which may be expanded by cofactors through the last column

$$(ka_{n+1} - 1) \left\| \begin{pmatrix} ka_1(h+1) - 1 & ka_2(h+1) & \dots & ka_n(h+1) \\ ka_1(h+1) & ka_2(h+1) - 1 & \dots & ka_n(h+1) \\ \vdots & \vdots & \ddots & \vdots \\ ka_1(h+1) & ka_2(h+1) & \dots & ka_n(h+1) - 1 \end{pmatrix} \right| \tag{5.40}$$

which by induction (i.e. using Eq.(5.38)) yields

$$|kA_{n+1} - I| \;=\; (ka_{n+1} - 1)\,(-1)^{n+1} \left[k(h+1) \sum_{j=1}^{n} a_j - 1 \right] \tag{5.41}$$

and by substituting $h = -ka_{n+1}/(ka_{n+1} - 1)$ we obtain

$$|kA_{n+1} - I| \;=\; (-1)^{n+2} \left[k \sum_{j=1}^{n+1} a_j - 1 \right] \tag{5.42}$$

This proves our claim.

Now that we know that the origin is stable for no delay, then the next step is to find the critical delay, T=T_{cr}, where the bifurcation occurs and the equilibrium point, given by (5.22), loses its stability. We start by assuming solutions of the form

$$\eta_i = A_i \exp(\lambda t) \tag{5.43}$$

$$\xi_i = B_i \exp(\lambda t) \tag{5.44}$$

substitute them into (5.29)-(5.30)

$$(\lambda + \mu)\, B_i = \frac{e^{-\lambda T}}{N+1} \sum_{j=0}^{N} K_{j1} A_j \tag{5.45}$$

$$(\lambda + \mu)\, A_i = B_i \tag{5.46}$$

eliminate B_i from (5.45)-(5.46), and set T=T_{cr} and λ=iω to obtain

$$A_i = \frac{c}{N+1} \sum_{j=0}^{N} K_{j1} A_j \tag{5.47}$$

where

$$c = \frac{e^{-\mathrm{i}\omega T_{cr}}}{(\mathrm{i}\omega + \mu)^2} \in \mathbb{C} \tag{5.48}$$

The N+1 algebraic equations (5.47) will have solutions if

$$\det(cK - I) = 0 \tag{5.49}$$

where K is given by Eq.(5.32). Using Eq.(5.49) on (5.38) we find

$$c \sum_{j=0}^{N} K_{j1} = N + 1 \tag{5.50}$$

which implies

$$\mathrm{Im}(c) = 0 \quad \Leftrightarrow \quad \frac{(\omega^2 - \mu^2)\sin(\omega T_{cr}) - 2\omega\mu\cos(\omega T_{cr})}{(\mu^2 + \omega^2)^2} = 0 \tag{5.51}$$

$$\Leftrightarrow \quad T_{cr} = \frac{1}{\omega} \arctan\left(\frac{2\omega\mu}{\omega^2 - \mu^2}\right) \tag{5.52}$$

In addition, equating the real parts of Eq.(5.50) yields the critical frequency

$$\begin{aligned} & \mathrm{Re}(c)\sum_{j=0}^{N} K_{j1} \;=\; N+1 \\ \Leftrightarrow \quad & \frac{(\mu^2-\omega^2)\cos(\omega T_{cr}) - 2\omega\mu\sin(\omega T_{cr})}{(\mu^2+\omega^2)^2}\sum_{j=0}^{N} K_{j1} = N+1 \qquad (5.53) \\ \Leftrightarrow \quad & \omega \;=\; \sqrt{-\mu^2 - \frac{1}{N+1}\sum_{j=0}^{N} K_{j1}} \qquad (5.54) \end{aligned}$$

where we have used the trig identities

$$\sin(\omega T_{cr}) \;=\; \sin\left(\arctan\left(\frac{2\omega\mu}{\omega^2-\mu^2}\right)\right) \;=\; \frac{2\omega\mu}{\omega^2+\mu^2} \qquad (5.55)$$

$$\cos(\omega T_{cr}) \;=\; \cos\left(\arctan\left(\frac{2\omega\mu}{\omega^2-\mu^2}\right)\right) \;=\; \frac{\omega^2-\mu^2}{\omega^2+\mu^2} \qquad (5.56)$$

Equation (5.52) is the critical delay, where the origin loses its stability, and Eq.(5.54) is the critical frequency in terms of the Taylor coefficients given by Eq.(5.26).

5.3.2 Nonlinear Analysis

In this section we use Lindstedt's perturbation method to find closed form approximate expressions for the amplitude of the limit cycle born at the Hopf. This will be accomplished by considering the full nonlinear system (5.24)-(5.25) and perturbing off of the critical delay value, T=T_{cr}. We start by combining Eqs.(5.24) and (5.25) into a second order DDE

$$\ddot{\eta}_i + 2\mu\dot{\eta}_i + \mu^2\eta_i \;=\; \sum_{j=0}^{N}\frac{K_{j1}}{N+1}\eta_{jd} + \sum_{j=0}^{N}\frac{K_{j2}}{N+1}\eta_{jd}^2 + \sum_{j=0}^{N}\frac{K_{j3}}{N+1}\eta_{jd}^3 + \ldots \qquad (5.57)$$

where K_{j1}, K_{j2}, and K_{j3} are the Taylor coefficients given by Eqs.(5.26)-(5.28), respectively. Next we introduce a small parameter ϵ via the following scaling

$$\eta_i \;=\; \epsilon u_i \qquad (5.58)$$

where $i = 0, 1, \ldots, N$. We stretch time by defining a new independent variable

$$\tau \;=\; \Omega t \tag{5.59}$$

and expand Ω in a power series in ϵ as follows

$$\Omega \;=\; \omega + \epsilon^2 k_2 + \ldots \tag{5.60}$$

where we omit the $O(\epsilon)$ term since it turns out to be zero. We substitute (5.58) and (5.59) into (5.57) to obtain

$$\Omega^2 \frac{d^2 u_i}{d\tau^2} \;+\; 2\mu\Omega \frac{du_i}{d\tau} \quad + \quad \mu^2 u_i \;-\; \sum_{j=0}^{N} \frac{K_{j1}}{N+1} u_{jd} \;= \\ \epsilon \sum_{j=0}^{N} \frac{K_{j2}}{N+1} u_{jd}^2 \;+\; \epsilon^2 \sum_{j=0}^{N} \frac{K_{j3}}{N+1} u_{jd}^3 \;+\; \ldots \tag{5.61}$$

Next we introduce a small detuning, Δ, about the critical delay, T_{cr},

$$T \;=\; T_{cr} + \Delta \;=\; T_{cr} + \epsilon^2 \delta \tag{5.62}$$

where Δ is scaled like ϵ^2. Substituting Eqs.(5.62) and (5.60) into $u_{jd} = u_j(\tau - \Omega T)$ and Taylor expanding about ϵ=0 we obtain

$$u_{jd} \;=\; u_j(\tau - \Omega T) \quad = \quad u_j(\tau - \omega T_{cr} - \epsilon^2(k_2 T_{cr} + \omega\delta) + \ldots) \tag{5.63}$$

$$= \quad u_j(\tau - \omega T_{cr}) - \epsilon^2(k_2 T_{cr} + \omega\delta) u_j'(\tau - \omega T_{cr}) + \ldots \tag{5.64}$$

Next we expand $u_j(\tau)$ in a power series in ϵ

$$u_j(\tau) \;=\; u_{j0}(\tau) + \epsilon u_{j1}(\tau) + \epsilon^2 u_{j2}(\tau) + \ldots \tag{5.65}$$

and by substituting the latter and Eqs.(5.60) and (5.64) into (5.61), and collecting like powers of ϵ we find

$$\omega^2 \frac{d^2 u_{i0}}{d\tau^2} + 2\mu\omega \frac{du_{i0}}{d\tau} + \mu^2 u_{i0} - \sum_{j=0}^{N} \frac{K_{j1}}{N+1} u_{j0}(\tau - \omega T_{cr}) = 0 \tag{5.66}$$

$$\omega^2 \frac{d^2 u_{i1}}{d\tau^2} + 2\mu\omega \frac{du_{i1}}{d\tau} + \mu^2 u_{i1} - \sum_{j=0}^{N} \frac{K_{j1}}{N+1} u_{j1}(\tau - \omega T_{cr}) = \sum_{j=0}^{N} \frac{K_{j2}}{N+1} u_{j0}^2(\tau - \omega T_{cr}) \tag{5.67}$$

$$\omega^2 \frac{d^2 u_{i2}}{d\tau^2} + 2\mu\omega \frac{du_{i2}}{d\tau} + \mu^2 u_{i2} - \sum_{j=0}^{N} \frac{K_{j1}}{N+1} u_{j2}(\tau - \omega T_{cr}) = \ldots \tag{5.68}$$

where $\ldots$ stands for terms in u_{i0} and u_{i1}, omitted here for brevity.

We take the solutions, u_{i0}, of the system (5.66) as

$$u_{i0}(\tau) = \hat{A} \cos\tau \tag{5.69}$$

where by Eq.(5.58) we know $\eta_{i0} = \epsilon u_{i0} = \epsilon \hat{A} \cos\tau = A \cos\tau$. Next we substitute (5.69) into (5.67) and obtain the following expression for u_{i1}:

$$u_{i1}(\tau) = m_1 \sin 2\tau + m_2 \cos 2\tau + m_3 \tag{5.70}$$

where m_1 is given by the equation:

$$m_1 = -\frac{2\,\hat{A}^2\,\hat{K}_2\,\mu\,\omega^3\,\left(2\,\mu^2 + 3\,\hat{K}_1\right)}{\hat{K}_1\,\left(16\,\mu^6 + 39\,\hat{K}_1\,\mu^4 + 18\,\hat{K}_1^2\,\mu^2 - 9\,\hat{K}_1^3\right)} \tag{5.71}$$

where

$$\hat{K}_1 = \sum_{j=0}^{N} \frac{K_{j1}}{N+1}, \quad \hat{K}_2 = \sum_{j=0}^{N} \frac{K_{j2}}{N+1}, \quad \text{and} \quad \hat{K}_3 = \sum_{j=0}^{N} \frac{K_{j3}}{N+1} \tag{5.72}$$

and where we omit the expressions for m_2 and m_3 for brevity.

Next we substitute Eqs.(5.69) and (5.70) into (5.68), and after trigonometric simplifications have been performed, we equate to zero the coefficients of the resonant terms $\sin\tau$ and $\cos\tau$. This yields the amplitude, A, of the limit cycle that was born in the Hopf bifurcation:

$$A^2 = \frac{P}{Q}\,\Delta \tag{5.73}$$

where

$$P = 8\,\hat{K}_1^2\,\omega^2\left(\mu^2-\hat{K}_1\right)\left(16\,\mu^6+39\,\hat{K}_1\,\mu^4+18\,\hat{K}_1^2\,\mu^2-9\,\hat{K}_1^3\right) \tag{5.74}$$

$$Q = Q_0\,T_{cr} + Q_1 \tag{5.75}$$

and

$$\begin{aligned} Q_0 = {} & 48\,\hat{K}_3\,\hat{K}_1^2\,\mu^8-16\,\hat{K}_2^2\,\hat{K}_1\,\mu^8+69\,\hat{K}_3\,\hat{K}_1^3\,\mu^6+32\,\hat{K}_2^2\,\hat{K}_1^2\,\mu^6-63\,\hat{K}_3\,\hat{K}_1^4\,\mu^4 \\ & +162\,\hat{K}_2^2\,\hat{K}_1^3\,\mu^4-81\,\hat{K}_3\,\hat{K}_1^5\,\mu^2+108\,\hat{K}_2^2\,\hat{K}_1^4\,\mu^2+27\,\hat{K}_3\,\hat{K}_1^6-30\,\hat{K}_2^2\,\hat{K}_1^5 \end{aligned} \tag{5.76}$$

$$\begin{aligned} Q_1 = {} & -96\,\hat{K}_3\,\hat{K}_1\,\mu^9+64\,\hat{K}_2^2\,\mu^9-138\,\hat{K}_3\,\hat{K}_1^2\,\mu^7+16\,\hat{K}_2^2\,\hat{K}_1\,\mu^7+126\,\hat{K}_3\,\hat{K}_1^3\,\mu^5 \\ & -308\,\hat{K}_2^2\,\hat{K}_1^2\,\mu^5+162\,\hat{K}_3\,\hat{K}_1^4\,\mu^3-296\,\hat{K}_2^2\,\hat{K}_1^3\,\mu^3-54\,\hat{K}_3\,\hat{K}_1^5\,\mu+12\,\hat{K}_2^2\,\hat{K}_1^4\mu \end{aligned} \tag{5.77}$$

and where the $\hat{K}_i$'s are given by Eq.(5.72) and Eqs.(5.26)-(5.28).

Eq.(5.73) is the expression for the limit cycle amplitude. Notice that the expression for A found in this section is the generalization of the single gene amplitude found in Section 4.3 Eq.(4.43). Also notice that each gene unit behaves identically at steady state. As we will see, this behavior is in contrast to the exponential weighting case, where each gene unit has a different amplitude of oscillation.

5.4 Exponential Weighting: Two Gene Network

In this section we analyze Case 2 (Exponential weighting) presented in Section 5.2.1 Eqs.(5.11)-(5.12), where we choose $G_{ij}=e^{-|i-j|}$. In this case, each protein product is shared unequally, with nearby gene promoter sites being repressed

to a greater extent than more distant ones. We choose the Hill function as in Eq.(5.10) and use the system (5.11)-(5.12) for our analysis.

5.4.1 Steady State Solutions

We begin our analysis by considering the following 4-dimensional system

$$\dot{m}_0 = -\mu m_0 + H(p_{0d}) + e^{-1}H(p_{1d}), \quad \dot{p}_0 = m_0 - \mu p_0 \tag{5.78}$$

$$\dot{m}_1 = -\mu m_1 + e^{-1}H(p_{0d}) + H(p_{1d}), \quad \dot{p}_1 = m_1 - \mu p_1 \tag{5.79}$$

with an associated geometric representation given by Figure 5.4 in Section 5.2.1. The steady state will satisfy $\dot{p}_i$=$\dot{m}_i$=0, p_i=p_i^*, m_i=m_i^*, which gives

$$\mu^2 p_0^* = H(p_0^*) + e^{-1}H(p_1^*) \tag{5.80}$$

$$\mu^2 p_1^* = e^{-1}H(p_0^*) + H(p_1^*) \tag{5.81}$$

and by using (5.10)

$$\mu^2 p_0^* = \left(1 - p_0^* + \alpha {p_0^*}^3\right) + e^{-1}\left(1 - p_1^* + \alpha {p_1^*}^3\right) \tag{5.82}$$

$$\mu^2 p_1^* = e^{-1}\left(1 - p_0^* + \alpha {p_0^*}^3\right) + \left(1 - p_1^* + \alpha {p_1^*}^3\right) \tag{5.83}$$

Since Eqs.(5.82) and (5.83) are invariant (symmetric) $p_0^* \leftrightarrow p_1^*$, then steady state satisfies $p^* = p_0^* = p_1^*$ and Eq.(5.82) becomes

$$\mu^2 p^* = \left(1 + \frac{1}{e}\right)\left(1 - p^* + \alpha {p^*}^3\right) \tag{5.84}$$

which will give the steady state as a function of μ and α.

As an example consider $\mu = 0.2$ and $\alpha = 0.01$. Using Macsyma's root_by_bisection on Eq.(5.84) gives $p^* \approx 0.98075$. The latter agrees with Matlab's dde23 numerical simulation of Eqs.(5.78)-(5.79) given in Figure 5.6.

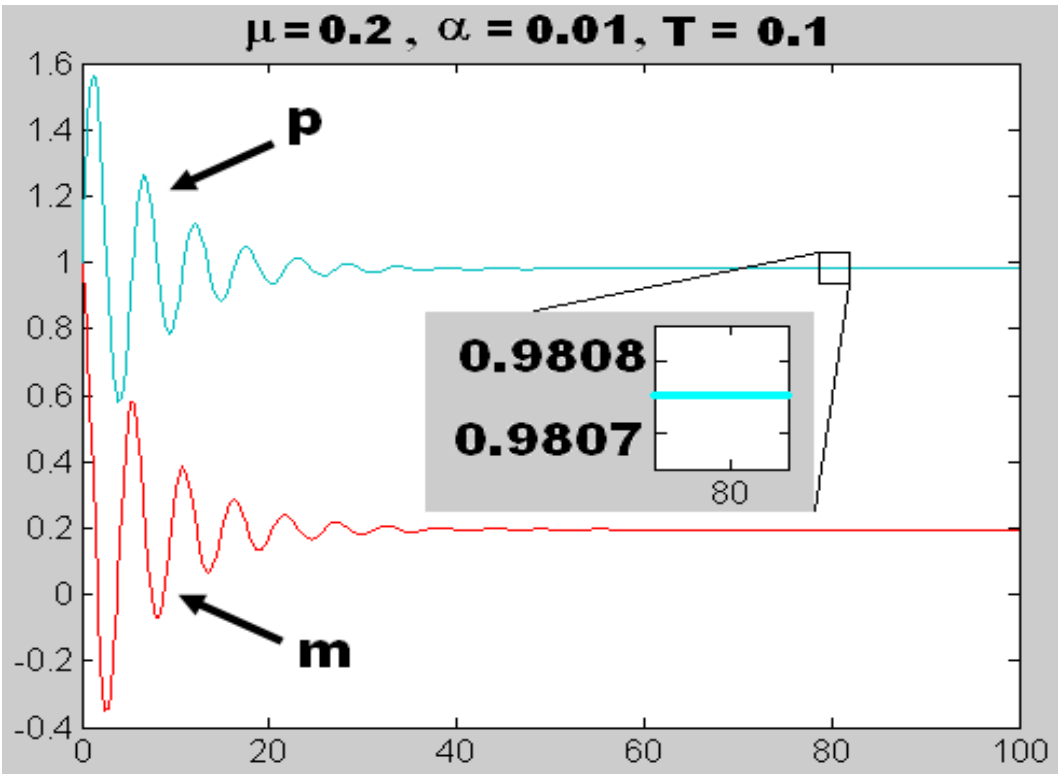

Figure 5.6: Matlab numerical simulation for Eqs.(5.78)-(5.79). Notice that the steady state is approximately p^*=0.98075

5.4.2 Linear Stability Analysis

If ξ_i and η_i (i=0,1) are deviations from equilibrium $\xi_i=m_i-m^*$ and $\eta_i=p_i-p^*$, then substitution into Eqs.(5.78)-(5.79) yields

$$\dot{\xi}_0 = -\mu(\xi_0 + m^*) + H(\eta_{0d} + p^*) + e^{-1}H(\eta_{1d} + p^*), \quad \dot{\eta}_0 = \xi_0 - \mu\eta_0 \tag{5.85}$$

$$\dot{\xi}_1 = -\mu(\xi_1 + m^*) + e^{-1}H(\eta_{0d} + p^*) + H(\eta_{1d} + p^*), \quad \dot{\eta}_1 = \xi_1 - \mu\eta_1 \tag{5.86}$$

which become

$$\dot{\xi}_0 = -\mu\xi_0 + G(\eta_{0d}) + e^{-1}G(\eta_{1d}), \quad \dot{\eta}_0 = \xi_0 - \mu\eta_0 \tag{5.87}$$

$$\dot{\xi}_1 = -\mu\xi_1 + e^{-1}G(\eta_{0d}) + G(\eta_{1d}), \quad \dot{\eta}_1 = \xi_1 - \mu\eta_1 \tag{5.88}$$

where

$$G(\eta) = \left(-1 + 3\alpha p^{*2}\right)\eta + 3\alpha p^* \eta^2 + \alpha\eta^3 \tag{5.89}$$

To find the critical frequency, ω_{cr}, and its associated critical delay, T_{cr}, we linearize Eqs.(5.87)-(5.88) for small η_i to obtain

$$\dot{\xi}_0 = -\mu\xi_0 + \left(-1 + 3\alpha p^{*\,2}\right)\eta_{0d} + e^{-1}\left(-1 + 3\alpha p^{*\,2}\right)\eta_{1d} \tag{5.90}$$

$$\dot{\eta}_0 = \xi_0 - \mu\eta_0 \tag{5.91}$$

$$\dot{\xi}_1 = -\mu\xi_1 + e^{-1}\left(-1 + 3\alpha p^{*\,2}\right)\eta_{0d} + \left(-1 + 3\alpha p^{*\,2}\right)\eta_{1d} \tag{5.92}$$

$$\dot{\eta}_1 = \xi_1 - \mu\eta_1 \tag{5.93}$$

If $\xi_i = A_i e^{\lambda t}$ and $\eta_i = B_i e^{\lambda t}$ then Eqs.(5.90)-(5.93) become

$$(\lambda + \mu)A_0 = \left(-1 + 3\alpha p^{*\,2}\right)B_0 e^{-\lambda T} + e^{-1}\left(-1 + 3\alpha p^{*\,2}\right)B_1 e^{-\lambda T} \tag{5.94}$$

$$(\lambda + \mu)B_0 = A_0 \tag{5.95}$$

$$(\lambda + \mu)A_1 = e^{-1}\left(-1 + 3\alpha p^{*\,2}\right)B_0 e^{-\lambda T} + \left(-1 + 3\alpha p^{*\,2}\right)B_1 e^{-\lambda T} \tag{5.96}$$

$$(\lambda + \mu)B_1 = A_1 \tag{5.97}$$

which yields

$$-e^{\lambda T}(\lambda + \mu)^2 B_0 = \left(1 - 3\alpha p^{*\,2}\right)B_0 + e^{-1}\left(1 - 3\alpha p^{*\,2}\right)B_1 \tag{5.98}$$

$$-e^{\lambda T}(\lambda + \mu)^2 B_1 = e^{-1}\left(1 - 3\alpha p^{*\,2}\right)B_0 + \left(1 - 3\alpha p^{*\,2}\right)B_1 \tag{5.99}$$

The eigenvalue problem $MB = rB$ given by

$$M = \begin{pmatrix} \left(1 - 3\alpha p^{*\,2}\right) & e^{-1}\left(1 - 3\alpha p^{*\,2}\right) \\ e^{-1}\left(1 - 3\alpha p^{*\,2}\right) & \left(1 - 3\alpha p^{*\,2}\right) \end{pmatrix} \tag{5.100}$$

$$B = \begin{pmatrix} B_0 \\ B_1 \end{pmatrix} \tag{5.101}$$

$$r = -e^{\lambda T}(\lambda + \mu)^2 \tag{5.102}$$

will have nontrivial solutions when

$$\det(M - rI) = 0 \Leftrightarrow \left[\left(1 - 3\alpha p^{*\,2}\right) - r\right]^2 - e^{-2}\left(1 - 3\alpha p^{*\,2}\right)^2 = 0 \tag{5.103}$$

$$\Leftrightarrow \left(1 - 3\alpha p^{*\,2}\right) - r = \pm e^{-1}\left(1 - 3\alpha p^{*\,2}\right) \tag{5.104}$$

$$\Leftrightarrow r = \left(1 \pm e^{-1}\right)\left(1 - 3\alpha p^{*\,2}\right) \tag{5.105}$$

Now that r is known we have two cases:

(i) When $T = 0$ Eq.(5.102) gives

$$r = -(\lambda + \mu)^2 \quad \Rightarrow \quad \lambda = -\mu \pm \sqrt{-r} \tag{5.106}$$

If $r > 0$ then $\mathrm{Re}(\lambda) = -\mu < 0$ (for $\mu > 0$) and the system has a stable steady state.

(ii) When $T = T_{cr}$ and $\lambda = i\omega$, Eq.(5.102) becomes

$$r = -e^{i\omega T_{cr}}(i\omega + \mu)^2 \tag{5.107}$$

which gives the two real equations

$$r = 2\mu\omega \sin\omega T_{cr} + \left(\omega^2 - \mu^2\right)\cos\omega T_{cr} \tag{5.108}$$

$$0 = \left(\omega^2 - \mu^2\right)\sin\omega T_{cr} - 2\mu\omega \cos\omega T_{cr} \tag{5.109}$$

Solving Eqs.(5.108),(5.109) for $\sin\omega T_{cr}$ and $\cos\omega T_{cr}$ we obtain

$$\omega = \sqrt{r - \mu^2} \tag{5.110}$$

where we have used the trig identity $\sin^2\omega T_{cr} + \cos^2\omega T_{cr} = 1$. Dividing the expressions for $\sin\omega T_{cr}$ and $\cos\omega T_{cr}$ and solving for T_{cr} we also obtain

$$T_{cr} = \frac{1}{\omega}\arctan\left(\frac{2\mu\omega}{\omega^2 - \mu^2}\right) \tag{5.111}$$

As before, we compare our results when $\mu = 0.2$ and $\alpha = 0.01$. Using Eqs.(5.105) and (5.84) we obtain

$$r = \left(1 \pm e^{-1}\right)\left(1 - 3(.01)(0.98075)^2\right) = 1.32841 \text{ or } 0.61388 \tag{5.112}$$

which gives

$$\omega_{cr} = \sqrt{r - \mu^2} = 1.13508 \text{ or } 0.75755 \tag{5.113}$$

$$T_{cr} = \frac{1}{\omega}\arctan\left(\frac{2\mu\omega}{\omega^2 - \mu^2}\right) = 0.30731 \text{ or } 0.68146 \tag{5.114}$$

which implies $T_{cr} \approx 0.30731$ by taking the smallest T_{cr} in (5.114). To confirm our previous results we numerically integrate Eqs.(5.78)-(5.79) using Matlab's dde23. The numerical results give $T_{cr} \approx 0.3087$ with an associated amplitude of oscillation of approximately $1.6441 - 0.96291 = 0.68119$, which comes from the difference between the approximate maximum value of the amplitude (Figure 5.7) and the approximate value of the steady state (Figure 5.6).

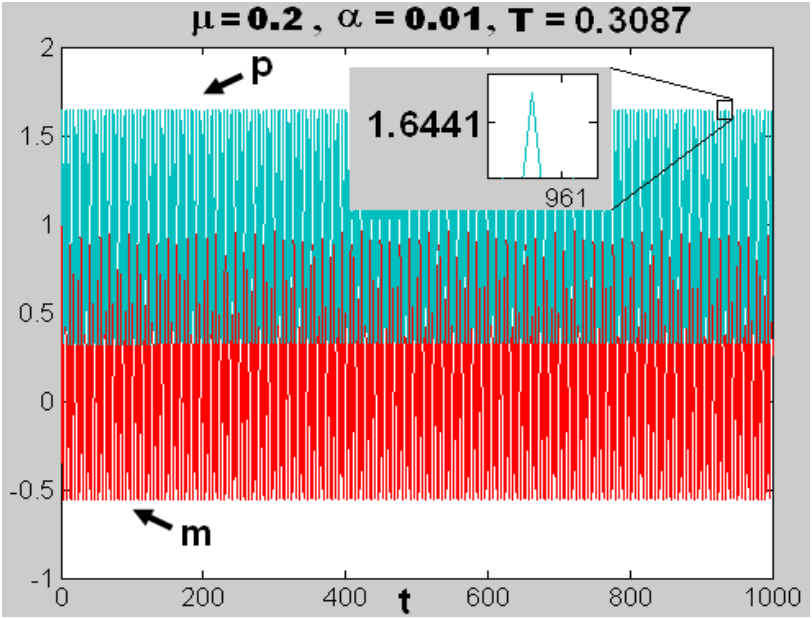

Figure 5.7: Matlab numerical simulation for $T = T_{cr} \approx 0.3087$. Notice that the maximum value of oscillation is approximately 1.6441

5.4.3 Nonlinear Numerical Investigations

In this section we investigate the nonlinear behavior of Eqs.(5.78)-(5.79) close to the Hopf when $T = T_{cr}$. We set $T = T_{cr} + \Delta$ and then repeat the analysis presented in Section 5.4.2 for various $\Delta = T - T_{cr}$. Using Matlab's dde23 we obtain Figure 5.8, which contains the numerical integration results by plotting the amplitude

curve for various Δ. In Figure 5.9 we show the solution curves for various points in the detuning-amplitude plot.

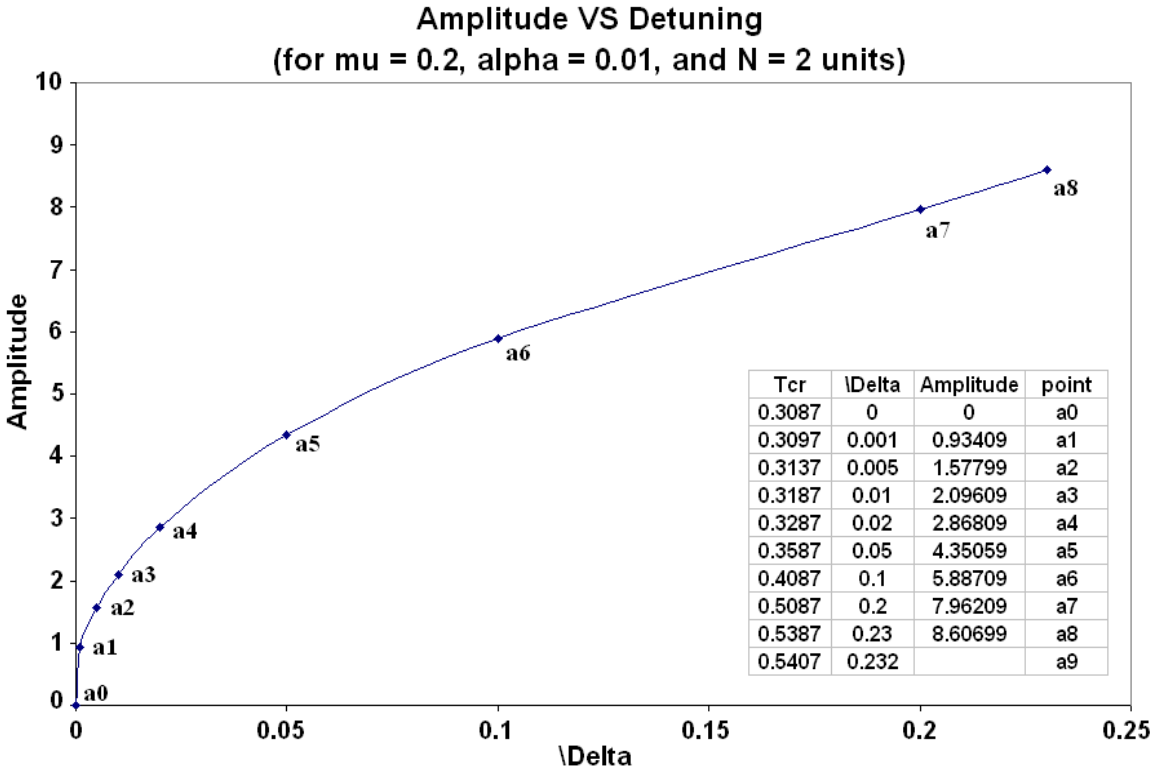

Figure 5.8: Amplitude VS Detuning graph. The corresponding solution curves for each point can be found in Figure 5.9. The amplitude is found by subtracting the largest value of p found in Figure 5.9 and p^* found in Figure 5.6.

We point out that Figure 5.10 is the plot of the numerical integration results for $\Delta = 0.232$ (see Figure 5.8 point "$a9$"). This is a limiting point where the behavior of the increasing amplitude changes. We hypothesize that an unknown bifurcation could be taking place (e.g. homoclinic bifurcation). Another possibility is that Matlab is not capable of numerically integrating the system when the oscillations become arbitrarily large.

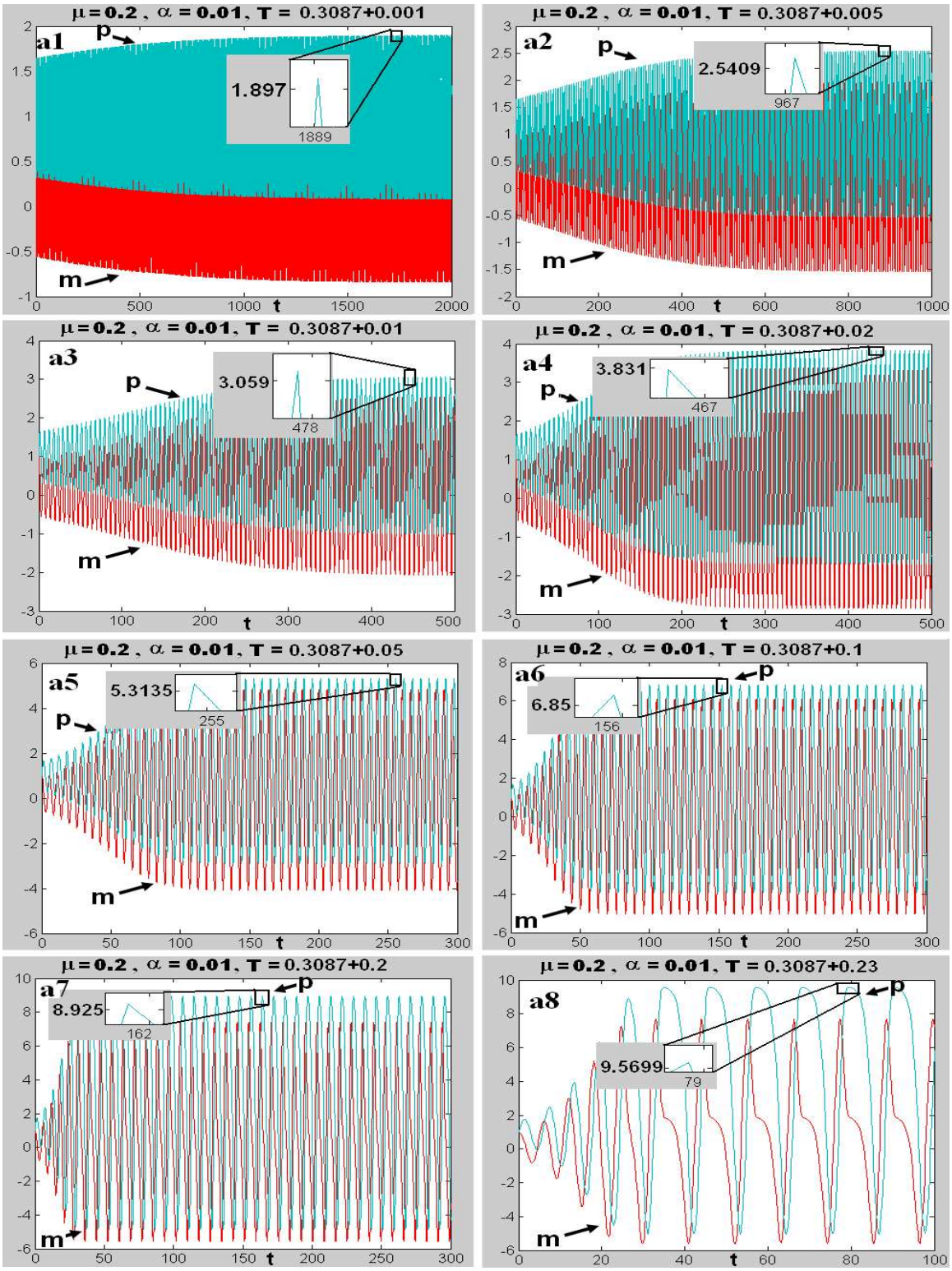

Figure 5.9: Solutions p and m for detuning-amplitude plot in Figure 5.8.

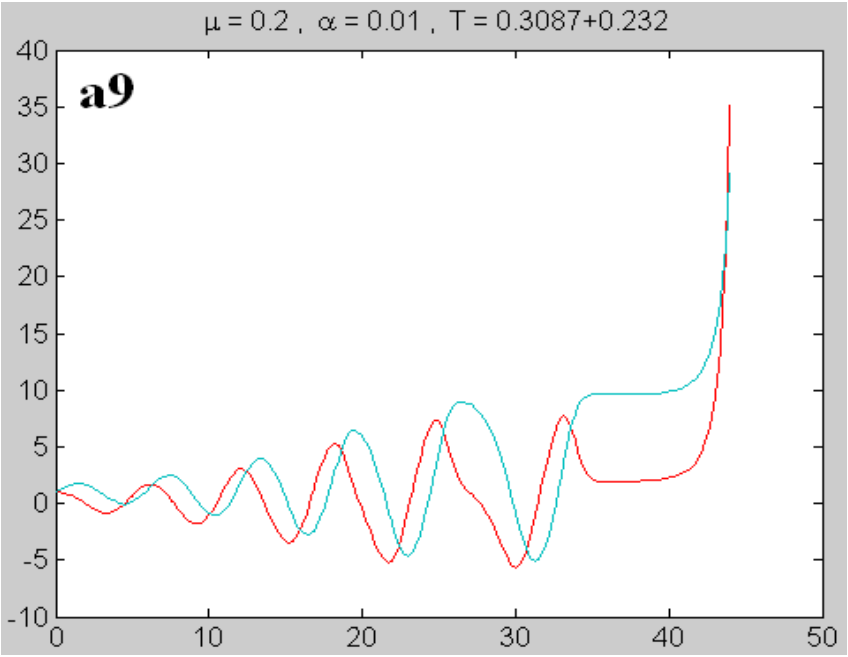

Figure 5.10: Solution curves when $\Delta = 0.232$.

5.5 Exponential Weighting: Multiple Gene Network

5.5.1 Steady State Solutions

Now we treat the multiple gene network with exponential weighting. We start by finding the equilibrium solutions of the system (5.17),(5.18) where $H(p)$ is given by Eq.(5.10). Setting $\dot{m}_i$=$\dot{p}_i$=0 in Eqs.(5.17) and (5.18) gives an equilibrium point of the form $(m_0^*, \ldots, m_N^*, p_0^*, \ldots, p_N^*)$, which will satisfy the following equations

$$\mu^2 p_i^* = \frac{1}{N} \sum_{j=0}^{N} e^{-|i-j|/N} H(p_j^*) \tag{5.115}$$

This (N+1)-dimensional system of equations may be solved numerically for different values of N, μ, and α.

Continuing our previous numerical example when $\mu = 0.2$ and $\alpha = 0.01$ we may use Macsyma's root_by_bisection to obtain Table 5.1 and Figure 5.11, both of which give a summary of our numerical results. Notice that the system is symmetric, so $p_j^* = p_{N-j}^*$.

Table 5.1: Numerical results for $\mu = 0.2$ and $\alpha = 0.01$. The system is symmetric and so the steady state, p^*, satisfies $p_j^* = p_{N-j}^*$.

N	p^* (where $p_j^* = p_{N-j}^*$)
1	p_0=0.98075 (2 gene network)
2	p_0=0.96281, p_1=0.98662
3	p_0=0.94847, p_1=0.98378
4	p_0=0.93714, p_1=0.97885, p_2=0.98565
5	p_0=0.92822, p_1=0.97310, p_2=0.98434
7	p_0=0.91538, p_1=0.96146, p_2=0.97863, p_3=0.98432
15	p_0=0.89269, p_1=0.92878, p_2=0.95139, p_3=0.96550, p_4=0.97423, p_5=0.97950, p_6=0.98248, p_7=0.98382
30	p_0=0.88043, p_1=0.90325, p_2=0.92129, p_3=0.93555, p_4=0.94680, p_5=0.95568, p_6=0.96268, p_7=0.96817, p_8=0.97247, p_9=0.97581, p_{10}=0.97837, p_{11}=0.98030, p_{12}=0.98170, p_{13}=0.98265, p_{14}=0.98320, p_{15}=0.98338

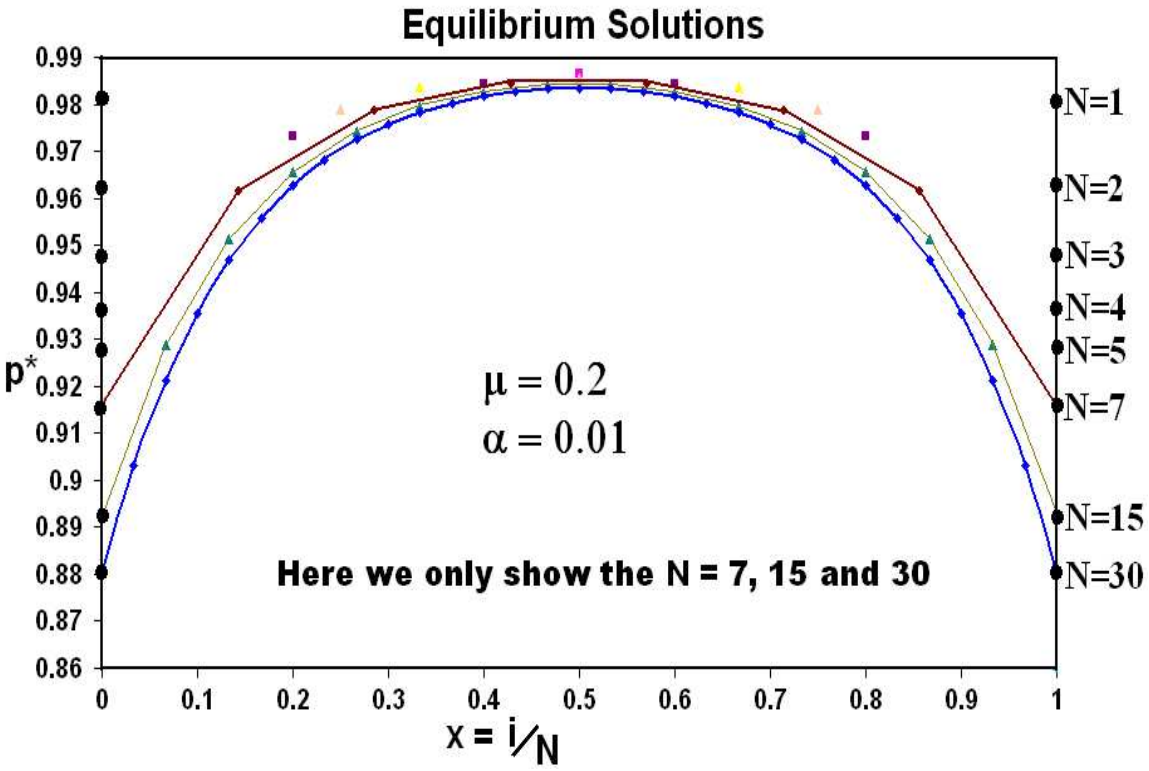

Figure 5.11: Steady state solutions for μ=0.2, α=0.01, and N=7, 15, and 30. The approximate values for the steady states can be found in Table 5.1.

In addition to the previous results, we may numerically integrate the original system given by Eqs.(5.17) and (5.18) to obtain the equilibrium solutions p^* and m^* for different N. These may be obtained using Matlab's dde23 by setting T=0.001 and waiting until the solutions decay to their steady state. The Matlab results for N=15 can be found in Figure 5.12 and for N=30 in Figure 5.13.

Notice that the approximate values found in Table 5.1 were obtained using Macsyma's root_by_bisection where as the results in Figures 5.12 and 5.13 were found using Matlab. Both of these agree.

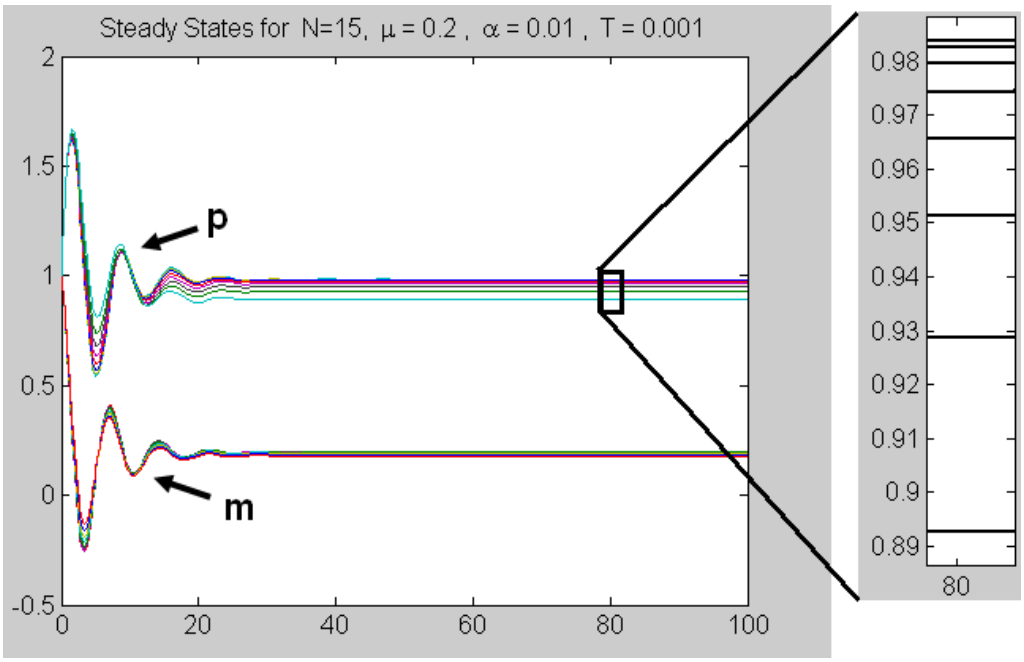

Figure 5.12: Equilibrium solutions when N=15.

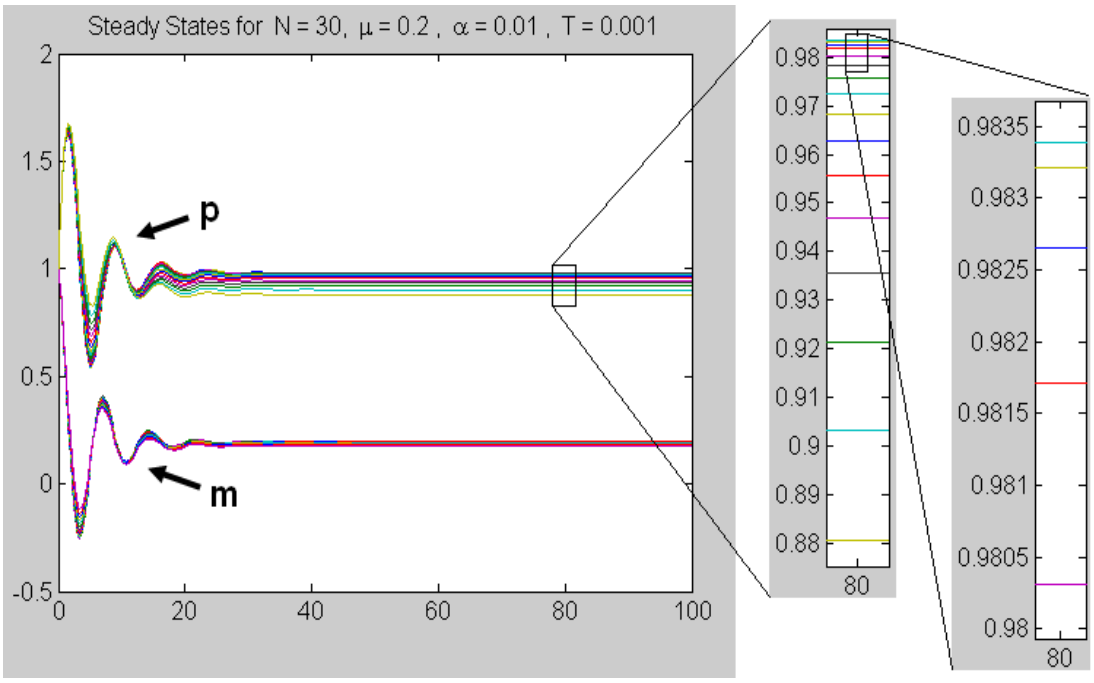

Figure 5.13: Equilibrium solutions when N=30.

5.5.2 Linear Stability Analysis

Next we define ξ_i and η_i to be deviations from equilibrium: ξ_i=m_i-m_i^*, η_i=p_i-p_i^*. Substituting these into (5.17) and (5.18) yields

$$\dot{\xi}_i = -\mu\,(\xi_i + m_i^*) + \frac{1}{N}\sum_{j=0}^{N} e^{-|i-j|/N} H(\eta_{jd} + p_j^*) \tag{5.116}$$

$$\dot{\eta}_i = \xi_i + m_i^* - \mu\,(\eta_i + p_i^*) \tag{5.117}$$

which become

$$\dot{\xi}_i = -\mu\,\xi_i + \frac{1}{N}\sum_{j=0}^{N} e^{-|i-j|/N} G(\eta_{jd}) \tag{5.118}$$

$$\dot{\eta}_i = \xi_i - \mu\,\eta_i \tag{5.119}$$

where

$$G(\eta_j) = \left(-1 + 3\alpha {p_j^*}^2\right)\eta_j + 3\alpha p_j^* \eta_j^2 + \alpha\,\eta_j^3 \tag{5.120}$$

To find the critical frequency, ω_{cr}, and its associated critical delay, T_{cr}, we linearize Eqs.(5.118)-(5.119) for small η to obtain

$$\dot{\xi}_i = -\mu\xi_i - \frac{1}{N}\sum_{j=0}^{N} e^{-|i-j|/N}(1 - 3\alpha {p_j^*}^2)\eta_{jd} \tag{5.121}$$

$$\dot{\eta}_i = \xi_i - \mu\eta_i \tag{5.122}$$

If $\xi_i = A_i e^{\lambda t}$ and $\eta_i = B_i e^{\lambda t}$ then Eqs.(5.121)-(5.122) become

$$-(\lambda+\mu)A_i = \frac{1}{N}\sum_{j=0}^{N} e^{-|i-j|/N}(1 - 3\alpha {p_j^*}^2)B_j e^{-\lambda T} \tag{5.123}$$

$$(\lambda+\mu)B_i = A_i \tag{5.124}$$

which yields

$$-Ne^{\lambda T}(\lambda+\mu)^2 B_i = \sum_{j=0}^{N} e^{-|i-j|/N}(1 - 3\alpha {p_j^*}^2)B_j \tag{5.125}$$

For nontrivial solutions, the system (5.125) must satisfy $\det(M - rI) = 0$, where M is the $(N+1)\times(N+1)$ symmetric matrix given by

$$M = [M_{ij}] = \left[(1 - 3\alpha p_j^{*2}) \exp(-|i - j|/N)\right] \tag{5.126}$$

and r is the associated eigenvalue given by

$$r = -Ne^{\lambda T}(\lambda + \mu)^2 \tag{5.127}$$

Since M is a symmetric matrix, then all of its eigenvalues are real which means r is real.

Continuing our example for $\mu = 0.2$ and $\alpha = 0.01$ we use the condition $\det(M - rI) = 0$ to obtain Table 5.2, which shows the numerical evaluation of the eigenvalues r for different values of N.

Table 5.2: Numerical results for the eigenvalues, r, when $\mu = 0.2$ and $\alpha = 0.01$

N	r
1	1.32763
2	2.00107
3	2.70349
4	3.41340
5	4.12635
7	5.55626
15	11.29060
30	22.05340

Now that r is known we have two cases:

(i) When $T = 0$ Eq.(5.127) gives

$$r = -N(\lambda + \mu)^2 \quad \Rightarrow \quad \lambda = -\mu \pm \sqrt{-r/N} \tag{5.128}$$

which for $r > 0$ gives $\mathrm{Re}(\lambda) = -\mu < 0$ (for $\mu > 0$) and thus the system has a stable steady state.

(ii) When $T = T_{cr}$ and $\lambda = i\omega$, Eq.(5.127) becomes

$$r = -Ne^{i\omega T_{cr}}(i\omega + \mu)^2 \tag{5.129}$$

which gives the two real equations

$$\frac{r}{N} = 2\mu\omega \sin\omega T_{cr} + \left(\omega^2 - \mu^2\right)\cos\omega T_{cr} \tag{5.130}$$

$$0 = \left(\omega^2 - \mu^2\right)\sin\omega T_{cr} - 2\mu\omega \cos\omega T_{cr} \tag{5.131}$$

As before, solving Eqs.(5.130),(5.131) for $\sin\omega T_{cr}$ and $\cos\omega T_{cr}$ gives

$$\omega = \sqrt{\frac{r}{N} - \mu^2} \tag{5.132}$$

and dividing the expressions for $\sin\omega T_{cr}$ and $\cos\omega T_{cr}$ and solving for T_{cr} we obtain

$$T_{cr} = \frac{1}{\omega}\arctan\left(\frac{2\mu\omega}{\omega^2 - \mu^2}\right) \tag{5.133}$$

We continue our example by setting $\mu = 0.2$ and $\alpha = 0.01$. Table 5.3 gives a summary of the numerical results found for T_{cr} and ω for different values of N. Notice that N=1 is the two gene network result found in Eqs.(5.113) and (5.114).

Table 5.3: Numerical results for r, ω, and T_{cr} when $\mu = 0.2$ and $\alpha = 0.01$

N	r	ω	T_{cr}
1	1.32763	1.13474	0.30749
2	2.00107	0.98007	0.41079
3	2.70349	0.92799	0.45749
4	3.41340	0.90186	0.48396
5	4.12635	0.88615	0.50099
7	5.55626	0.86819	0.52158
15	11.29060	0.84422	0.55108
30	22.05340	0.83373	0.56477

In addition to the previous results, another interesting finding is the associated bifurcation mode shape of the oscillation. This can be obtained from Eq.(5.125) by using the values $\mu = 0.2$, $\alpha = 0.01$, and the associated r for a given N (cf. Table 5.2). In Figures 5.14, 5.15, and 5.16 we present our numerical results for N=7, 15, and 30 respectively.

5.5.3 Nonlinear Numerical Analysis

In this section we generalize our results from Section 5.4.3 for the two gene model. Here again we let $\Delta = T - T_{cr}$ and repeat the analysis for various N. The numerical integration results are summarized in Figure 5.17 where we have plotted amplitude versus detuning about T_{cr} for $N = 1, 7, 15$, and 30.

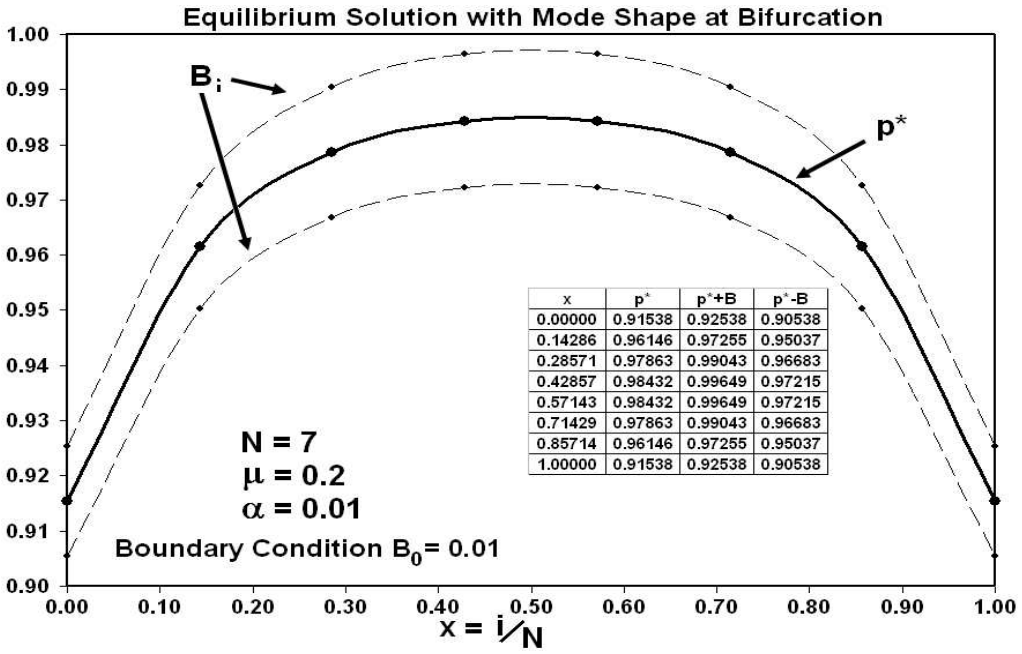

x	p*	p*+B	p*-B
0.00000	0.91538	0.92538	0.90538
0.14286	0.96146	0.97255	0.95037
0.28571	0.97863	0.99043	0.96683
0.42857	0.98432	0.99649	0.97215
0.57143	0.98432	0.99649	0.97215
0.71429	0.97863	0.99043	0.96683
0.85714	0.96146	0.97255	0.95037
1.00000	0.91538	0.92538	0.90538

Figure 5.14: Bifurcation mode shape from linearized analysis when μ=0.2, α=0.01, and N=7. The values for the steady states can be found in Table 5.1. The B_i's can be found by solving Eq.(5.125).

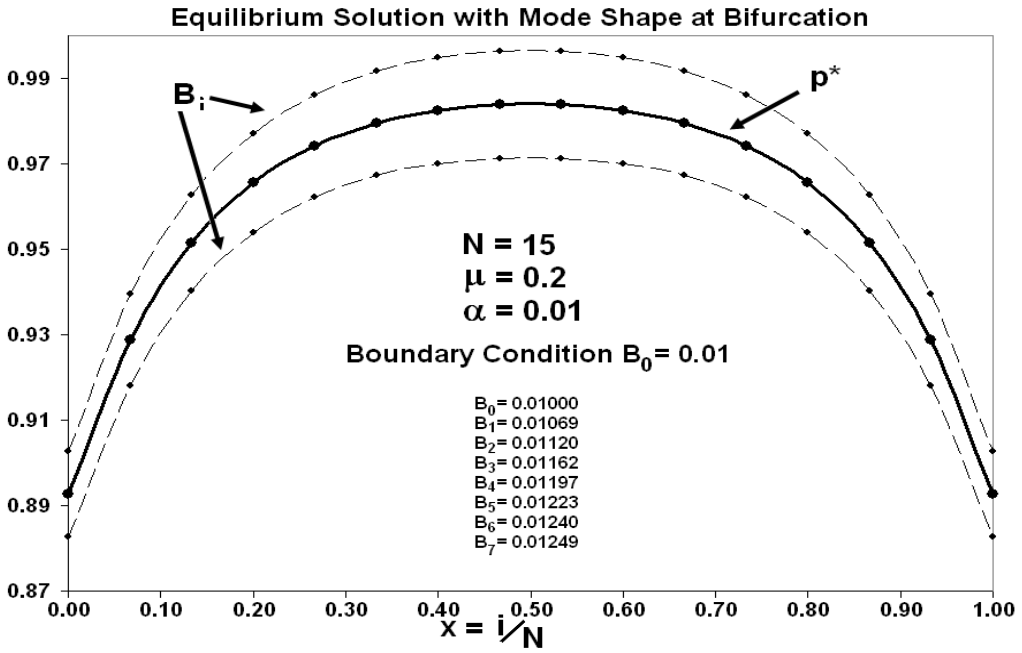

Figure 5.15: Bifurcation mode shape from linear stability analysis when μ=0.2, α=0.01, and N=15. See Table 5.1 for p^*.

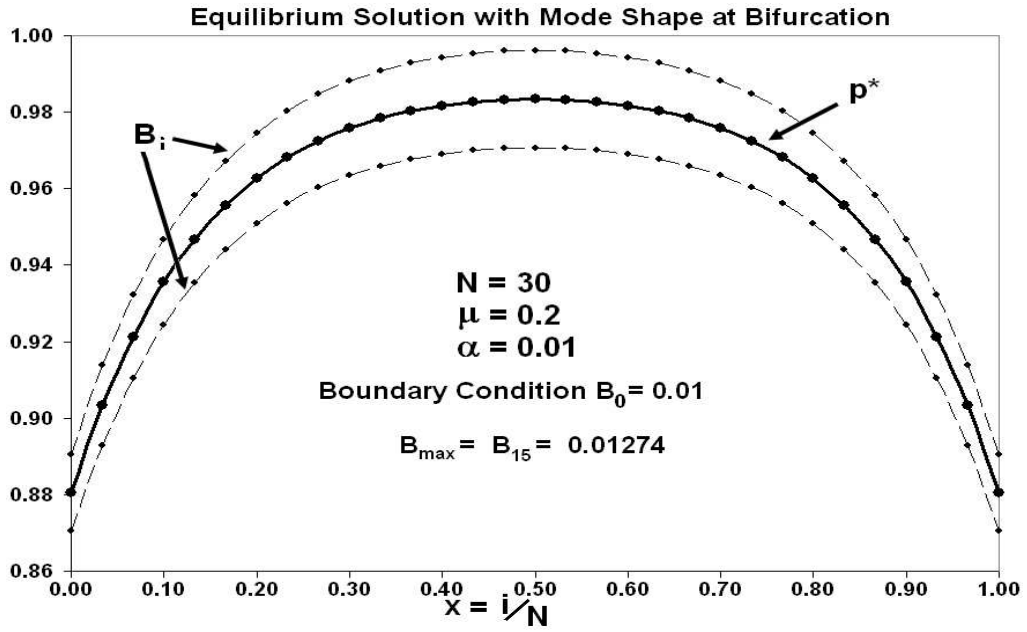

Figure 5.16: Bifurcation mode shape from linear analysis when μ=0.2, α=0.01, and N=30. See Table 5.1 for the values of p_i^*'s and Eq.(5.125) for B_i's.

Extending our study of the single gene-mRNA-protein unit into a network of N coupled gene units proved to be interesting and useful. Unlike the uniform weighting case, in the exponential weighting case, each protein product is shared unequally. That is, the production of protein of one gene represses the mRNA production of nearby gene sites to a greater extent than more distant genes.

As in our previous analyses, we were able to prove that the system exhibits a stable steady state when there is no delay. However, we highlight the fact that (unlike the uniform case) the steady state is not constant, but rather it depends on gene location. Interestingly, at the bifurcation delay (critical value when the steady state becomes unstable) the associated bifurcation mode shape of the oscillation gives the amplitudes of oscillation at the different gene locations. Fur-

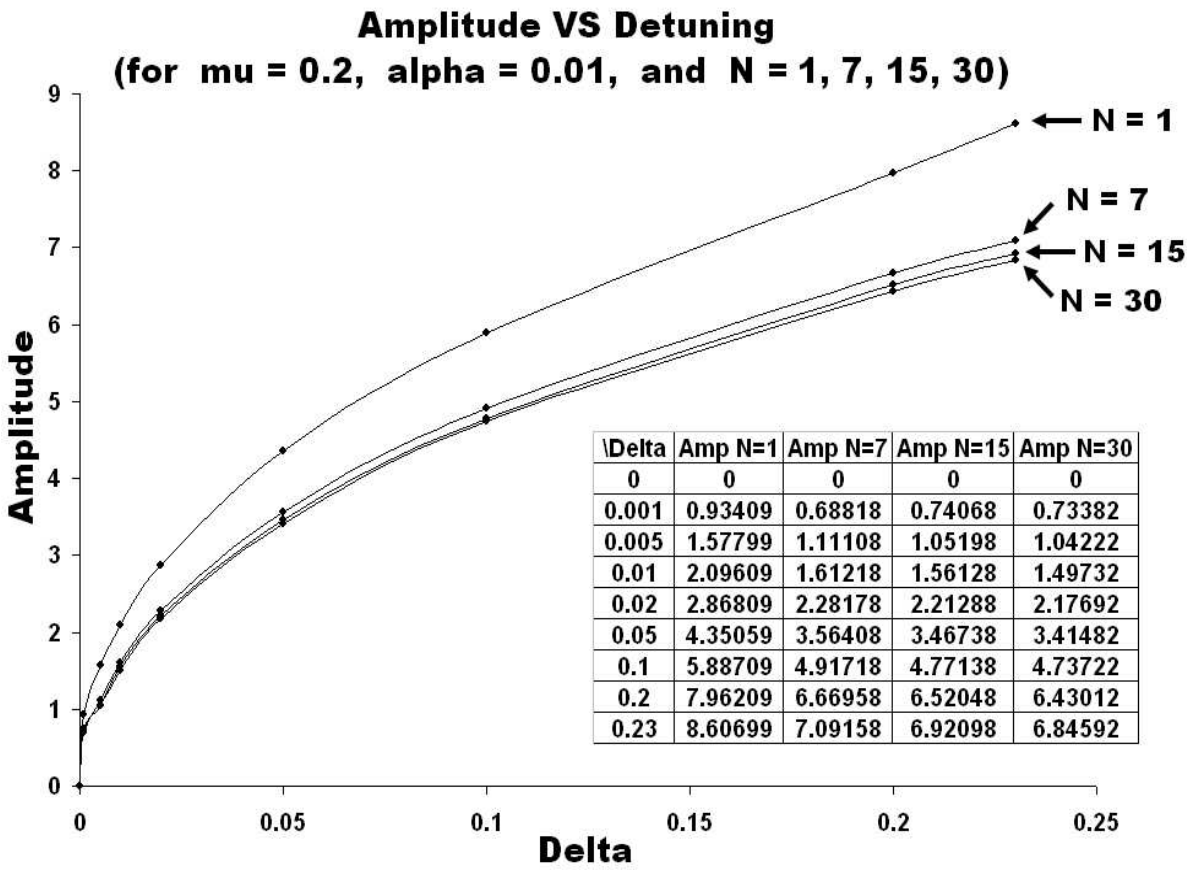

\Delta	Amp N=1	Amp N=7	Amp N=15	Amp N=30
0	0	0	0	0
0.001	0.93409	0.68818	0.74068	0.73382
0.005	1.57799	1.11108	1.05198	1.04222
0.01	2.09609	1.61218	1.56128	1.49732
0.02	2.86809	2.28178	2.21288	2.17692
0.05	4.35059	3.56408	3.46738	3.41482
0.1	5.88709	4.91718	4.77138	4.73722
0.2	7.96209	6.66958	6.52048	6.43012
0.23	8.60699	7.09158	6.92098	6.84592

Figure 5.17: Amplitude VS Detuning plot for N = 1, 7, 15, and 30.

thermore, the nonlinear numerical integration results imply that the amplitude of oscillation at each gene site converges to a fixed amplitude as $N \to \infty$. This can be confirmed by our numerical results in Figure 5.17 where we have plotted amplitude versus detuning about T_{cr} for N = 1, 7, 15, and 30.

CHAPTER 6

CONTINUOUS NETWORK MODEL

6.1 Introduction

In this chapter we will study a continuous network model. The model is characterized by a system of two coupled equations: an ordinary differential equation and a delay differential-*integral* equation. We will study two different cases with distinct integral kernels and Hill functions. The first case considers uniform weighting, where each ribosome produces a given quantity of protein which is then shared equally amongst all gene sites. The second case is characterized by an exponential weighting, where each protein product is shared unequally, with nearby gene units being repressed to a greater extent than more distant genes.

Both of these cases (uniform and exponential) exhibit a steady state, which is stable when there is no delay. Linear analysis then reveals that a critical delay exists, where the steady state becomes unstable. Closed form expressions for the critical delay T_{cr} and associated frequency ω are then found. Finally, we confirm our results for the exponential weighting case by discretizing the continuous system into an N-dimensional system and showing that the discrete system analysis (presented in Chapter 5) approach the continuous results as N becomes large.

6.2 From Discrete to Continuous

We start by presenting the continuous version of the discrete network model (5.15)-(5.16) when there is uniform weighting (Case 1 in Section 5.2.2):

$$\dot{m} = -\mu m + \int_0^1 \frac{1}{1+\left(\frac{p_d(\bar{x})}{p_0(\bar{x})}\right)^n} d\bar{x} \tag{6.1}$$

$$\dot{p} = m - \mu p \tag{6.2}$$

where $m{=}m(x,t)$, $p{=}p(x,t)$, $p_d(\bar{x}){=}p(\bar{x},t-T)$, and $p_0(\bar{x})$ is a reference concentration of protein at $\bar{x}$. In Eqs.(6.1) and (6.2) we made the following approximations

$$m_i \to m(x) \quad , \quad p_i \to p(x) \quad , \quad \text{and}$$
$$\sum_{j=0}^{N} \frac{1}{1+\left(\frac{p_j(t-T)}{p_{0j}}\right)^n} \frac{1}{N+1} \to \int_0^1 \frac{1}{1+\left(\frac{p_d(\bar{x})}{p_0(\bar{x})}\right)^n} d\bar{x} \quad \text{as} \quad N \to \infty \tag{6.3}$$

The geometric representation of Eqs.(6.1),(6.2) is given by Figure 6.1, which is the continuous version of Figure 5.5.

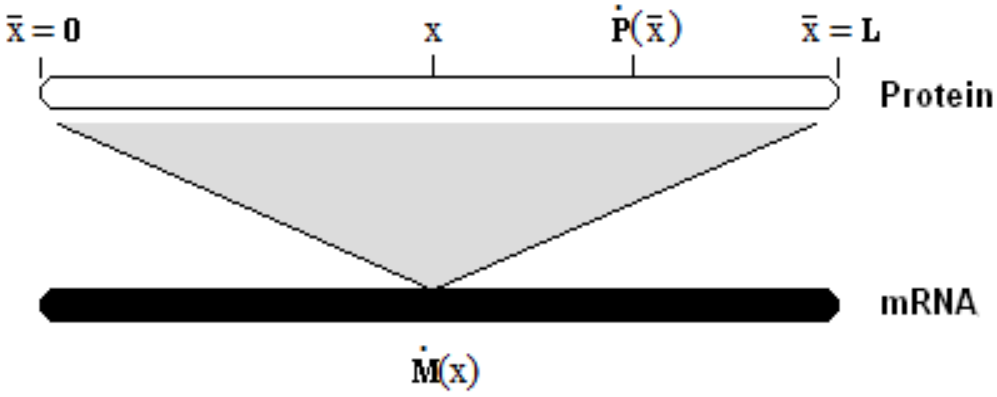

Figure 6.1: Geometric representation for the continuous model. Notice that Figure 6.1 is the continuous version of the discrete geometric representation for the N gene network given by Figure 5.5 in Section 5.2.2.

Next we present the continuous version of the exponential weighting case (Case 2 in Section 5.2.2), which was given by Eqs.(5.17) and (5.18) with $\alpha = 0$:

$$\dot{m} = -\mu m + \int_0^1 e^{-|x-\bar{x}|}\left(1 - p_d(\bar{x})\right) \tag{6.4}$$

$$\dot{p} = m - \mu p \tag{6.5}$$

where as before we have assumed

$$m_i \to m(x) \quad , \qquad p_i \to p(x) \quad , \qquad \text{and}$$
$$\sum_{j=0}^{N} e^{-|i-j|/N}\left(1 - p_{jd}\right)\frac{1}{N} \;\to\; \int_0^1 e^{-|x-\bar{x}|}\left(1 - p_d(\bar{x})\right)d\bar{x} \quad \text{as} \quad N \to \infty \tag{6.6}$$

An important biological remark about the continuum model is that genes are discrete (they are organized separately along the DNA). Thus the discrete model is more realistic. Mathematically, however, we may approximate the discrete system by assuming a "gene continuum" between genes and their associated mRNA and protein products. Thus, although biological realism is sacrificed, we are now able to transform the multidimensional DDE system (cf. Eqs.(5.17)-(5.18)) into a more compact mathematical model of two coupled equations given by (6.4) and (6.5). Notice that the latter approach is not an uncommon technique, since it has been regularly used on studies of predator-prey models, epidemiology, and population dynamics, all of which are inherently discrete biological systems but which have been conveniently extended to continuous models for their analysis.

6.3 Mathematical Model

As explained in the previous section, we may tag a given gene with a variable $x \in [0, 1]$, and generalize the system (5.13), and (5.14) to be of the form:

$$\dot{m} = -\mu m + \int_0^1 G(x - \bar{x}) H(p_d(\bar{x}))\, d\bar{x} \tag{6.7}$$

$$\dot{p} = m - \mu p \tag{6.8}$$

where $m = m(x, t)$, $p = p(x, t)$, $p_d(\bar{x}) = p(\bar{x}, t - T)$, and where the kernel, $G(x - \bar{x})$, and the Hill function, $H(p_d(\bar{x}))$ are given by the following two cases:

Case 1 (Uniform weighting): Here we assume $G(x - \bar{x}) = 1$. In this case each ribosome produces a given quantity of protein which is then shared equally amongst all gene sites. For the rate of production of mRNA $H(p_d(\bar{x}))$ we choose the following Hill function [72, 108]:

$$H(p_d(\bar{x})) = \frac{1}{1 + \left(\frac{p_d(\bar{x})}{p_0(\bar{x})}\right)^n} \tag{6.9}$$

where $p_d(\bar{x}) = p(\bar{x}, t - T)$ is the delayed protein concentration at location $\bar{x}$, and where $p_0(\bar{x})$ is a reference concentration of protein at $\bar{x}$, and n is a parameter. The resulting system is of the form:

$$\dot{m} = -\mu m + \int_0^1 \frac{1}{1 + \left(\frac{p_d(\bar{x})}{p_0(\bar{x})}\right)^n}\, d\bar{x} \tag{6.10}$$

$$\dot{p} = m - \mu p \tag{6.11}$$

Case 2 (Exponential weighting with linear Hill function): This case is characterized by the choice of the integral kernel $G(x - \bar{x}) = e^{-|x-\bar{x}|}$. Here each protein product is shared unequally, with nearby gene sites being repressed to a greater

extent than more distant ones. We choose the rate of production of mRNA $H(p_d(\bar{x}))$ to be given by the following function of p_d (cf.Eq.(5.10)):

$$H(p_d(\bar{x})) = 1 - p_d(\bar{x}) \tag{6.12}$$

The resulting system is of the form:

$$\dot{m} = -\mu\, m + \int_0^1 e^{-|x-\bar{x}|}(1 - p_d(\bar{x}))\, d\bar{x} \tag{6.13}$$

$$\dot{p} = m - \mu\, p \tag{6.14}$$

The following sections are organized as follows: In Section 6.4 we study the nonlinear system with uniform weighting (6.10)-(6.11). We start by presenting a study on the associated linear equations, and then we move to the nonlinear analysis. We point out that the results found in Section 6.4 are the generalizations of the results found in Section 5.5, where the sums are extended to integrals. In Section 6.5 we present the steady state and stability analysis for the linear equations (6.13) and (6.14).

6.4 Uniform Weighting

6.4.1 Linear Analysis

In this section we consider the steady state behavior of the system (6.10),(6.11). Setting $\dot{p}$=$\dot{m}$=0 we see that at steady state m^*=μp^* and p_d^*=p^*, where a * represents the steady state solution. Thus, at steady state, substituting Eq.(6.11) into (6.10) gives

$$\mu^2 p^*(x) = \int_0^1 \frac{1}{1 + \left(\frac{p^*(\bar{x})}{p_0(\bar{x})}\right)^n} d\bar{x} \tag{6.15}$$

Since the RHS of Eq.(6.15) is independent of x, we see that $p^*(x)=p^*$ is a constant. Because of the difficulty in evaluating the integral in Eq.(6.15) for a general function $p_0(\bar{x})$, numerical integration is required in order to obtain an approximate value for p^*. In order to illustrate the process we choose a tractable function $p_0(\bar{x}) = 1 + \bar{x}$, together with $n = 3$ and $\mu = 0.2$, in which case Eq.(6.15) gives $p^* = 2.9876$.

To study the stability of the steady state solution $(m^*(x), p^*(x))$ found above, we set $p(x,t)=p^*(x)+\eta(x,t)$ and $m(x,t)=m^*(x)+\xi(x,t)$ and linearize the resulting equations in $\eta(x,t)$ and $\xi(x,t)$. Since the steady state solution p^* is constant in x then Eqs.(6.10),(6.11) give

$$\dot{\xi} = -\mu\xi - \int_0^1 K_1(\bar{x})\,\eta_d(\bar{x})\,d\bar{x} \tag{6.16}$$

$$\dot{\eta} = \xi - \mu\eta \tag{6.17}$$

where

$$K_1(\bar{x}) = \frac{n\beta}{(1+\beta)^2\,p^*}, \quad \text{and } \beta = \beta(\bar{x}) = \left(\frac{p^*}{p_0(\bar{x})}\right)^n. \tag{6.18}$$

Assuming solutions for ξ and η of the form

$$\xi(x,t) = A(x)\,e^{\lambda t}, \qquad \eta(x,t) = B(x)\,e^{\lambda t} \tag{6.19}$$

substituting them into Eqs.(6.16) and (6.17), and solving for $B(x)$ yields the following integral equation

$$r\,B(x) = \int_0^1 K_1(\bar{x})\,B(\bar{x})\,d\bar{x} \tag{6.20}$$

where

$$r = -e^{\lambda T}(\lambda+\mu)^2 \tag{6.21}$$

To solve Eq.(6.20), we note that the RHS is independent of x, which tells us that $B(x)$=B is constant. Eliminating B from Eq.(6.20), we obtain

$$r = \int_0^1 K_1(\bar{x})\, d\bar{x} \tag{6.22}$$

Here $K_1(\bar{x})$ is given by Eq.(6.18), so that r is known. We are left with the problem of determining λ from Eq.(6.21) when r is known. This problem is common to both cases: the present case of uniform weighting as well as to the exponential weighting case. To avoid repeating the treatment, we handle this problem in the Appendix.

There are two important situations: **(i)** when $T = 0$, in which case λ determines the stability of the system with no delay, and **(ii)** when $T = T_{cr}$, where the delay T_{cr} corresponds to pure imaginary λ and corresponds to a change in stability.

(i) When $T = 0$, Eq.(6.87) in the Appendix gives

$$\lambda = -\mu \pm \sqrt{-\int_0^1 K_1(\bar{x})\, d\bar{x}} \tag{6.23}$$

which shows that the system with no delay is stable since $K_1(\bar{x})$>0 from (6.18).

(ii) When $T = T_{cr}$, Eqs.(6.92),(6.91) in the Appendix give

$$T_{cr} = \frac{1}{\omega} \arctan\Big(\frac{2\omega\mu}{\omega^2 - \mu^2}\Big) \tag{6.24}$$

$$\omega = \sqrt{-\mu^2 + \int_0^1 K_1(\bar{x})\, d\bar{x}} \tag{6.25}$$

We continue the example given in the previous section, namely, $p_0(\bar{x}) = 1 + \bar{x}$, $n = 3$ and $\mu = 0.2$, which yielded the steady state $p^* = 2.9876$. By substituting Eq.(6.18) into (6.25) we obtain $\omega = 0.24977$ which we substitute into (6.24) to obtain the critical delay $T_{cr} = 5.40638$, where the steady state becomes unstable.

6.4.2 Nonlinear Analysis

In this section we will study the full nonlinear system by using Lindstedt's perturbation method. We start by combining Eqs.(6.10) and (6.11) into a second order DDE and expanding for small η_d

$$\begin{aligned} \ddot{\eta} + 2\mu\dot{\eta} + \mu^2\eta &= \int_0^1 K_1(\bar{x})\eta_d(\bar{x})\,d\bar{x} + \int_0^1 K_2(\bar{x})\eta_d^2(\bar{x})\,d\bar{x} \\ &\quad + \int_0^1 K_3(\bar{x})\eta_d^3(\bar{x})\,d\bar{x} + \ldots \end{aligned} \tag{6.26}$$

where $K_1(\bar{x})$, is given by Eq.(6.18) and $K_2(\bar{x})$, and $K_3(\bar{x})$ are the Taylor coefficients given by

$$K_2(\bar{x}) = \frac{n\beta_j\left(\beta_j n - n + \beta_j + 1\right)}{2\left(1+\beta_j\right)^3\, p^{*2}}, \quad \text{where} \quad \beta_j = \left(\frac{p^*}{p_0(\bar{x})}\right)^n \tag{6.27}$$

$$K_3(\bar{x}) = -\frac{n\beta_j\left(\beta_j^2 n^2 - 4\beta_j n^2 + n^2 + 3\beta_j^2 n - 3n + 2\beta_j^2 + 4\beta_j + 2\right)}{6\left(1+\beta_j\right)^4\, p^{*3}} \tag{6.28}$$

Next we introduce a small parameter ϵ via the following scaling

$$\eta(x) = \epsilon u(x) \tag{6.29}$$

stretch time by defining a new independent variable

$$\tau = \Omega t \tag{6.30}$$

and expand Ω in a power series in ϵ as follows

$$\Omega = \omega + \epsilon^2 k_2 + \ldots \tag{6.31}$$

where we omit the $O(\epsilon)$ term since it turns out to be zero. We substitute (6.29) and (6.30) into (6.26) to obtain

$$\Omega^2\frac{d^2u}{d\tau^2} + 2\mu\Omega\frac{du}{d\tau} + \mu^2 u - \int_0^1 K_1(\bar{x})u_d(\bar{x})\,d\bar{x} = \tag{6.32}$$

$$\epsilon\int_0^1 K_2(\bar{x})\,u_d^2(\bar{x})\,d\bar{x} + \epsilon^2\int_0^1 K_3(\bar{x})\,u_d^3(\bar{x}) + \ldots \tag{6.33}$$

Next we introduce a small detuning, Δ, about the critical delay, T_{cr},

$$T \;=\; T_{cr} + \Delta \;=\; T_{cr} + \epsilon^2\delta \tag{6.34}$$

where Δ is scaled like ϵ^2. Substituting Eqs.(6.34) and (6.31) into $u_d(\bar{x}) = u(\tau - \Omega T, \bar{x})$ and Taylor expanding about ϵ=0 we obtain

$$u_d(\bar{x}) \;=\; u(\tau - \Omega T, \bar{x}) \;=\; u(\tau - \omega T_{cr} - \epsilon^2(k_2 T_{cr} + \omega\delta) + \ldots, \bar{x}) \tag{6.35}$$

$$\;=\; u(\tau - \omega T_{cr}, \bar{x}) - \epsilon^2(k_2 T_{cr} + \omega\delta)u'(\tau - \omega T_{cr}, \bar{x}) + \ldots \tag{6.36}$$

Next we expand $u(\tau, \bar{x})$ in a power series in ϵ

$$u(\tau, x) \;=\; u_0(\tau, x) + \epsilon u_1(\tau, x) + \epsilon^2 u_2(\tau, x) + \ldots \tag{6.37}$$

and by substituting the latter and Eqs.(6.31) and (6.36) into (6.33), and collecting like powers of ϵ we find

$$Lu_0 \;=\; 0 \tag{6.38}$$

$$Lu_1 \;=\; \int_0^1 K_2(\bar{x})\, u_0^2(\tau - \omega T_{cr}, \bar{x})\, d\bar{x} \tag{6.39}$$

$$Lu_2 \;=\; \ldots \tag{6.40}$$

where $\ldots$ stands for terms in u_0 and u_1 (omitted here) and where Lf stands for

$$Lf \;=\; \omega^2 \frac{d^2 f}{d\tau^2} + 2\mu\omega \frac{df}{d\tau} + \mu^2 f - \int_0^1 K_1(\bar{x}) f(\tau - \omega T_{cr}, \bar{x})\, d\bar{x} \tag{6.41}$$

We take the solution, $u_0(\tau, x)$, of the system (6.38) as

$$u_0(\tau, x) \;=\; \hat{A}\cos\tau \tag{6.42}$$

where by Eq.(6.29) we know $\eta_0(\tau, x) \;=\; \epsilon u_0(\tau, x) \;=\; \epsilon\hat{A}\cos\tau \;=\; A\cos\tau$. Next we substitute (6.42) into (6.39) and obtain the following expression for u_1:

$$u_1(\tau) = m_1 \sin 2\tau + m_2 \cos 2\tau + m_3 \tag{6.43}$$

where m_1 is given by the equation:

$$m_1 = -\frac{2\,\hat{A}^2\,\hat{K}_2\,\mu\,\omega^3\,\left(2\,\mu^2+3\,\hat{K}_1\right)}{\hat{K}_1\,\left(16\,\mu^6+39\,\hat{K}_1\,\mu^4+18\,\hat{K}_1^2\,\mu^2-9\,\hat{K}_1^3\right)} \tag{6.44}$$

where

$$\hat{K}_1 \;=\; \int_0^1 K_1(\bar{x})\,d\bar{x}\,, \quad \hat{K}_2 \;=\; \int_0^1 K_2(\bar{x})\,d\bar{x}\,, \quad \text{and} \quad \hat{K}_3 \;=\; \int_0^1 K_3(\bar{x})\,d\bar{x} \tag{6.45}$$

and where we omit the expressions for m_2 and m_3 for brevity. Next we substitute Eqs.(6.42) and (6.43) into (6.40), and after trigonometric simplifications have been performed, we equate to zero the coefficients of the resonant terms $\sin\tau$ and $\cos\tau$. This yields the amplitude, A, of the limit cycle that was born in the Hopf bifurcation:

$$A^2 = \frac{P}{Q}\,\Delta \tag{6.46}$$

where

$$P \;=\; 8\,\hat{K}_1^2\,\omega^2\,\left(\mu^2-\hat{K}_1\right)\left(16\,\mu^6+39\,\hat{K}_1\,\mu^4+18\,\hat{K}_1^2\,\mu^2-9\,\hat{K}_1^3\right) \tag{6.47}$$

$$Q \;=\; Q_0\,T_{cr} \;+\; Q_1 \tag{6.48}$$

and

$$\begin{aligned} Q_0 \;=\;& 48\,\hat{K}_3\,\hat{K}_1^2\,\mu^8-16\,\hat{K}_2^2\,\hat{K}_1\,\mu^8+69\,\hat{K}_3\,\hat{K}_1^3\,\mu^6+32\,\hat{K}_2^2\,\hat{K}_1^2\,\mu^6-63\,\hat{K}_3\,\hat{K}_1^4\,\mu^4 \\ &+162\,\hat{K}_2^2\,\hat{K}_1^3\,\mu^4-81\,\hat{K}_3\,\hat{K}_1^5\,\mu^2+108\,\hat{K}_2^2\,\hat{K}_1^4\,\mu^2+27\,\hat{K}_3\,\hat{K}_1^6-30\,\hat{K}_2^2\,\hat{K}_1^5 \end{aligned} \tag{6.49}$$

$$\begin{aligned} Q_1 \;=\;& -96\,\hat{K}_3\,\hat{K}_1\,\mu^9+64\,\hat{K}_2^2\,\mu^9-138\,\hat{K}_3\,\hat{K}_1^2\,\mu^7+16\,\hat{K}_2^2\,\hat{K}_1\,\mu^7+126\,\hat{K}_3\,\hat{K}_1^3\,\mu^5 \\ &-308\,\hat{K}_2^2\,\hat{K}_1^2\,\mu^5+162\,\hat{K}_3\,\hat{K}_1^4\,\mu^3-296\,\hat{K}_2^2\,\hat{K}_1^3\,\mu^3-54\,\hat{K}_3\,\hat{K}_1^5\,\mu+12\,\hat{K}_2^2\,\hat{K}_1^4\mu \end{aligned} \tag{6.50}$$

and where the $\hat{K}_i$'s are given by Eq.(6.45), which are the generalized versions of Eq.(5.72) in Chapter 5. In addition, notice that Eqs.(6.46)-(6.50) are the same expressions found in Section 5.3.2, with the difference that the K_i's are now integrals instead of sums.

6.5 Exponential Weighting

6.5.1 Steady State Solutions

In this section we consider the steady state behavior of the system (6.13),(6.14). Setting $\dot{p}=\dot{m}=0$ we see that at steady state $m^*=\mu p^*$ and $p_d^*=p^*$, where a * represents the steady state solution.

At steady state, Eqs.(6.13),(6.14) give

$$\mu^2 p^*(x) \;=\; \int_0^1 e^{-|x-\bar{x}|} H(p^*(\bar{x}))\, d\bar{x} \tag{6.51}$$

where $H(p^*(\bar{x})) = 1 - p^*(\bar{x})$ and which may be written in the form:

$$\mu^2 p^*(x) \;=\; e^{-x} \int_0^x e^{\bar{x}} H(p^*(\bar{x}))\, d\bar{x} \;+\; e^{x} \int_x^1 e^{-\bar{x}} H(p^*(\bar{x}))\, d\bar{x} \tag{6.52}$$

Differentiating Eq.(6.52) twice [49] we obtain the equivalent second order ODE for the steady state solution $p^*=p^*(x)$:

$$\frac{d^2 p^*}{dx^2} - p^* \;=\; -\frac{2}{\mu^2} H(p^*) \tag{6.53}$$

where the boundary conditions are given by

$$p^*(0) \;=\; \frac{1}{\mu^2} \int_0^1 e^{-\bar{x}} H(p^*(\bar{x}))\, d\bar{x} \tag{6.54}$$

$$p^*(1) \;=\; \frac{1}{e\mu^2} \int_0^1 e^{\bar{x}} H(p^*(\bar{x}))\, d\bar{x}. \tag{6.55}$$

For $H(p^*(\bar{x})) = 1 - p^*(\bar{x})$, Eq.(6.53) becomes

$$\frac{d^2 p^*}{dx^2} - \gamma\, p^* \;=\; 1 - \gamma \tag{6.56}$$

where

$$\gamma \;=\; 1 + \frac{2}{\mu^2} \;>\; 0 \tag{6.57}$$

Thus

$$p^*(x) \;=\; c_1 \sinh \sqrt{\gamma}\, x \;+\; c_2 \cosh \sqrt{\gamma}\, x \;+\; \frac{2}{\mu^2 \gamma} \tag{6.58}$$

where c_1 and c_2 are determined by substituting Eq.(6.58) into (6.54) and (6.55):

$$c_1 \;=\; \left(1 - e^{\sqrt{\gamma}}\right) K \tag{6.59}$$

$$c_2 \;=\; \left(1 + e^{\sqrt{\gamma}}\right) K \tag{6.60}$$

where

$$K \;=\; \frac{1 - \sqrt{\gamma} - \left(1 + \sqrt{\gamma}\right) e^{\sqrt{\gamma}}}{\gamma\left[\left(\mu^2\sqrt{\gamma} + \mu^2 + 1\right) e^{2\sqrt{\gamma}} + \mu^2\sqrt{\gamma} - \mu^2 - 1\right]} \tag{6.61}$$

For example, in the case that $\mu = 0.2$, we obtain

$$p^*(x) \;=\; 0.12040 \sinh \sqrt{51}\, x \;-\; 0.12059 \cosh \sqrt{51}\, x \;+\; \frac{50}{51} \tag{6.62}$$

which we have plotted in Figure 6.2.

6.5.2 Stability of Steady State

To study the stability of the steady state solution $(m^*(x), p^*(x))$, we set $p(x,t)$= $p^*(x)$+$\eta(x,t)$ and $m(x,t)$=$m^*(x)$+$\xi(x,t)$ and linearize the resulting equations in $\eta(x,t)$ and $\xi(x,t)$. The latter gives the variational equations around the equilibrium solution $(m^*(x), p^*(x))$ as follows

$$\xi_t \;=\; -\mu\,\xi - \int_0^1 e^{-|x-\bar{x}|}\,\eta_d(\bar{x})\,d\bar{x} \tag{6.63}$$

$$\eta_t \;=\; \xi - \mu\,\eta \tag{6.64}$$

If $\xi(x,t)$=$\phi(x)e^{\lambda t}$ and $\eta(x,t)$=$\psi(x)e^{\lambda t}$ then Eqs.(6.63) and (6.64) become

$$-e^{\lambda T}\,(\lambda+\mu)\phi(x) \;=\; \int_0^1 e^{-|x-\bar{x}|}\,\psi(\bar{x})\,d\bar{x} \tag{6.65}$$

$$(\lambda+\mu)\psi(x) \;=\; \phi(x) \tag{6.66}$$

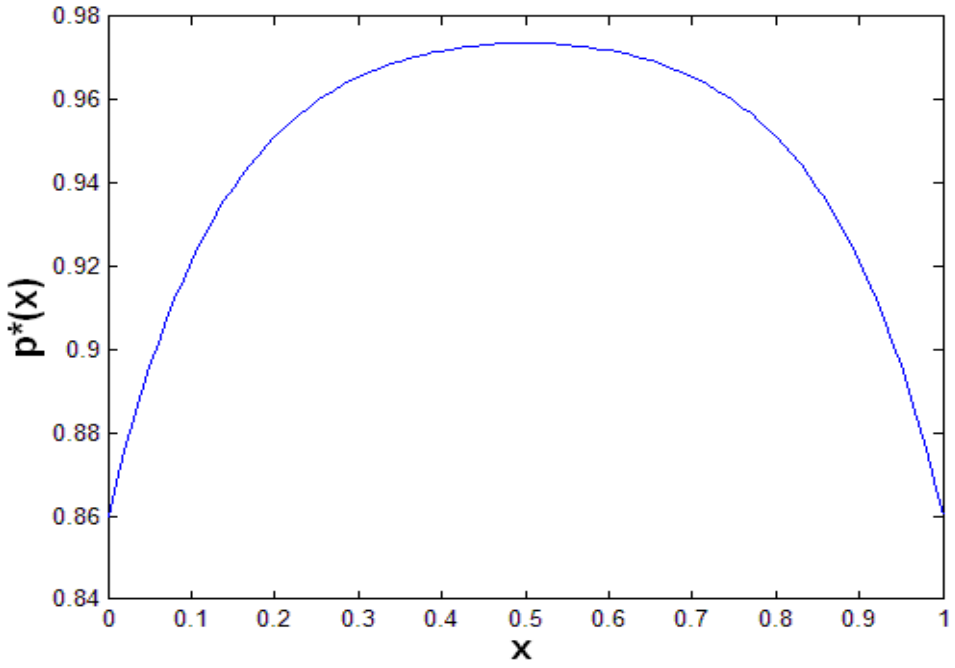

Figure 6.2: Steady state for exponential weighting case when $\mu = 0.2$. Here we have plotted $p^*(x)$ vs. x from Eq.(6.62).

Substituting Eq.(6.66) into (6.65) gives

$$r\,\psi(x) \;=\; \int_0^1 e^{-|x-\bar{x}|}\,\psi(\bar{x})\,d\bar{x} \tag{6.67}$$

where r is given by Eq.(6.84) in the Appendix. Next we transform the integral equation (6.67) to the following equivalent second order ODE [49] (as in Eqs.(6.51)-(6.55))

$$\frac{d^2\psi}{dx^2} + \left(\frac{2}{r} - 1\right)\psi \;=\; 0 \tag{6.68}$$

which will have solutions of the form

$$\psi(x) \;=\; c_1\,\sin(\rho\,x) + c_2\,\cos(\rho\,x) \tag{6.69}$$

where c_1 and c_2 are constants and $\rho = \sqrt{\frac{2}{r} - 1}$.

The endpoint boundary conditions of the second order ODE (6.68) are obtained from Eq.(6.67) as follows

$$\psi(0) = \frac{\rho^2+1}{2}\int_0^1 e^{-\bar{x}}\psi(\bar{x})\,d\bar{x} \tag{6.70}$$

$$\psi(1) = \frac{\rho^2+1}{2e}\int_0^1 e^{\bar{x}}\psi(\bar{x})\,d\bar{x}. \tag{6.71}$$

Substituting Eq.(6.69) into (6.70) and (6.71) gives a system of equations on the constants c_1 and c_2 which yields the following condition on ρ for nontrivial solutions

$$\begin{vmatrix} \rho\,\sin\rho - \cos\rho - e & -\sin\rho - \rho\,\cos\rho + e\rho \\ e\rho\,\sin\rho - e\,\cos\rho - 1 & -e\,\sin\rho - e\rho\,\cos\rho + \rho \end{vmatrix} = 0 \tag{6.72}$$

or equivalently

$$\left(\rho^2 - 1\right)\sin\rho - 2\rho\,\cos\rho = 0 \tag{6.73}$$

Eq.(6.73) has an infinite number of roots, the first three of which are $\rho = 1.30654$, 3.67319, 6.58462, $\cdots$ which give the following corresponding values for r:

$$r = \frac{2}{1+\rho^2} = 0.73881,\ 0.13800,\ 0.04509,\ \cdots \tag{6.74}$$

In addition to the previous results we may also use Eq.(6.72) and Eq.(6.69) to find the following relationship

$$c_2 = \rho\, c_1 \tag{6.75}$$

which gives Figure 6.3 by choosing $c_1 = 1$. Notice that by Eqs.(6.69) and (6.75) the endpoint boundary condition is given by $\psi(0) = c_2 = \rho = 1.30654$. This is confirmed by Figure 6.3.

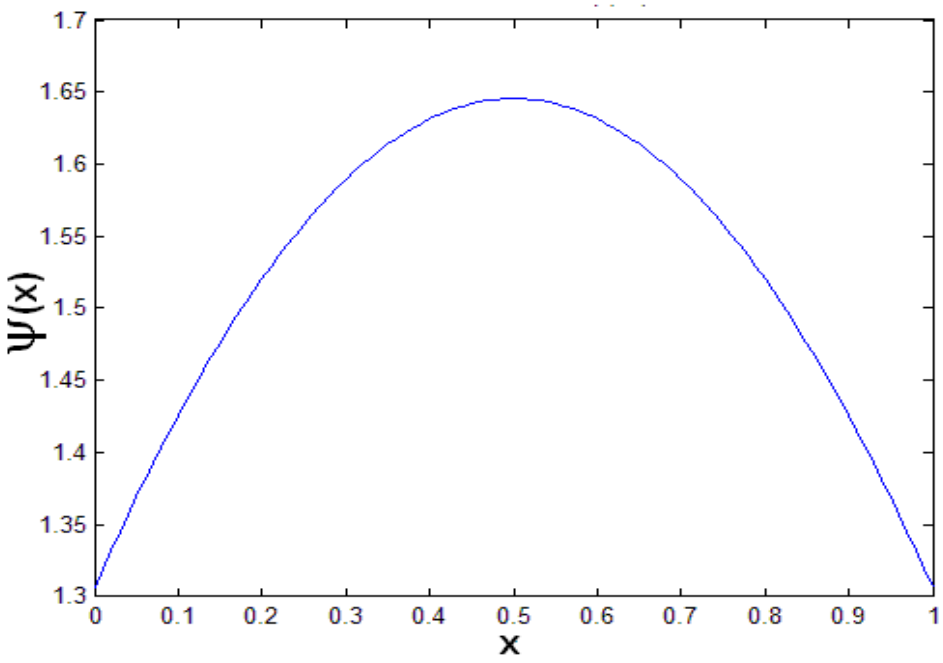

Figure 6.3: Bifurcation mode shape from linearized stability analysis. Here we have plotted $\psi(x)$ vs. x by using Eqs.(6.69) and (6.75) with $c_1 = 1$ and $c_2 = \rho = 1.30654$

Now that we know r from Eq.(6.74), we may use the results in the Appendix to determine stability of the steady state:

(i) When $T = 0$, Eq.(6.87) in the Appendix gives $\lambda = -\mu \pm \sqrt{-r}$ which, in view of the fact that all the values of r are positive (see Eq.(6.74)), shows that the system with no delay is stable.

(ii) When $T = T_{cr}$, Eqs.(6.91) and (6.92) in the Appendix give expressions for ω and T_{cr}. Since we are interested in the smallest value for T_{cr}, we take $r = 0.73881$, which gives, for $\mu = 0.2$, the values $\omega = 0.83595$ and $T_{cr} = 0.56184$.

In order to check this result, we replace the continuous variables $\xi(x,t)$ and $\eta(x,t)$ in Eqs.(6.63),(6.64) by a discrete set of N+1 variables $\xi_i(t)$ and $\eta_i(t)$ as in

Chapter 5. This corresponds to a model of N+1 coupled gene units, and replaces the integral in Eq.(6.63) by a sum of N+1 terms. As we now demonstrate, analysis of this system shows that $T_{cr} \to 0.56184$ as N goes to infinity for $\mu = 0.2$.

We start by discretizing the continuous system (6.63)-(6.64) into a (2N+2)-dimensional system given by (cf. Eqs.(5.17)-(5.18))

$$\dot{\xi}_i = -\mu\,\xi_i - \frac{1}{N+1}\sum_{j=0}^{N} e^{-|i-j|/N}\,\eta_j(t-T) \tag{6.76}$$

$$\dot{\eta}_i = \xi_i - \mu\,\eta_i \tag{6.77}$$

where $i = 0, 1, \ldots, N$. Next we assume solutions of the form

$$\xi_i = \phi_i\, e^{\lambda t} \tag{6.78}$$

$$\eta_i = \psi_i\, e^{\lambda t} \tag{6.79}$$

and substitute them into (6.76),(6.77) to obtain

$$-e^{\lambda T}(\lambda+\mu)\,\phi_i = \frac{1}{N+1}\sum_{j=0}^{N} e^{-|i-j|/N}\,\psi_j \tag{6.80}$$

$$(\lambda+\mu)\,\psi_i = \phi_i \tag{6.81}$$

eliminating ϕ_i we obtain

$$c\,\psi_i = \sum_{j=0}^{N} e^{-|i-j|/N}\,\psi_j \tag{6.82}$$

where $c = (N+1)r$ and r is given by (6.84). For nontrivial solutions, the system (6.82) of N+1 algebraic equations, must satisfy $\det(K - cI) = 0$ where K is the (N+1)×(N+1) matrix K=[K_{ij}]=[exp(−|$i - j$|/N)] and c is its associated eigenvalue. Since K is a symmetric matrix, all of its eigenvalues are real and thus c is a real number. Numerical evaluation of these eigenvalues c shows that they are all positive (see Table 6.1). The stability results for the steady state are summarized as follows:

(i) When $T = 0$, we see from Eq.(6.87) in the Appendix with $r = c/(N+1)$ that the steady state in the system with no delay is stable.

(ii) When $T = T_{cr}$, we choose the smallest value of c for a given truncation size N, and use Eqs.(6.91) and (6.92) in the Appendix to obtain values for ω and T_{cr} where we take $r = c/(N+1)$. Table 6.1 shows results for $\mu = 0.2$ for various values of N.

Table 6.1: Numerical results for $\mu = 0.2$

N	c	ω	T_{cr}
1	1.3678	0.8024	0.6089
2	2.0612	0.8044	0.6059
3	2.7844	0.8100	0.5977
5	4.2494	0.8175	0.5870
7	5.7215	0.8216	0.5813
10	7.9338	0.8253	0.5761
15	11.6246	0.8285	0.5718
30	22.7034	0.8320	0.5671
50	37.4783	0.8336	0.5649
100	74.4173	0.8348	0.5634
200	148.2960	0.8353	0.5627
300	222.1740	0.8355	0.5623

6.6 Conclusions

In this chapter we investigated the steady state solutions and stability of two different versions of a continuous gene regulatory network model. In both cases the model took the form of an ordinary differential equation coupled to a delay differential-integral equation having time, t, and gene location, x, as independent variables. These two versions were mainly defined by the integral kernel and Hill function as follows: **(1) uniform weighting** where the kernel G=1 and the Hill function was given by Eq.(6.9), and **(2) exponential weighting** where the kernel was of the form $G(x,\bar{x})$=exp$(-|x-\bar{x}|)$ and the associated Hill function given by Eq.(6.12). For the uniform weighting case we showed that the steady state is not only constant in time but in space as well. This allowed us to solve the associated eigenvalue problem and prove that the system is stable when there is no delay. Subsequently, we showed that the system becomes unstable for a critical delay and found closed form expressions for the critical delay, frequency, and amplitude of oscillation. For the exponential weighting case we found that the steady state solution depends on gene location. This was accomplished by transforming the steady state integral equation into a second order differential equation. By solving the differential equation we found a closed form expression for the x-dependent steady state. Stability analysis then revealed that the nondelayed system is stable and expressions for the critical delay and associated frequency were found. We confirmed our results by means of a numerical approximation where the continuous system was discretized, which resulted in a multidimensional system with delay. Numerical evaluations for different N were performed and good agreement was found with the continuous counterpart as N became large.

APPENDIX

In Eqs.(6.20) and (6.67) we have the following eigenvalue problem

$$r\, f(x) \;=\; \int_0^1 K(x,\bar{x}) f(\bar{x}) d\bar{x} \tag{6.83}$$

where $K(x,\bar{x})$ is a *symmetric* integral kernel, $f(x)$ is the eigenfunction, and r is the associated eigenvalue given by

$$r \;=\; -e^{\lambda T}(\lambda+\mu)^2 \tag{6.84}$$

Note that r is real since the RHS of (6.83) contains a symmetric kernel and thus is a self-adjoint operator of the form

$$L(\cdot) = \int_0^1 K(x,\bar{x})(\cdot)\, d\bar{x} \tag{6.85}$$

which has real eigenvalues.

Now given r we wish to determine λ in two special situations: **(i)** when $T = 0$, and **(ii)** when $T = T_{cr}$ and λ is pure imaginary, corresponding to a change in stability.

(i) When $T = 0$, Eq.(6.84) becomes

$$r \;=\; -(\lambda+\mu)^2 \tag{6.86}$$

and gives

$$\lambda = -\mu \pm \sqrt{-r} \tag{6.87}$$

If $r > 0$ then the $\mathrm{Re}(\lambda) = -\mu < 0$ (for positive μ), and we have stability of the system with no delay.

(ii) When $T = T_{cr}$ and $\lambda = i\omega$, Eq.(6.84) becomes

$$r = -e^{i\omega T_{cr}}(i\omega + \mu)^2 \tag{6.88}$$

which gives the two real equations

$$r = 2\mu\omega \sin\omega T_{cr} + \left(\omega^2 - \mu^2\right)\cos\omega T_{cr} \tag{6.89}$$

$$0 = \left(\omega^2 - \mu^2\right)\sin\omega T_{cr} - 2\mu\omega \cos\omega T_{cr} \tag{6.90}$$

Solving Eqs.(6.89),(6.90) for $\sin\omega T_{cr}$ and $\cos\omega T_{cr}$, and using the identity $\sin^2 + \cos^2 = 1$ we obtain

$$\omega = \sqrt{r - \mu^2} \tag{6.91}$$

Dividing the expressions for $\sin\omega T_{cr}$ and $\cos\omega T_{cr}$ and solving for T_{cr} we also obtain

$$T_{cr} = \frac{1}{\omega}\arctan\left(\frac{2\mu\omega}{\omega^2 - \mu^2}\right) \tag{6.92}$$

CHAPTER 7

CONCLUSIONS AND FUTURE WORK

7.1 Summary

This thesis deals with one of the greatest mysteries in modern science: gene regulation. It is our goal to find a geometrical and dynamical description of how proteins within the cell regulate their own production. Unfortunately, most cellular processes involve many different molecules interconnected. Thus the difficulty in understanding gene regulatory networks (GRNs) comes from finding the mechanisms that relate multiple biochemical processes inside the cell. Furthermore, recent findings [62, 72, 108] show that there are time delays associated with gene regulation. These delays arise naturally as transcriptional delays (time it takes the gene to get copied into mRNA) and translational delays (time it takes the ribosome to translate mRNA into protein). Incorporating these time delays into the dynamics of these mathematical models is thus becoming an important part of theoretical biology [4, 57, 104, 105].

In Chapter 4 we analyzed a single gene-mRNA-protein model. The model takes the form of an ordinary differential equation coupled to a delay differential equation, the state variables being concentrations of messenger RNA and protein. Section 4.2 provided a linear stability analysis and gave a critical time delay beyond which a periodic motion was born in a Hopf bifurcation. In Sections 4.3 and 4.4 we analyzed the model when the delay is constant, and in Section 4.5 when the delay depends on the state of the system.

In Chapter 5 we studied the dynamics of two different GRN models with multiple genes interconnected. Both of these models are characterized by a system of coupled ODEs and DDEs. The first model considers uniform weighting, where each ribosome produces a given quantity of protein which is then shared equally amongst all gene sites. The second model is characterized by an exponential weighting, where each protein product is shared unequally, with nearby gene sites being repressed to a greater extent than more distant genes. Both of these cases exhibited a steady state, which is stable when there is no delay. Linear and nonlinear analysis then reveal that a critical delay exists, where the steady state becomes unstable and a limit cycle is born.

Chapter 6 presents a continuous network model, which is characterized by a system of two coupled equations: an ordinary differential equation and a delay differential-integral equation. Two different cases with distinct integral kernels and Hill functions are studied. The first case considers an integral kernel of the form $G(x, \bar{x}) = 1$ and the second case consider a kernel $G(x, \bar{x}) = \exp(-|x - \bar{x}|)$. Both of these cases exhibited a steady state when there is no delay. Closed form expressions for the critical delay (when the equilibrium becomes unstable) and associated frequency are then found. Finally, we confirmed our results for the continuous exponential weighting case by discretizing the continuous system into an N-dimensional system and showing that the discrete system analysis (presented in Chapter 5) approaches the continuous results as N becomes large.

7.2 Final Remarks

The biological literature [20, 62, 72, 108] shows that long time behavior of gene expression dynamics can consist of both stable equilibrium as well as periodic behavior. In this thesis we have shown (for several models with delays) that the transition between these states is due to a Hopf bifurcation. Our linear and nonlinear analyses provide expressions for the critical delays, amplitudes, and frequency of oscillation as functions of the model parameters. In the case of constant delay in Chapter 4, Figure 4.3 shows that the Hopf bifurcation may not occur if the rates of degradation μ are too large. Also, inspection of Figure 4.4 shows that for a given detuning Δ off of the Hopf bifurcation, the amplitude of the oscillation depends on both p_0 (initial protein concentration) and μ (protein degradation rate). In this manner, the parameter study presented in Section 4.3.2 gives a well-rounded description of how the dynamics of the system depends on the biological constants.

The highly technical center manifold analysis presented in Section 4.4 provides a rigorous mathematical framework for the study of the infinite dimensional DDE system given by Eqs.(4.5) and (4.6). Since the center manifold theorem guarantees the existence of a curved two dimensional subspace, then the local flow about the steady state will be the same as the flow generated by the full nonlinear system. The center manifold analysis extended the study in Section 4.3 by providing approximations of general motions (slow flow), including the periodic motion itself. In particular, using the center manifold results we were able to show that the origin is asymptotically stable for the critical (bifurcation) value of the delay parameter.

We point out that by using Lindstedt's method (which is an approximation method) we obtained the same results as the center manifold theorem (which is based on a more rigorous mathematical foundation). However, as it can be seen in Section 4.4, the center manifold procedure is much more complicated than the Hopf calculation. In [81] (Chapter 14), 2 pages are spent explaining the application of Lindstedt's method to DDE's, whereas 10 pages are required for explanation of the center manifold approach. Thus the main advantage of using Lindstedt's method is that it is simpler to understand and easier to execute than the center manifold reduction. Furthermore, in Section 4.5 we investigated the effect of state-dependency on delay by using Lindstedt's method on the nonlinear system. We showed that Lindstedt's method can be used to deal with state-dependent delays and found the approximate expressions for amplitude and frequency of the steady state oscillation, which are in good agreement with those obtained by numerical integration (see Figure 4.9). Unfortunately, a constructive method for the state dependent version of the center manifold reduction is not available in the literature.

Extending our study of the single gene-mRNA-protein unit into a network of N coupled gene units proved to be interesting and useful. Both of the network models were characterized by a system of coupled ODEs and DDEs. The coupling between gene units was mainly given by the repression effect of one gene over another. If the coupling is uniform (as in Case 1 in Section 5.2.2) then the protein produced from each gene will repress equally (and with equal strength) the production of all other mRNAs. In this case, our nonlinear results give an expression for the amplitude of oscillation, Eq.(5.73), which turns out to be the generalization of the single gene amplitude found in Section 4.3 Eq.(4.43). This result means that each gene unit behaves identically at steady state. In particu-

lar, the protein concentrations oscillate with the same amplitude (even though they are all interconnected!). This behavior is in contrast to the exponential weighting case, where each gene unit has a different amplitude of oscillation.

Unlike the uniform weighting case, in the exponential weighting case, each protein product is shared unequally. That is, the production of protein of one gene represses the mRNA production of nearby gene sites to a greater extent than more distant genes. As in our previous analysis, we were able to prove that the system exhibits a stable steady state when there is no delay. However, we highlight the fact that (unlike the uniform case) the steady state is not constant, but rather it depends on gene location. In addition, another interesting result at the bifurcation delay (critical value when the steady state becomes unstable) is the associated bifurcation mode shape of the oscillation. Several bifurcation mode shapes are given in Figures 5.14, 5.15, and 5.16 for N=7, 15, and 30 respectively. The nonlinear numerical integration results are summarized in Figure 5.17 where we have plotted amplitude versus detuning about T_{cr} for N = 1, 7, 15, and 30.

Extending the multiple gene network analysis to a continuous network study is the goal of Chapter 6. An important biological remark about the continuum model is that genes are physically discrete, that is, they are organized separately along the DNA. Thus the discrete model is more realistic. Mathematically, however, we may approximate the discrete system by assuming a "gene continuum" between genes and their associated mRNA and protein products. Thus, although biological realism is sacrificed, we were able to transform the multidimensional DDE system (cf. Eqs.(5.17)-(5.18)) into a more compact mathematical model of two coupled equations given by (6.4) and (6.5). Notice that the latter

approach is not an uncommon technique, since it has been regularly used on studies of predator-prey models, epidemiology, and population dynamics, all of which are inherently discrete biological systems but which have been conveniently extended to continuous models for their analyses.

The two continuous models take the form of an ordinary differential equation coupled to a delay differential-integral equation having time, t, and gene location, x, as independent variables. For the uniform weighting case we showed that the steady state is not only constant in time but in space as well. On the other hand, for the exponential weighting case, we found that the steady state solution depends on gene location. This was accomplished by transforming the steady state integral equation into a second order differential equation. By solving the differential equation we found a closed form expression for the x-dependent steady state. Stability analysis then revealed that the nondelayed system is stable and expressions for the critical delay and associated frequency were found. We confirmed our results by means of a numerical approximation where the continuous system was discretized. Numerical evaluations for different N were performed and good agreement was found with the continuous counterpart as N became large.

7.3 Future Work

The results presented in this thesis lay the groundwork for a good understanding of the dynamics of DDEs and their applications to gene networks. However, numerous directions for future investigations have emerged from this work. Here we present several directions of future research which could be pursued:

Bifurcation Analysis

In our study of the single gene model (cf.Eqs.(4.5) and (4.6) in Chapter 4), we perturbed off of $T = T_{cr}$. However, there are other ways of setting up the perturbation analysis. From Eq.(4.27) we have:

$$\ddot{\eta} + 2\mu\dot{\eta} + \mu^2\eta = -K\eta_d + H_2\eta_d^2 + H_3\eta_d^3 + \cdots \tag{7.1}$$

which for small μ, small T, and small η transforms into

$$\ddot{\eta} + 2\mu\epsilon\dot{\eta} + \mu^2\epsilon^2\eta = -K\eta_d + \epsilon H_2\eta_d^2 + \epsilon^2 H_3\eta_d^3 + \cdots \tag{7.2}$$

where $\eta_d = \eta(t - \epsilon T)$. When $\epsilon = 0$ we have

$$\ddot{\eta} + K\eta = 0 \tag{7.3}$$

where K is given by Eq.(4.15).

A few immediate questions arise: (1) what would slow flow look like if we perturb off of Eq.(7.3) using averaging? (2) Can we use computer software (e.g. AUTO or BIFTOOL) to understand the slow flow of the perturbed system?

In Chapter 4 we found conditions on T_{cr} for a periodic solution. However, there may be other parameter combinations which also give pure imaginary roots. For example, setting $T = 0$ and $\mu = 0$ in Eq.(7.1) gives a periodic solution:

$$\ddot{\eta} + K\eta_d = H_2\eta_d^2 + H_3\eta_d^3 + \cdots \tag{7.4}$$

However, if we allow μ and T to take small nonzero values, then we could expect to get two limit cycles in (7.1): one from our analysis in Chapter 4 and one from (7.4). The use of AUTO or BIFTOOL would prove useful at this stage.

Large Delays

What would happen if the delay becomes large compared to the system's time scale? Biologically this means that the time it takes the cell to produce mRNA is very large compared to the rest of the processes. Mathematically we may define the delay as $T = 1/\epsilon$ and use Eq.(7.1) for our analysis. Preliminary numerical integration results for $T = 5000$ using Matlab's dde23 are given in Figure 7.1.

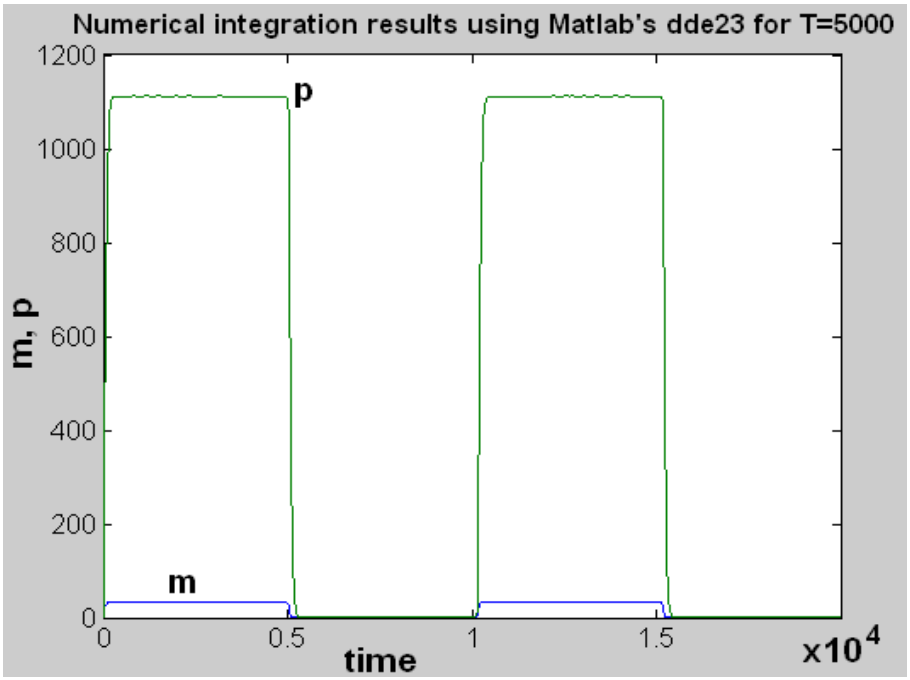

Figure 7.1: Numerical integration results using Matlab's dde23 for large delay.

The first step in studying large time delays is to understand the square wave response in Figure 7.1. It is clear that for small ϵ the outer layer (non-boundary layer) will have one solution, which will probably be an iterative map. The previous study has not been done before and it would be worth pursuing.

State Dependent Delays

Following the investigations described in Section 4.5 we may extend our study to more general state dependent delays. Two possibilities are

$$T = T_0 + c_1 M(t) + c_2 P(t) \tag{7.5}$$

$$T = T_0 + c_1 M(t) + c_2 M(t)^2 \tag{7.6}$$

where the delay in (7.5) includes the protein concentration P, and where the delay in (7.6) includes quadratic terms of $M(t)$. Possible questions to investigate would include the existence of limit cycles: does the original limit cycle found in Section 4.5 still exist if $c_2 \neq 0$? does it stop existing for a certain critical c_2? Using Matlab's *ddesd* would be a first step in understanding the previous.

Nonlinear Hill Function

The results presented in Chapter 6 show how to deal with a delay differential-integral equation. However, we could extend our analysis to include a more complicated Hill function. The next step could be to study a system of the following form

$$\dot{m} = -\mu m + \int_0^1 e^{-|x-\bar{x}|}\left(1 - p_d(\bar{x}) + \alpha p_d(\bar{x})^3\right) d\bar{x} \tag{7.7}$$

$$\dot{p} = m - \mu p \tag{7.8}$$

where α could be a small number and defined as $\alpha = \epsilon\alpha_1 + \epsilon^2\alpha_2$ for $\epsilon << 1$. Several difficulties soon arise when working with the previous equations, for example, the steady state solutions now become complicated to find. If we set $\dot{p}=\dot{m}=0$ then the steady state (m^*,p^*) satisfies $m^*=\mu p^*$, $p_d^*=p^*$, and the system (7.7)-(7.8) can be combined to give

$$\mu^2 p^* = \int_0^1 e^{-|x-\bar{x}|}\left(1 - p^* + \alpha {p^*}^3\right) d\bar{x} \tag{7.9}$$

By using the procedure presented in Chapter 6 Eq.(7.9) can be transformed into the following ODE

$$\frac{d^2p^*}{dx^2} - \left(1 + \frac{2}{\mu^2}\right)p^* = -\frac{2}{\mu^2} - \alpha\frac{2}{\mu^2}p^{*\,3} \tag{7.10}$$

Finding the steady state solutions would entail solving the second order ODE (7.10), which has a cubic nonlinearity. The latter has proven to be nontrivial.

Distributed Delays

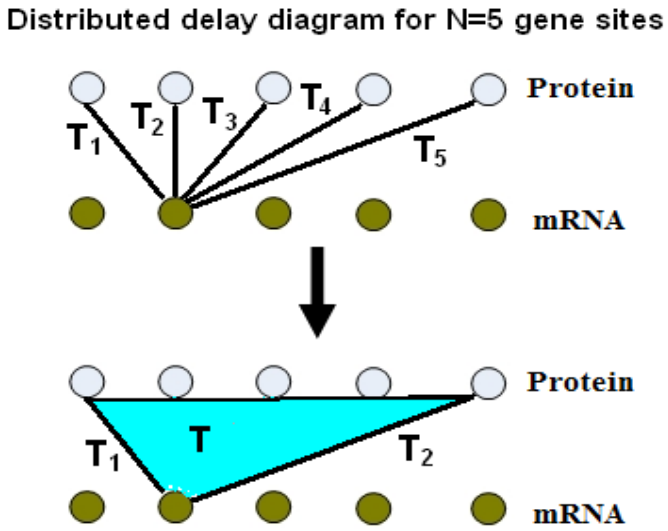

Figure 7.2: Distributed delay diagram for five genes. This diagram shows the extension of the system with "discrete" delays into a system with a "continuum" of delays.

According to Figure 7.2, future work in the area of distributed delays might entail studying the system

$$\dot{m} = -\mu m + \int_{T_1}^{T_2} \frac{1}{1 + \left(\frac{p(t-T)}{p_0}\right)^n} dT \tag{7.11}$$

$$\dot{p} = m - \mu p \tag{7.12}$$

where $m = m(x,t)$ and $p = p(x,t)$ and where the integral is over a continuum of delays from one gene site to another.

BIBLIOGRAPHY

[1] Abouheif E., Wray G.A. 'Evolution of the gene network underlying wing polyphenism in ants', *Science,* 297:249-252 (2002).

[2] Aldana M., Balleza E., Kauffman S., Resendiz O. 'Robustness and evolvability in genetic regulatory networks', *J. Theor. Biol.,* 245:433-448 (2007).

[3] Alla H., David R. 'Continuous and hybrid petri nets', *J. Circ. Syst. Comp.,* 8(1):159-188 (1998).

[4] Batchelor E., Mock C.S., Bhan I., Loewer A., Lahav G. 'Recurrent Initiation: A Mechanism for Triggering p53 Pulses in Response to DNA Damage', *Molecular Cell,* 30(3):277-289 (2008).

[5] Beer M.A., Tavazoie S. 'Predicting gene expression from sequence'. *Cell,* 117:185-198 (2004).

[6] Becskei A., Serrano L. 'Engineering stability in gene networks by autoregulation', *Nature,* 405:590-593 (2000).

[7] Bellman R., Cooke K.L. *Differential Difference Equations,* Academic Press, New York (1963).

[8] Bratsun D., Volfson D., Tsimring L.S., Hasty J. 'Delay-induced stochastic oscillations in gene regulation', *PNAS,* 102(41):14593-14598 (2005).

[9] Brazhnik P. 'Inferring gene networks from steady-state response to single-gene perturbations', *J. Theor. Biol.,* 237:427-440 (2005).

[10] Breda D., Maset S., Vermiglio R. 'Computing the characteristic roots for delay differential equations', *IMA J Numer Anal,* 24:1-19 (2004).

[11] Campbell S.A., Belair J., Ohira T., and Milton J. 'Complex Dynamics and Multistability in a Damped Harmonic Oscillator with Delayed Negative Feedback', *Chaos* 5:640-645 (1995).

[12] Campbell S.A., Edwards R., van den Driessche P. 'Delayed coupling between two neural network loops', *SIAM J Appl Math,* 65(1):316-335 (2004).

[13] Casal, A. and Freedman M. 'A Poincare-Lindstedt Approach to Bifurcation Problems for Differential-Delay Equations', *IEEE Transactions on Automatic Control,* 25:967-973 (1980).

[14] Carr, J., *Applications of Centre Manifold Theory,*Springer-Verlag, New York (1981).

[15] Casey R., Jong H., Gouze J. 'Piecewise-linear models of genetic regulatory networks: Equilibria and their stability', *J. Math. Biol.,* 52:27-56 (2006).

[16] Chaves M., Albert R., Sontag E.D. 'Robustness and fragility of Boolean models for genetic regulatory networks', *J. Theor. Biol.,* 235:431-449 (2005).

[17] Chen K., Rajewsky N. 'The evolution of gene regulation by transcription factors and microRNAs', *Nature Rev Gen,* 8:93-103 (2007).

[18] Ciliberti S., Martin O.C., Wagner A. 'Robustness can evolve gradually in complex regulatory gene networks with varying topology', *PLOS Comp. Biol.,* 3(2):164-173 (2007).

[19] Ciliberti S., Martin O.C., Wagner A. 'Innovation and robustness in complex regulatory gene networks', *PNAS,* 104(34):13591-13596 (2007).

[20] Ciliberto A., Novak B., Tyson J.J. 'Steady states and oscillations in the p53/Mdm2 network', *Cell Cycle,* 4(3):488-493 (2005).

[21] Ciupea M.S., Bivortb B.L., Bortzc D.M., Nelson P.W. 'Estimating kinetic parameters from HIV primary infection data through the eyes of three different mathematical models', *Math Biosci,* 200(1):1-27 (2006).

[22] Cooke K., Kuang Y., Li B. 'Analysis of an antiviral immune response model with time delays', *Proc 3rd Butler conf,* 6:321-354 (1998).

[23] Cooke K., van den Driessche P., Zou X. 'Interaction of maturation delay and nonlinear birth in population and epidemic models', *J Math Biol,* 39:332-352 (1999).

[24] Conrad E.D., Tyson J.J. 'Modeling molecular interaction networks with nonlinear ordinary differential equations', *Cambridge, MA: MIT Press,* 97-123 (2006).

[25] Coutinho R., Fernandez B., Lima R., Meyroneinc A. 'Discrete time piecewise affine models of genetic regulatory networks', *J. Math. Biol.,* 52:524-570 (2006).

[26] Davidson E.H., Erwin D.H. 'Gene regulatory networks and the evolution of animal body plans', *Science,* 311:796-800 (2006).

[27] DHaeseleer P., Liang S., Somogyi R. 'Genetic network inference: From co-expression clustering to reverse engineering', *Bioinformatics,* 16:707726 (2000).

[28] Diekmann O., van Gils S.A., Lunel S.M.V., Walther H-O. *Delay Equations: Functional, Complex, and Nonlinear Analysis,* New York, Springer-Verlag (1995).

[29] Edwards R., van den Driessche P., Wang L. 'Periodicity in piecewise-linear switching networks with delay', *J. Math. Biol.,* 55:271-298 (2007).

[30] Elowitz M.B., Leibler S. 'A synthetic oscillatory network of transcriptional regulators'. *Nature,* 403:335-338 (2000).

[31] Friedman N., Linial M., Nachman I., Peer D. 'Using Bayesian networks to analyze expression data'. *J. Comp. Biol.,* 7:601-620 (2000).

[32] Gambin A., Lasota S., Rutkowski M. 'Analyzing stationary states of gene regulatory network using Petri nets', *In Silico Biology,* 6:0010 (2006).

[33] Gardner T.S, Bernardo D., Lorenz D., Collins J.J. 'Inferring genetic networks and identifying compound mode of action via expression profiling', *Science,* 301:102-105 (2003).

[34] Gardner T.S., Cantor C.R., Collins J.J. 'Construction of a genetic toggle switch in Escherichia coli', *Nature,* 403:339-342 (2000).

[35] Geva-Zatorsky N., Rosenfeld N., Itzkovitz S., Milo R., Sigal A., Dekel E., Yarnitzky T., Liron Y., Polak P., Lahav G., Alon U. 'Oscillations and variability in the p53 system', *Mol Syst Biol,* 2:2006.0033 (2006).

[36] Goodwin B.C. 'Temporal Organization in Cells. A Dynamic Theory of Cellular Control Processes', *New York: Academic Press* (1963).

[37] Goodwin B.C. 'Oscillatory behavior in enzymatic control processes', *Advances in Enzyme Regulation*, 3:425-438 (1965).

[38] Goutsias J., Kim S. 'Stochastic transcriptional regulatory systems with time delays: A mean-field approximation', *J. Comp. Biol.*, 13(05):1049-1076 (2006).

[39] Guckenheimer J. and Holmes P. *Nonlinear Oscillations, Dynamical Systems, and Bifurcations of Vector Fields,* Springer-Verlag, New York, 1983.

[40] Guss K.A., Nelson C.E., Hudson A., Kraus M.E., Carroll S.B. 'Control of a genetic regulatory network by a selector gene', *Science,* 292:1164-1167 (2001).

[41] Halberg F. 'Transdisciplinary unifying implications of circadian findings in the 1950s', *J Circ Rhythms* 1:1-61 (2003).

[42] Hale J.K. *Theory of Functional Differential Equations,* Springer-Verlag (1977).

[43] Hale J.K. *Functional Differential Equations of Retarded Type,* 7o Coloquio Brasileiro de Matematica, Pocos de Caldas (1969).

[44] Hale J.K., Verduyn-Lunel S.M. *Introduction to Functional Differential Equations,* Applied Math Sciences 99, Springer-Verlag (1991).

[45] Hassard B.D., Kazarinoff N.D., Wan Y-H. *Theory and Applications of Hopf Bifurcation,* Cambridge University Press, Cambridge (1981).

[46] Hasty J., Dolnik M., Rottschafer V., Collins J.J. 'Synthetic gene network for entraining and amplifying cellular oscillations', *Phys. Rev. Let.*, 88(14):148101 (2002).

[47] Hasty J., McMillen D., Isaacs F., Collins J.J. 'Computational studies of gene regulatory networks: In numero molecular biology', *Nature,* 2:268-279 (2001).

[48] He G., Siddik Z.H., Huang Z., Wang R., Koomen J., Kobayashi R., Khokhar A.R., Kuang J. 'Induction of p21 by p53 following DNA damage inhibits both Cdk4 and Cdk2 activities', *Oncogene,* 24:2929-2943 (2005).

[49] Hildebrand F.B. 'Methods of Applied Mathematics', *Prentice Hall,* (1965).

[50] Hill R., Bodzak E., Blough M.D., Lee P.W.K. 'p53 binding to the p21 promoter is dependent on the nature of DNA damage', *Cell Cycle,* 7:2535-2543 (2008).

[51] Hu W., Feng Z., Ma L., Wagner J., Rice J.J., Stolovitzky G., Levine A.J. 'A single nucleotide polymorphism in the MDM2 gene disrupts the oscillation of p53 and MDM2 levels in cells', *Cancer Res,* 67:2757-2765 (2007).

[52] Insperger T., Stepan G., Hartung F. and Turi J. 'State-dependent Regenerative Delay in Milling Processes', *Proc ASME IDETC,*Long Beach CA (2005), DETC2005-85282.

[53] Insperger T., Stepan G., and Turi J. 'State-dependent Delay in Regenerative Turning Processes', *Nonlinear Dynamics,* 47:275283 (2007).

[54] Jong H. 'Modeling and simulation of genetic regulatory systems: A literature review', *J Comp Biol,* 9(1):67-103 (2002).

[55] Jong H., Gouze J., Hernandez C., Page M., Sari T., Geiselmann J. 'Qualitative simulation of genetic regulatory networks using piecewise-linear models', *Bulletin of Mathematical Biology,* 66:301-340 (2004).

[56] Kalmar-Nagy T., Stepan G., Moon F.C. 'Subcritical Hopf Bifurcation in the Delay Equation Model for Machine Tool Vibrations', *Nonlinear Dynamics,* 26:121-142 (2001).

[57] Karlebach G., Shamir R. 'Modelling and analysis of gene regulatory networks', *Nature,* 9:770-780 (2008).

[58] Kohn M.C., Lemieux D.R. 'Identification of regulatory properties of metabolic networks by graph theoretical modeling', *J Theor Biol,* 150:3-25 (1991).

[59] Lahav G, Rosenfeld N, Sigal A, Geva-Zatorsky N, Levine AJ, Elowitz MB, Alon U. 'Dynamics of the p53-Mdm2 feedback loop in individual cells', *Nat Genet,* 36(2):147-50 (2004).

[60] Lane D. 'Awakening angels', *Nature,* 394:616-617 (1998).

[61] Lee D., Rieger H. 'Comparative study of the transcriptional regulatory networks of E. coli and yeast: Structural characteristics leading to marginal dynamic stability', *J. Theor. Biol.,* 248:618-626 (2007).

[62] Lewis J. 'Autoinhibition with transcriptional delay: A simple mechanism for the zebrafish somitogenesis oscillator', *Current Biology,* 13:1398-1408 (2003).

[63] Ma L., Wagner J., Rice J.J., Hu W., Levine A.J., Stolovitzky G.A. 'A plausible model for the digital response of p53 to DNA damage', *PNAS,* 102(40):14266-71 (2005).

[64] Mahaffy J.M. 'Genetic Control Models with Diffusion and Delays', *Mathematical Biosciences* 90:519-533 (1988).

[65] Mahaffy J.M., Jorgensen D.A., Vanderheyden R.L. 'Oscillations in a model of repression with external control', *J Math Biol,* 30:669-691 (1992).

[66] Matsuno H., Doi A., Nagasaki M., Miyano S. 'Hybrid Petri net representation of gene regulatory network', *Pac Symp Biocomput,* 5:338-349 (2000).

[67] Merrow M., Spoelstra K., Roenneberg T. 'The circadian cycle: daily rhythms from behaviour to genes', *EMBO Reports,*6(10):930-935 (2005).

[68] Mestl T., Plahte E., Omholt S.W. 'A mathematical framework for describing and analysing gene regulatory networks', *J Theor Biol,* 176:291-300 (1995).

[69] Mincheva M., Roussel M.R. 'Graph-theoretic methods for the analysis of chemical and biochemical networks', II. Oscillations in networks with delays', *J Math Biol,* 55:87-104 (2007).

[70] Mocek W.T., Rudbicki R. and Voit E.O. 'Approximation of delays in biochemical systems', *Mathematical Biosciences* 198:190-216 (2005).

[71] Mochizuki A. 'Structure of regulatory networks and diversity of gene expression patterns', *J Theor Biol,* doi:10.1016/j.jtbi.2007.09.019 (2007).

[72] Monk N.A.M. 'Oscillatory expression of Hes1, p53, and NF-κB driven by transcriptional time delays', *Current Biology,* 13:1409-1413 (2003).

[73] Monk N.A.M. 'Supplemental Data to *Oscillatory Expression of Hes1, p53, and NF-κB Driven by Transcriptional Time Delays', Current Biology,* 13:1409-1413 (2003). Available online at: www.current-biology.com/cgi/content/full/13/16/1409/DC1

[74] Muller S., Hofbauer J., Endler L., Flamm C., Widder S., Schuster P. 'A generalized model of the repressilator', *J Math Biol,* 53:905-937 (2006).

[75] Nayfeh A., Mook D. *Nonlinear Oscillations,* Wiley Classics Library, John Wiley and Sons (1995).

[76] Novak B., Tyson J.J. 'Design principles of biochemical oscillators', *Nat Rev Molec Cell Biol,* 9:981-991 (2008)

[77] Namachchivaya N.S. and Beddini R. 'Spindle Speed Variation for the Suppression of Regenerative Chatter', *J. Nonlinear Science* 13:265-288 (2003).

[78] Oktem H., Pearson R., Egiazarian K. 'An adjustable aperiodic model class of genomic interactions using continuous time Boolean networks (Boolean delay equations)', *Chaos,* 13(4):1167-1174 (2003).

[79] Pabla N., Huang S., Mi Q.S., Daniel R., Dong Z. 'ATR-Chk2 signaling in p53 activation and DNA damage response during cisplatin-induced apoptosis', *J Biol Chem,* 283(10):6572-83 (2008).

[80] Perkins T.J., Hallett M., Glass L. 'Dynamical properties of model gene networks and implications for the inverse problem', *BioSystems,* 84:115-123 (2006).

[81] Rand, R.H. *Lecture Notes on Nonlinear Vibrations (version 48)*, available online at http://audiophile.tam.cornell.edu/randdocs/nlvibe52.pdf (2005).

[82] Rand R.H. and Armbruster D. *Perturbation Methods, Bifurcation Theory and Computer Algebra,* Springer-Verlag, New York (1987).

[83] Rand R. and Verdugo A. 'Hopf Bifurcation Formula for First Order Differential-Delay Equations', *Comm Nonlin Sci Numer Simul,* 12:859-864 (2007).

[84] Ribeiro A., Kauffman S.A. 'Noisy attractors and ergodic sets in models of gene regulatory networks', *J. Theor. Biol.,* 247:743-755 (2007).

[85] Ribeiro A., Zhu R., Kauffman S.A. 'A general modeling strategy for gene regulatory networks with stochastic dynamics', *J Comp Biol,* 13(9):1630-1639 (2006).

[86] Satyanarayana A., Hilton M.B., Kaldis P. 'p21 inhibits Cdk1 in the absence of Cdk2 to maintain the G1/S phase DNA damage checkpoint', *Molec Biol Cell,* 19:6577 (2008).

[87] Scheper T., Klinkenberg D., Pennartz C., Pelt J. 'A mathematical model for the intracellular circadian rhythm generator', *J Neurscience,* 19(1):40-47 (1999).

[88] Schlitt T., Brazma A. 'Current approaches to gene regulatory network modelling', *BMC Bioinformatics,* 8(Supp 6):S9 (2007).

[89] Sible J.C. and Tyson J.J. 'Mathematical modeling as a tool for investigating cell cycle control networks', *Methods,* 41(2):238-47 (2007).

[90] Smith J., Theodoris C., Davidson E.H. 'A gene regulatory network subcircuit drives a dynamic pattern of gene expression', *Science,* 318:794-797 (2007).

[91] Smolen P., Baxter D.A., Byrne J.H. 'A reduced model clarifies the role of feedback loops and time delays in the Drosophila circadian oscillator', *Biophysical Journal,* 83:2349-2359 (2002).

[92] Smolen P., Baxter D.A., Byrne J.H. 'Modeling transcriptional control in gene networksmethods, recent results, and future directions', *Bulletin of Mathematical Biology,* 62:247-292 (2000).

[93] Smolen P., Baxter D.A. 'Mathematical modeling of gene networks', *Neuron,* 26:567-580 (2000).

[94] Srividhyaa J., Gopinathan M.S. 'A simple time delay model for eukaryotic cell cycle', *J Theo Biol* 241(3):617-627 (2006).

[95] Stepan G. *Retarded Dynamical Systems: Stability and Characteristic Functions,* Longman Scientific and Technical, Essex (1989).

[96] Strogatz S. 'Nonlinear dynamics and chaos: With applications to physics, biology, chemistry, and engineering', Perseus Books, 1994.

[97] Strogatz S. 'Death by delay', *Nature,* 394:316317 (1998).

[98] Tao Y. 'Intrinsic and external noise in an auto-regulatory genetic network', *J. Theor. Biol.,* 229:147-156 (2004).

[99] Tegner J., Yeung M.K.S., Hasty J., Collins J.J. 'Reverse engineering gene networks: Integrating genetic perturbations with dynamical modeling', *PNAS,* 100(10):5944-5949 (2003).

[100] Turchin P. 'Rarity of density dependence or population regulation with lags?', *Nature,* 344:660-663 (1990).

[101] Turner S., Sherratt J.A., Painter K.J. 'From a discrete to a continuous model of biological cell movement', *Phys. Rev. E,* 69:021910 (2004).

[102] Tyson J.J. 'Another turn for p53', *Mol Syst Biol,* 2:2006.0032 (2006).

[103] Tyson J.J. 'Monitoring p53's pulse', *Nat Genet,* 36(2):113-114 (2004).

[104] Tyson J.J., Chen K.C., Novak B. 'Network dynamics and cell physiology', *Nature Rev,* 2(12):908-916(2001).

[105] Tyson J.J., Chen K.C., Novak B. 'Sniffers, buzzers, toggles and blinkers: dynamics of regulatory and signaling pathways in the cell', *Curr Opin Cell Biol,* 15(2):221-231 (2003).

[106] Tyson J.J., Novak B. 'Temporal organization of the cell cycle', *Curr Biol,* 18:R759-768 (2008).

[107] Vass M., Allen N., Shaffer C.A., Ramakrishnan N., Watson L.T., Tyson J.J. 'The JigCell model builder and run manager', *Bioinformatics,* 20(18):3680-1 (2004).

[108] Verdugo A., Rand R. 'Hopf bifurcation in a DDE model of gene expression', *Communications in Nonlinear Science and Numerical Simulation,* 13:235-242 (2008).

[109] Verdugo A., Rand R. 'Center manifold analysis of a DDE model of gene expression', *Communications in Nonlinear Science and Numerical Simulation,* 13:1112-1120 (2008).

[110] Verdugo A., Rand R. 'Delay Differential Equations in the Dynamics of Gene Copying', *Proc IDETC-ASME,* paper no. DETC2007-34214 (2007).

[111] Verdugo A., Rand R. 'DDE Model of Gene Expression: A Continuum Approach', *Proc IMECE-ASME,* paper no. IMECE2008-66321 (2008).

[112] Verheyden K., Luzyanina T., Roose D. 'Efficient computation of characteristic roots of delay differential equations using LMS methods', *J Comp App Math,* 214(1):209-226 (2008)

[113] Villasana M., Radunskaya A. 'A delay differential equation model for tumor growth', *J Math Biol,* 47(3):270-294 (2003).

[114] Vogelstein B, Lane D, Levine A.J. 'Surfing the p53 network', *Nature,* 408:307-10 (2000).

[115] Volterra V. 'Variazioni e fluttuazioni del numero d'individuali in specii animali conviventi', *Mem. R. Accad. Naz. Lincei,* VI Vol. 2, pp. 3778 (1926).

[116] Wagner J., Stolovitzky G. 'Stability and time-delay modeling of negative feedback loops', *Proceedings of the IEEE,* 96(8):1398-1410 (2008).

[117] Wang R., Chen L., Aihara K. 'Construction of genetic oscillators with interlocked feedback networks', *J. Theor. Biol.,* 242:454-463 (2006).

[118] Zeiser S., Muller J., Liebscher V. 'Modeling the Hes1 oscillator', *J. Comp. Biol.,* 14(7):984-1000 (2007).

[119] Zhu R., Ribeiro A.S., Salahub D., Kauffman S.A. 'Studying genetic regulatory networks at the molecular level: Delayed reaction stochastic models', *J. Theor. Biol.,* 246:725-745 (2007).